博士論文（要約）

Assessing Impacts of Human Disturbance and Fire on Forests in the Protected Area of Russian Far East using Remote Sensing Data

（リモートセンシングデータを利用したロシア極東の自然保護区の森林における人為攪乱と火災が及ぼす影響評価）

KHATANCHAROEN Chulabush

カタンチャルン　チュラブッシュ

Assessing Impacts of Human Disturbance and Fire on Forests in the Protected Area of Russian Far East using Remote Sensing Data

（リモートセンシングデータを利用したロシア極東の自然保護区の森林における人為攪乱と火災が及ぼす影響評価）

By

Chulabush Khatancharoen

Supervisor: Professor Satoshi Tsuyuki

A thesis

submitted in partial fulfillment

of the requirements for the degree of

Doctor of Philosophy

The University of Tokyo, Department of Global Agricultural Sciences,

Graduate School of Agricultural and Life Sciences

2021

Acknowledgements

I sincerely thank Dr.Satoshi Tsuyuki for supervising this thesis. This thesis will not be successful without his supervision. I would like to thank Dr.Naoya Wada from University of Toyama and Center for Far Eastern Studies (CFES) for sponsoring and giving me opportunity to conduct research in Russia. I also want to thank my coauthors: Dr.Tatsuyuki Seino, Dr.Konosuke Sugiura, Dr.Semyon Bryanin, Dr.Irina G. Borisova, for helping me achieve professional level of academic career. Without them, I would not have come this far.

I would like to thank Institute of Geology and Nature Management, Far East Branch, Russian Academy of Sciences, and Zeya State Nature Reserve for a great collaboration during field visits. And finally thank to those who support me and help me throughout the research works.

I would like to thank my friends in GFES: (list name of GFES) for supporting me during the lab. The enjoyment and the atmosphere of GFES motivate me to achieve the higher education level without fear or discouragement. The lab is full of fun and friendship and teamwork. I also thank to my family who always give me warmness and always encourage me to work hard and finished the thesis.

Lastly, I want to say that I was deeply saddened by the news of Viktor passing during my PhD research. I want to send my heartfelt sympathy for the loss of one of my colleagues to his family. And I would like to specially thank him for being one of the best colleagues. His support and care will be missed and he will never be forgotten, may his soul rest in peace.

Abstract

Anthropogenic effects have altered forest globally. Russia is one of the few countries that has remaining large intact forest. The forest in the Russian Far East is now on a long-term decline due to major forest fires and illegal cutting. Because of the low protection and lack of accessibility, the impacts of forest fires and human disturbances in far east region is not well studied, raising concerns in the scientific community about the impact of forest loss and degradation. Major tree die-off and shrinking forest sequestration areas are expected.

The thesis aims to raise awareness within the scientific community to find solution for future challenge of the current impacts on forest loss in the Russian Far East. Many studies pointed out that monitoring the fire influence and possible causes of human disturbances may provide the scientific community with a way to avoid the catastrophic effects of future consequence. The protected area served as important targeted area for my field experiment because the protected area keeps the environment away from human activities and allowing the full potential of ecosystem functioning and the development of forest regrowth after disturbance.

In terms of protected areas, the Russian Federation has its own separate governance structure. The study chose the highest-level restriction area, Zapovednik type as the study area. I selected Zeya Zapovednik, or Zeya State Nature Reserve (hence “The Reserve”) as my study area. The Reserve located in the Zeya city in Amur oblast, the Russian Far East. The Reserve is home to more than 1000 of plant and wildlife species. Many species are red-listed by the International Union for Conservation of Nature (IUCN). Human settlements and recreational activities are strictly prohibited; only staff cabins and instructional activities licensed by the park rangers are permitted. This particular research site is has recently become more vulnerable to anthropogenic threats such as fires and clear-cutting. The Reserve is facing more frequent burning inside the Reserve and illegal clearcutting area around the edge of the Reserve.

Extreme impacts from human disturbances degrade forest development and ecological processes, affecting forest cover transitioning over time. Tracking forest disturbance and forest cover transition is therefore essential to protect its natural complexity, biological diversity, and ecological role.

Remote sensing methods are the most advanced way to collect information from large ground area. Using remote sensing data to track and analyze forest changes and disturbances on the environment provides critical information to help scientists address global warming problems. The study used high-quality Landsat images from 1975 to 2019 with less than 10% cloud during the growing season acquired from the United States Geological Survey (USGS) Data Center. The center housed the most extensive continuously collected database of space-based moderate-resolution data, to which scientists and non-scientists from all academic disciplines had free access.

The overall objectives of the study were to analyze forest cover change around protected area in The Russian Far East and evaluate an effectiveness of protected area using remote sensing data. Three critical questions that lead to new insights for my interested in the Reserve locations included: 1) If the areas did not have frequent image data available, how can we monitor forest cover change and disturbances and effectiveness of protected area by using long-time interval satellite image analysis? 2) How did disturbances distribute around the protected area in relation to environmental and climatic factors? 3) After new images available that allow the research to conduct single image classification, how did forest and disturbance covers change around protected area and can we monitor the stableness of the forest and disturbance covers around protected area based on vegetation indices using short-time interval satellite image analysis? addressing these questions gave me the opportunity to discover how human activities impact interacted to shape the forest ecosystem, particularly in comparison between the protected area and outside protected area.

The outline of the thesis included introduction, study areas, research data, experiment, and discussion. Chapter 1 addressed the study context, general goal, and three specific questions. The background of study area's biodiversity, conservation status, and ecosystem benefits was guided by the study field was described in Chapter 2 with the remote sensing data information. Chapters 3-5 included research questions, approaches, and an interpretation of the results of each experiment to answer the overall objectives and specific questions. From 2016 to 2019, a forest investigation in the field was conducted. There are a total of 23 plots. Six plots were developed in August 2016, eleven in August 2017, and six in August 2018. These data provided information on the physical characteristics of each site, such as habitat type, species composition, disturbance evidence, and vegetation group structure. When doing analysis, these plot-level data are used to check forest cover style position on satellite imagery around protected areas—chapter 3 used six plots from 2016 to address the first question while chapter 5 used all the plots. Chapter 6 presented the general discussion and summarized the conclusions of Chapters 3-5 and addressed the broad questions of whether using remote sensing data can enhance forest cover change detection and whether such research can add value to park information for future management.

For a long term, long-time intervals of two-year-overlaid object-based segmentation classification using nearest neighbors (NNs) classification algorithm were developed using plot surveys and high-resolution photos as references to understand forest dynamics and forest successional stage path. The aim of Chapter 3 was to investigate the effects of disturbance and forest dynamics in the Reserve and surroundings. The chapter used two-year overlaid Landsat images from the Landsat 5 Thematic Mapper (TM) and the Landsat 8 Operational Land Imager (OLI) to produce forest-cover-change maps from 1988 to 1999, 1999 to 2010, and 2010 to 2016. I look at the course of forest successional stages to see how successful the protected area is at preventing fire and human-caused disturbances using vegetation indices. The vegetation

indices included the normalized burn ratio (NBR), the normalized difference vegetation index (NDVI), and the normalized difference water index (NDWI). The NDWI was used to distinguish between areas with and without water. The mean NBR and NDVI values were determined to assess the forest successional stages of fire, woodland regeneration, grassland, mixed forest, oak forest, and birch and larch trees. Land dimensions, field photos, and high-resolution photographs were used as sources to determine the accuracy. Overall, the classification results for all three maps are highly accurate more than 80% accuracy. The most disturbed period was from 2010 to 2016. The reserve was well-protected, with no human disturbances. During the period 1999–2010, however, large areas of burned area (137 km2) was discovered inside the Reserve. Burned areas also appeared in the buffer zone and outside of the reserve. Over the period 2010–2016, mixed disturbance rose to nearly 50 km2 in the buffer zone and outside the reserve. Future research could apply the two-year overlaid image technique in Chapter 3 to compare forest succession and disturbance within and outside the protected area in other ecosystem zones.

The chapter 4 analyzed disturbance types (forest fire, clearcutting for timber and agriculture and mixed disturbance) from Chapter 3 classification results, comparing with environmental factors and climatic factors. The elevation gradient, slope and aspect were obtained from digital elevation model (DEMs) of NASA Shuttle Radar Topographic Mission (SRTM). The study analyzed as patch-wise to calculate largeness and frequency of the disturbance area in different types. The MaxEnt model have been used to produce disturbance vulnerability maps. The climatic data of BIO1-BIO19 bioclimatic factors from Worldclim Version 2.0, averages for the years 1970-2020, were used together with environmental factors, as variable inputs. The results showed most of the disturbance occurrence follow the trend rarely occurred in larger patch size but very frequent in smaller patch size. Most of disturbance in all types have been occurring at the lower elevation, the area closer to the road and at the

narrower slope angle, with some exception of forest fire inside of the Reserve that found upon the high elevation and steeper slope angle. Some mixed disturbance was found high in elevation outside of the Reserve and steep slope in the buffer area. Most disturbances occurred in the easily accessible areas. The MaxEnt showed that several climatic factors might potentially influence how the disturbance were distributed around the Reserve, such as, temperature seasonality, annual precipitation, and annual mean temperature. The technique acquired essential information without vast field-based information gathering. The study provided vulnerable area information based on an open-source Landsat data and freely-analyzing software to understand the distribution of disturbances around protected area.

With substantial field investigation and more high-resolution and medium-resolution images, it helps me to use the data until major infrastructure was constructed in the late 1970s. The chapter employed object-based classification using nearest neighbors (NNs) classification algorithm similar to Chapter 3 to classify eleven single-year images (1975, 1988, 1993, 1996, 1999, 2001, 2005, 2010, 2014, 2016, 2019) and eleven time-series forest cover maps were generated. Then, I roughly estimated area changes of forest covers and disturbances. I proposed a change vector analysis (CVA) method to evaluate the change of stableness of forest cover and disturbance classes in the inside, buffer, and outside zones of the Reserve by using spectral characteristics based on vegetation indices: the NDVI and NBR. Because there was neither a SWIR band nor an additional NIR band in the Landsat 2 MSS, the study excluded 1975 for the NDVI and NBR vegetation index analysis. The vegetation index was calculated pixel-wise. The average index value of pixels representing each class were compare between years. Mixed disturbance and forest fire showed a significant increasing trend while grassland showed the opposite trend. The disturbance classes showed large change magnitude of change (S) or stableness between pre-and post- period compared with the forest classes. The classes inside the Reserve contain smaller change of stableness between pre- and post- period, indicating that

the inside of the Reserve is effective in term of preventing human disturbance and maintaining the forest area from the past to present.

The thesis results showed that the overall objective and specific questions were mostly accomplished using remote sensing data. Such tools are very essential to detect forest fire and forest cover changes around the Reserve's protected area. The large and remote spatial extents only allowed remote sensing as feasible method to observed forest dynamics from a far. By applying object-based segmentation classification method using long-time interval classification technique or single year technique could provide details of forest cover change and disturbance in more meaningful way.

Even though the Reserve is very well protected, there is no guarantee that the forest cover and disturbance patterns around the reserve will not affect forest dynamics inside the reserve. If there are more frequent massive burning, the reserve will face difficulty in maintaining its biological diversity and ecological function. There is an urgent need of multi spatial-scale study of how forest fire behaved in recent time. The frequency, intensity, and severity data will enrich more knowledge of susceptible area. Unexpected climate events could cause severe damage to boreal forest, thus more understanding about the impacts of forest fires and human disturbance is needed to establish better management for preserving biological diversity and ecological resources. The study provides supporting evidence of forest fires in remote protected area. I recommend that future studies to apply knowledge from the thesis to other protected areas, so that we can understand the effectiveness of forest conservation there as well.

Table of Contents

List of Figures

List of Tables

Assessing Impacts of Climate Change and Human Disturbance on Forests in the Protected Area of Russian Far East using Remote Sensing Data

Chapter I

Introduction

1.1 Background

1.1.1 Boreal forest and forest fire in the Russian Far East

The Russian Far East contains one of the most extensive intact boreal forests on earth (Potapov et al., 2008b). This biome offers various ecosystem services, including mitigating the global climate (Melillo et al., 1993). A large area of this northern hemisphere is less likely to be explored, preserving unique permafrost forest ecosystem that most plant species and permafrost soil depend on fire, protecting wildlife habitats and biodiversity from human activities (Sofronov and Volokitina, 2010). This area is considered a reservoir that controls the flux of water and CO_2, exchanges gas for many living organisms (Kasischke and Stocks, 2000; Sellers et al., 1995). The boreal forest consists of fire-resisted species such as oaks, aspens, larch, spruce, and even some grasses. This species-rich community depends on a forest fire to be able to regenerate its offspring and restore its successional stages from grass, lower shrub vegetation, to a deciduous tree and replaced by confers at a later stage (Chistyakova and Leonova, 2003; Jasinski and Angelstam, 2002; Kämpf et al., 2016; Marozas et al., 2007).

The region faces numerous issues during the modern era, including illegal logging, increasing returning massive fire, and climate change (Shuman et al., 2017; Wu et al., 2018). The evidence of growing population and urban expansion is seen in the higher demand for timber harvesting in young forests, creating depletion in carbon stocks over the last several decades (Goodale et al., 2002; Uotila et al., 2002). The changing climate is also another driver, challenging the weather during the millennium era that to be hardly predicted and the

consequences of an extreme climatic condition such as the high intensity of forest fire from June to August to be more severed (Conard et al., 2002; Damoah et al., 2004; Feurdean et al., 2020; Stocks et al., 1998). The estimate of forest loss and the impact of dramatic events is still complicated and not fully understand. It raises awareness within the scientific community to find the solution for future management practices.

The boreal forest serves as an essential role in keeping earth's climate; however, many areas are still empty and unoccupied by humans, making it susceptibility to infrastructure, wildfire, and other human activities. The potential of massive tree die-off and the decreasing forest sequestration areas is expected, resulting in a release of CO_2 to the atmosphere and the possibility of air pollution (Conard and A. Ivanova, 1997; Potapov et al., 2017). The effects of natural devastation and human impacts are still underestimated (Bondur et al., 2019). The warmer climate increase vegetation shifts toward higher latitude or move upward higher elevation and outcompete several rare species (Shuman et al., 2011; Soja et al., 2007).

There is the need of monitoring forest fire in the boreal forest to estimate the unfavorable condition that could depreciate plant development and the causes which influence massive fire in order to maximize the survival rate of the young population within the community (Feurdean et al., 2020; Shvetsov et al., 2019; Suleymanova et al., 2019). The young and mature forest are crucial roles in maintaining carbon flux within the community after forest fire, especially larch species that contain most gas exchanges (Chen et al., 2016; Goetz et al., 2007; Shuman et al., 2017). Larch and birch forest dominated Siberian, expanding its range from low to high altitude (Chen et al., 2017). The forest community contains regrowth and resilience to its successional stage after significant fire disturbance, making it the most resistant group of forest in the region to succeed and outcompete other species in the past decades (Chen et al., 2016). However, the potential of warming climate leads to more frequent extreme fire

effects and magnificent loss of the forest community (Chen et al., 2018; Kharuk et al., 2016, 2011).

In recent decades, climate change led to uncertainty of fire frequency and magnitude in this region, unable to predict the impacts of an upcoming catastrophe or even underestimate the aptitude of the fire effects (Kukavskaya et al., 2013; Stocks et al., 1998). The loss of dominant forest in the Russian Far East enhances radiation balance alternation, losing its strange to hold soil moisture, creating positive feedback loops that magnify the next summer fire (Amiro et al., 2006; Betts, 2000; Soja et al., 2007). Several studies point out that increasing magnitude of forest fire severity across boreal region emitted a large amount of carbon and affect species composition and structure, which could make climate susceptible; or, in worst-case scenarios, could collapse the entire ecosystem (Bonan et al., 1992; Conard and A. Ivanova, 1997; de Groot et al., 2013; Randerson et al., 2006). Thus, monitoring climate impact and potential causes of disturbances in this region provide a solution to the scientific community to avoid devastating effects from climate change.

1.1.2 Effectiveness of Protected Areas in Russia

The Russian Federation has a unique geographical landscape, expanding from far west Eurasia to the Russian Far East (Potapov et al., 2008b). This largest territory has its independent governing system in terms of the protected area. Due to the large area and disappearance of existing humans, many forest areas are still untouched. This region has become a high interest in the scientific community after the more frequent forest fire in recent decades has been found to have connections with anthropogenic activities (Gromtsev and Petrov, 2014). The protected area showed significant importance in the ecosystem, controlling temperature within its region, and also develop the growth of forest community, creating wildlife habitats and protection to some species to take advantage of the development of the successional stage, and also changing climate direction (Zyryanova et al., 2010). The natural resources had been extensively used,

more than the forest's protection status available for its use, around 26% of the Russian natural reserves have been located in the Russian Far East (Kondrashov, 2004). The protection status postponed or delayed the opportunity of upcoming human-related disturbance activity; some highly restricted area even benefits from its resource use. Three categories of protected areas in Russia served to be important ecological areas cover many large intact remote areas across the regions; Zapovednik, national parks, and federal zakazniks (Degteva et al., 2015; Kondrashov, 2004). The level of strictness is high to low accordingly. With Zapovednik to be the prohibited areas of all uses, national parks allow some recreational activity that follows national policy, and the least restricted multiple-uses federal zakazniks allow several activities set by the regionals. After the Soviet collapse, the disturbances were sharply decreased in the highly protected area compared to the other two types, indicating the high effectiveness of protected areas (Wendland et al., 2015).

The protected area's role was found to avoid forest canopy and stabilizing landscape from human activity that intensified forest use, resulting in a drastic change of forest landscape (Bragina et al., 2015). Several studies found significant positivity of having forest areas protected. After intensified land use for agricultural farming in 1988 and abandoned after 1991, Oksky and Mordovsky State Nature Reserve have been regrowth its forest (Sieber et al., 2013). The area contained fewer disturbances compared to the outside of the protected area. This land-cover change represented conservation planning success that protected biodiversity and stabilized the landscape (Norton, 1996; Tishkov et al., 2020). Many forest areas have long been exposed to a forest fire in the ecological cycle, thus, protecting this area allowed the forest community to adapt and restore to its original state after post-fire (Ostroukhov et al., 2020)

The protection areas serve as a control location for a research experiment that allows an analyst to take advantage in measuring tree cover loss, wildlife habitat vulnerability, fire effect, and disturbance behavior in the future, such that they can mitigate and set a standard

way of conservation practices and management to avoid high severity damage from anthropogenic activities (Marcot et al., 1997; Volokitina et al., 2019; Wade et al., 2020). Even though that protected area in Russia is still well effective after the post-Soviet era, illegal and unregulated resource harvest are still concerned due to the lack of information and difficulty accessing many remote territories (Newell and Henry, 2016). The expansion of infrastructure and human habitats increased the risk of reconstructing the protection policy that could pose the forest community (Fiorino and Ostergren, 2011). Russia included many last intact forests of the world, the need for conservation priority depended on the region's management and development strategies. The protected areas' effectiveness needs to be determined to avoid future threats and unpredicted consequences (Scullion et al., 2019).

1.1.3 The Use of Remote Sensing in the Russian Far East

The Russian Far East covers vast areas from the eastern Siberia to the Pacific Ocean. The majority of the region is inaccessible, creating difficulty for scientists to obtain ground information (Potapov et al., 2008b, 2017). To understand the landscape structure and the environment changes, including forest conditions, the most practical ways to receive information from this region are remote sensing techniques (Gaston, 1997; Potapov et al., 2008b). Using remote sensing data to monitor and observe the change of forest and disturbance on the landscape provide essential information to guide scientists to solve global climate issues (Cohen and Goward, 2004; Coppin et al., 2004; Kerr and Ostrovsky, 2003; Turner et al., 2003). Many organizations used satellite data to monitor global change; including The European Space Agency (ESA), The European Commission (EC), Food, and Agriculture Organization of the United Nations (FAO), The National Aeronautics and Space Administration of the United States (NASA), and The Japan Aerospace Exploration Agency (JAXA). Many of the programs focused on forested and non-forested areas and how they changed corresponding to each driver. Several studies set experiments and observe forest cover change in the field;

however, the studies of protected area in the Russian Far East is still limited (Chen et al., 2016; Potapov et al., 2008b). In the past decades, many researchers lack interests due to difficulty accessing those regions and limited access to technology such as satellite data (Potapov et al., 2008b). So, the forest dynamics and fire-dependent ecosystem information are hardly found nor understood in the literature (Chen et al., 2016; Dubinin et al., 2010; Potapov et al., 2011).

In recent years, modern technology and high cloud storage capacity allow scientists to utilize the open-accessed remote sensing data (e.g., Landsat) and various software available on the online platform (Potapov et al., 2008b; Song et al., 2001; Turner et al., 2003). The availability of high-resolution images from several websites also gave opportunities for researchers to detect and confirm forest cover change and disturbance areas that may have been easily observed in the open-access data (Hansen et al., 2013). After 2000, satellite observation provided a deeper understanding of Siberian larch forest dynamics that the growing of young forested areas associated with large fire events (Chen et al., 2016; Kharuk et al., 2010). An increasing trend of forest loss was detected in the Russian Far East compared to other regions using the normalized difference vegetation index (NDVI), an index detecting the health of vegetation growth on satellite images for 30-meter spatial resolution (Hansen et al., 2013). These open-accessed images can be obtained from The United States Geological Survey (USGS) website, a survey conducted by the United States government's agency to monitor natural hazards, trends of landscape change around the worlds, and environmental issues that cover all scope of academic disciplines (Chander et al., 2009).

This study focused on forest cover change in the protected area in the Russian Far East. Adapting this advanced technology can estimate the number of trees affected by fire in different timing and model the distribution of future forest types on the different landscapes (Krylov et al., 2014). (Potapov et al., 2017) is another mega-study that used Landsat-based imagery to monitor forest loss in the Russian Federation from 1990 to 2005 to monitor forest change

related to political power transition. A dramatic increment of annual forest fire was found to be ranged from 33 to 73 thousand hectares per year during 1990 and 2005. The situation of forest fire in the Russian Far East by (Chen et al., 2016) also agreed there were massive burned areas, accounting for more than 8,000 km^2 annually during the past 24 years. The most affected forest to the massive fire included birch and larch forests. Using available Landsat Multispectral Scanner (MSS) imagery of post-2000 using spectral characteristics of forest stand ages to produce a comprehensive assessment of the pre-2000 "wall-to-wall" stand age distribution map of Siberian larch forest. For the Russian Far East region, (Loboda et al., 2012) studied the change of land cover regarding forest fire in the Russian Far East using Landsat image between 1972-2002; they found an expansion of burn area expanding from cropland, grassland, to the extent of sizeable mature forest land, and the surprising annual burn of around 520,000 ha on average between 2001-2005. The pattern of forest disturbance history and the accuracy of reliability in remote regions are still not fully available and hardly achieved across the region because Landsat data's spectral characteristics still limit. The study of (Shishov and Vaganov, 2010) found the use of NDVI trend and temperature change associated with Russia's vegetation growth rate. Some studies also found human activity associated with the increasing forest fire in the Russian Far East. A significant decrease of the young forest from intensifying harvesting appeared nearby forest fire area and nearby village on the satellite images (Hitztaler and Bergen, 2013). This result showed interest in this research to study further the areas where previous studies have not covered. Remote sensing data increased the detectability of forest cover change and disturbances in remote areas (Chen et al., 2016; García and Caselles, 1991; Loboda et al., 2012; Potapov et al., 2008b). This provides sufficient data for scientists to improve forest management and policy and accuracy to predict forest conversion, forest fire, logging, post-disturbance succession along with other potential data without endangering themselves (Krylov et al., 2014).

1.2 Objectives of the study

Many previous studies provide useful information for researchers to conduct research experiments in the Russian Far East using remote sensing data such as satellite imagery, creating a target for conservation planning and forestry management. However, the application of remote sensing techniques is limited to only the area where the location is easily accessible or having enough advanced technology to produce such kinds of data. Many areas that contain high interests of research are found to locate nearby human settlements or contain tremendous amounts of high-quality image data. There is still limited information on forest cover change in areas where specific transportation types and limited time can access fewer human settlements and farther places. After intensive literature review, I found that the research in the protected area in the Russian Far East were very few and lacks of information on forest cover changes. Most literature were produced in Russian-language basis, yet still quite a few. The historical information on disturbances were still rare, especially clearcutting and forest fire in areas located in a very remote region. Most of the literature monitored forest fire in the very broad study area which may overlook the local scale forest dynamics. With so much land and a few humans inhabited in the remote area in the Russian Far East, the effectiveness of the protected area in this region has not been well studied. The overall objective of this thesis is to analyze forest cover change around protected area in The Russian Far East and monitor an effectiveness of protected area using remote sensing data. This thesis provided an understanding of forest dynamics around remote protected area and evaluate whether or not the protected area can achieve protecting its environment from experiencing various threats and preserve forest stability. I found three research questions that needed to be answered to generate more useful knowledge for scientists, particularly those interested in exploring remote regions that are challenging to conduct experiments and may be difficult to access or obtain ground information: 1) If the areas did not have frequent image data available, how can we monitor

forest cover change and disturbances and effectiveness of protected area by using long-time interval satellite image analysis? 2) How did disturbances distribute around the protected area in relation to environmental and climatic factors? 3) After new images available that allow this research to conduct single image classification, how did forest and disturbance covers change around protected area and can we monitor the stableness of the forest and disturbance covers around protected area based on vegetation indices using short-time interval satellite image analysis? Resolving these mysterious questions helped the environmentalist community find a way to overcome hardness in the research planning and discover the ecological structure and forest dynamics related to climate and human activities—this research question developed strategies for conservationists and ecologists to develop a better forest conservation planning and management.

The first question was set to explore the different methods that could not be achieved when data availability is rare. Ecologists often overlook the remote areas because of its inaccessibility and inability to obtain satellite images because the summer season in this study is limited to only a few months (Potapov et al., 2008a). The other season contained much of high snow on the mountainous region and some other high latitude places, closing the satellite's possibility to capture high-quality ground information (Schroeder et al., 2011). Thus, few images are available for the research to use. During the master thesis (Khatancharoen, 2017), a previous study found that using single image classification diminishes the classes' stability, producing a lower accuracy for the forest cover interpretation. The use of a two-year overlaid image completed with higher accuracy and producing a promising result on forest cover change. For the first part, this Ph.D. thesis continues to use two-year-overlaid images classification results to analyze the distribution of forest cover change and disturbance around a protected area in the Russian Far East. Additionally, the analysis included the forest successional stage to see the effectiveness of the protected area. This question contributed to

the importance of park protection status compared to unprotected surroundings, highlighted the points of achievement in conservation and management, and raised concerns of endangering in other hotspot areas that might be vulnerable if no protection plan for the future (Elbakidze et al., 2013). The analysis of Long-time interval satellite image tackled down the existing problem when there were limited satellite images available in the study area. It also provided an alternative way of assess forest cover change and disturbances and monitor the effectiveness of the protected area.

The forest cover change classification results allow further usage to help understand the dynamics of the forest. However, few studies have explored the dynamics through the environmental factors. This study provided the first in-depth information data of forest cover changes related to environmental factors, including climatic factors, to show the different effects of different factors and different effects on both inside and outside of the protected area. The second question of this thesis is to focus on how did disturbances spread throughout the region based on environmental factors elevation, slope, aspect, distance to the nearest road) and climatic data (min. and max. temp., precipitation, etc.) This analysis gave an essential understanding of the environmental impacts and the scale of different effects, proving the impacts from anthropogenic activity (Loranty et al., 2016). The study provided essential information based on the distribution of the disturbances to cope with the existing problem that lacked knowledge of climatic and environmental factor information. The distribution of those factors allowed researchers to gain knowledge of the location of disturbances and whether or not the protected area was effective at preventing the disturbances. The assessment of climate and environmental impacts on disturbances can help researcher find a solution to reduce the risk of reoccurrence of unexpected consequences in the future (Conard et al., 2002).

Even though understanding the effect of environment on forest cover change can be essential in the research community, measuring impact is another exciting research that needs

to be comprehended. Research on the magnitude of forest loss or recovery and disturbance effects was seldom in the Russian Far East (Zyryanova et al., 2010). This thesis touched on the third question that gained more knowledge of how forest covers and disturbances change in frequent time series analysis of satellite data. This thesis was not only the first study to undertake analysis on forest cover change and disturbances around the study area but also compare variation of vegetation index values between inside and outside of the protected area to evaluate the stableness of the forest and disturbance cover inside, buffer, and outside of the Reserve. The analysis upscale the scope of the use of remote sensing to be more applicable to other researchers. The data on vegetation indices around the protected area helped researchers understand the different effects in each conservation zone of the protected area, such that they can improve conservation management and planning to protect biodiversity and forest community structure (Biswal et al., 2013).

Lastly, this thesis comprises several research questions to gain in-depth knowledge and understanding of forest structure in the remote ecosystem (Norton, 1996). The Russian Far East information is quite rare and often misunderstood because fewer humans neither exploring nor conducting research in this area (Gaston, 1997; Kondrashov, 2004; Loboda et al., 2012). Most of the research based on remote sensing in the Russian Far East only provided rough information on changes in landscape over time and how forest fire had spread across regions, but not how the effectiveness of the specific remote protected area was accomplished due to the difficulty in ground investigation (Turner et al., 2003). This thesis provided an alternative way to obtain rigorous information on forest cover change and historical disturbance effects to understand the role of protected area in forest conservation without endangering and intensive ground surveying on extensive remote area (Cohen and Goward, 2004). Thus, this thesis enabled researchers to understand the health of the forest and expand their ideas on how to develop the solution for future climate change and human disturbance activities.

1.3 Organization of thesis chapters

The thesis contained introduction, study areas, research experiments, and discussion chapters, as summarized in the study design (figure 1.1). The research background and general aim, and three specific objectives have been discussed in Chapter 1. The study area introduced in Chapter 2 guided the importance of the location in terms of biodiversity, protection status, and ecosystem benefits. Chapter 3-5 provided research questions, methods, and analysis of each study's findings. Forest investigation took place from 2016 to 2019. The total plot numbers are 23 plots. 6 plots established in August 2016, 11 plots in August 2017, and 6 plots in August 2018. These data provided information on each location's physical attributes, including forest type, species diversity, disturbance evidence, and vegetation community structure. These plot-level data are used to verify forest cover type location on satellite images around protected areas when conducting research—chapter 3 used six plots from 2016 to answer the first question.

Long-time intervals of two-year-overlaid image classification maps were produced using plots survey and high-resolution images as references to understand forest dynamics and forest successional stage direction for a long time. This chapter also analyzed the significant importance of park protection status and whether the protection's effectiveness can be seen in this area. Chapter 4 used the previous chapter's classification maps to analyze the forest cover change trend around the protected area. The relationships between forest cover change, and each environmental factor were compared. The inside and outside of the protected area were compared. The major environmental factors and climatic data were used to model and identify each factor's contribution to the forest cover change. The predicted climatic data were also used to estimate forest cover's vulnerability level in different climate scenarios. The new remote sensing data were uploaded on the archive at the end of 2018 and 2019, allowing the

thesis to obtain more image data to classify more frequent single images—chapter 5 hence used several more high-quality images to produce forest cover classification maps.

Along with substantial field investigation and more high-resolution data available, this allows me to use such data to analyzed forest cover patterns before human mega-infrastructure had been built in 1975 and after the construction has been finished. The chapter analyzed each forest cover class's change and identified the different spectral characteristics in each year's image. Chapter 6 summarized the findings of Chapter 3-5 and answered the whole scope questions whether using remote sensing data can improve forest cover change detection and whether such analysis can gain values and attain some importance of the park management in the remote area. This chapter also included the limitation and recommendation of future research to tackle future challenges and other difficulties.

Figure 1.1. Study Design of the thesis

Chapter II

Study Area and Data

2.1 Study Area Information

Zeysky State Nature Reserve (Зейский заповедник) or "Zeysky Zapovednik" (hereafter "the Reserve") located 13km. north of Zeya city, in the Zeysky District of Amur oblast in East Russia. The region of study area covered the entire protected area and some areas outside the Reserve. UTM coordinates of image extents were 345,105 to 403,695 Easting and 5,959,755 to 6,025,965 Northing, total area 3,881.78 km^2. The datum is World Geodetic System 1984 (WGS84). I selected this study region because the Reserve placed in the northern hemisphere in the eastern region of Russia (Figure 2.1). The Reserve is located at a number of boundaries, including the southern limit of Taiga and the longitudinal divide between oceanic (Pacific) and continental (east Siberian) climates and biomes. The ecosystems adjacent to such boundaries will be particularly vulnerable to climate change and subsequent changes in forest fire regimes. The Reserve is already facing more frequent burning inside the Reserve and illegal clearcutting area around the edge of the Reserve in the past decades. Extreme impacts from human disturbances degrade forest development and ecological processes, affecting forest cover transitioning over time. Tracking forest disturbance and forest cover transition is therefore essential to protect its natural complexity, biological diversity, and ecological role.

The Reserve was established on October 3rd, 1963, with a total area of 99,390 hectares and located in the north of the Amur River in the eastern end of the Tukuringra Ridge, a part of the four mountain ridges, Yankan-Tukuringra-Soktakhan-Djagdy ridge. The elevation of the Reserve was categorized into four levels: 40% of the area has an elevation of up to 700 m a.s.l., 35% for 700-1,000 m a.s.l., 18% for 1,000-1,300 m a.s.l., and 7% for over 1,300 m a.s.l. The largest rivers located in the state reserve are Motovaya River (length of 27 km) and Bolshaya

Garmakan River (length of 20 km). The area contained more than two hundred small rivers and streams that supply water to nearby and Zeya reservoirs.

Winds prevail in the north and northeast direction during winter and autumn and in the south and southeast direction in spring and summer. The state in which the cold and dry spring, followed by the wet hot summer, leads to the slow mineralization phase of dead organic matter, resulting in the formation of coarse humus. In January, the average temperature is around -28.8 ° C, and in July, during the summer, the average temperature is around +19.7 ° C. The mean annual precipitation is 515.2 mm (Naprasnikov et al. 1983). Up to 75 percent of northeastern wind speed range from 1.2 to 2.2 m/s (Ministry of Natural Resources of the Russian Federation. 2011).

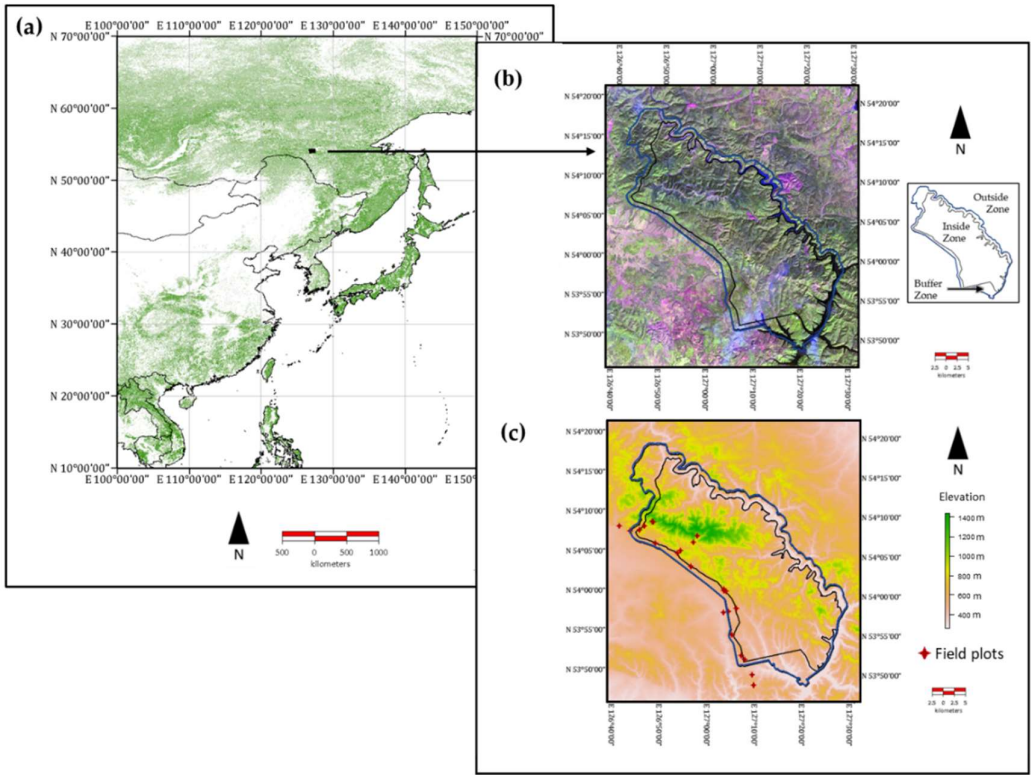

Figure 2.1. The study area and field plots established at Zeya State Nature Reserve. (**a**) The normalized different vegetation index (NDVI) distribution map of East Asia. (**b**) Zeya State Nature Reserve. (**c**) The study area elevation (m) and field plots.

Due to high acidity and low biological activity in the soils, soils in the Zeya State Nature Reserve do not favor vegetation growth. The mountains in the Reserve are primarily formed by many large peaks (area of more than 3 hectares), many large saddles (more than 3 hectares) and variable slopes from shallow (steepness 5-7 °), gently sloping (steepness up to 14-16 °) to very steep (up to 40 °). More than two hundred small rivers and streams in the reserve. In the winter, the water freezes to the bottom. In summer, though, water flows quicker in steep valleys; high water levels often increase as glacier melts or rains.

The river valleys act as pathways for animals to migrate to the Amur area from the southern Amur Basin. The fauna is more prosperous in the Zeya State Nature Reserve than in any other reserve in the Russian Far East. The 240 species represent birds. The most numerous and prevalent in this region is the hazel grouse (*Tetrastes bonasia*). You will find the Western Capercaillie (*Tetrao urogallus*) in the Reserve. Two species of partridge inhabit the ponds of the Tukuringra Range, grey partridge (*Perdix perdix*) and snow partridge (*Lerwa lerwa)*. The most endemic and rare bird is the dikusha, black grouse (*Tetrao tetrix*). This species is listed in the Red Book of the IUCN.

In the state reserve, 47 species of mammals are found. There are very few populations of ungulates in the Tukuring River Range. Occasionally, the boars (*Sus scrofa*) migrate up to the northern valley of Zeya and come down to breed in the valleys south of Zeya. The Siberian musk deer (*Moschus moschiferus*) is present in several places at the upper part of the mountain tundra belt at many sites. In the Reserve, the most impressive species are the Manchurian wapiti (*C. c. xanthopygus*), the roe deer (*C. capreolus*), Manchurian wapiti (*C. c. xanthopygus*), the roe deer (*C. capreolus),* and the moose (*Alces alces*). The Wapitis of Manchuria are primarily found in the Manchu fauna area. For their scrambling, they favor river valleys and slopes in the lower part of the forest belt. In the southern section of the Reserve, roe deer are evenly spread and can be seen only in the summer. The southeastern tip of the Reserve is restricted to

the wintering roe deer. For the Tukuringra Range foothills, two distinct subspecies of moose are found: The East Siberian moose (*A. alces cameloides*) or Kolyma moose (*A. alces buturlini*) and the Western Siberian moose or Ussuri Moose. The Altai elk (*C. c. sibiricus)* is found throughout the Reserve; however, they are mostly seen in the river valleys. They visit the mountain tundra in summer, because of the forage available. The stoat (Mustela erminea) and the sable (*Martes zibellina*) are abundant. The Siberian tiger (*Panthera tigris altaica*) sometimes shows up in the Reserve and leaves its footprint along the trails. The permanent inhabitant species of the Reserve is the gray wolf (*Canis lupus lupus*). These animals prefer river valleys. The East Siberian brown bear (*Ursus arctos collaris*) is found in all high-altitude belts. For invertebrate species, about 2000 species were recorded in 2014. These included Equilateral Crayfish, horsetails, Caddisflies, flies, beetles, sawflies, wasps, bees, ants, etc. Two species of insects are listed in the Red Book of the Russian Federation: Longhorn beetles (*Callipogon relictus)* and Northern Yellow Bumble Bee (*Bombus distinguendus*) and two endemic species of butterflies. A total of 23 species of cyclostomes and fish are found in Zeya District; two common species are the Siberian salmon (*Hucho taimen*) and Manchurian trout (*Brachymystax lenok*). The Amur pike (*Esox reichertii*) and roaches (*Rutilus lacustris)* are common in the Zeya reservoir. Simultaneously, in the rivers, the gudgeon (*Gobio gobio)* and Arctic charr (*Salvelinus alpinus*) are mostly found. The Zeya State Nature Reserve has also recorded 4 species of amphibians and 3 species of reptiles.

More than 90% of the land of the Reserve is covered with forests. Along the Zeya reservoir on well-warmed rocky slopes with an altitude between 350 and 500 m over sea level, oak and black walnut forests are prevalent. Mongolian oak, Chinese magnolia vine, Amur linden, Lesredets, Maximovitch are found under the canopy of pine and black birch woods. Above the pine and black birch forests are larch forests, which spread across the mountain in a variety of habitat and end up in the mountain tundra belt (1,000 m above sea level). Larch

forms together with all the birch flat-leaf, spruce and aspen. Vegetation located under the canopy of larch forests include cowberries, Ledum marsh, Rhododendron Daurian and green mosses. The mountain tundra belt of dark green coniferous woods is located at the altitudes of 1,000-1,300 m a.s.l. These woods were formed by Siberian spruce and Ayan spruce. Spruce is also located in the valleys of mountain rivers, and sometimes mixed with larch on the mountain slopes of northern exposures. Above the spruce forests (1,100-1,300 m a.s.l.), there are congregated of cedar pine tree. They frame the shirts of the Tukurings mountain range. They can be found together with Siberian Juniper, Golden Rhododendron, and Pallas mountain ash in certain areas. With an altitude of 1,100-1,142 m a.s.l.., three major biomorphs of tundra vegetation communities (i.e. lichens, shrubs and leaf-stalked mosses) are present. Along the river valley, willow and Chosenia-poplar woods are dispersed with Gmelin larch and birch. Other kinds of vegetation along the river valley are including five-leafed shrub, white syringe, purine reed, and sedge.

Meadow vegetation or grasslands are scattered in several areas such as forest fire disturbed area and floodplains. Marshes, however, occupy small area inside the Reserve. The lands at the Zeya State Nature Reserve are not favoring the plant growth because of high acidity and reduced biological activity in the soils. The mountain reliefs in the book are primarily formed by several enormous peaks (region of over 3 hectares), several enormous saddles (greater than 3 hectares), and variant slopes from shallow (steepness 5 -7 °), gently sloping (steepness around 14-16 °), into a very steep (up to 40 °)—over two hundreds of little rivers and lakes in the Reserve. In winter, the water trickle to the bottom.

The Reserve landscapes offered various ecosystems from mountain tundra vegetation on the highest altitude, lichen tundra, shrub tundra, moss tundra, and dwarf pine forest, cedar trees, fir trees, birch forests, larch forests, pine forests, oak forests, to the valley meadow. Human settlements and recreational activities are prohibited, only cabins and educational

activities approved by park rangers allowed. These ecosystems have been described and mapped by Dudov's Zeya State Nature Reserve vegetation (2018) and translated to English-language data to represent each forest cover type in this thesis (Table 2.1). Mountain tundra vegetation is dominated by dry heath alpine tundra species, such as *Vaccinium uliginosum* L., *Arctous alpina* (L.) Niedenzu, *Betula nana* L., and edge-surrounded by a Siberian dwarf (Makoto et al. 2016) Spruce species, *Picea ajanensis,* occurs in two elevation classes, high altitude on the mountain and river valleys. *Larix gmelinii and Betula divarivata* species occupy the majority of the area in the reserve and Amur regions. Grasses and willows are present in the river valleys and floodplains in lower elevation—*Querqus mongolica,* oak species present in the lower elevation near the Zeya reservoir, and the agricultural area.

There are 710 species of vascular plants in the Zeya State Nature Reserve. 28 species listed below are red-listed species of the International Union for Conservation of Nature (IUCN) (Table 2.2). 9 species are listed in the Red Data Book of Russia in 2008 (Table 2.3). This specific research site is full of biodiversity and well protected but lately become more vulnerable to anthropogenic threats, like fires and clear-cutting. It is crucial for forest conservation studies. The Reserve faces more regular massive burning and a sizable loggings area, particularly the buffer zone area. The extreme pressures from fires and loggings degrade forest resources and ecological functions, influencing forest cover change during time. Thus, to preserve its natural complexity, biological diversity, and ecological function, tracking forest disturbance and forest cover change is required.

Table 2.1. Major land cover types of Zeya District.

Abbrev. Name	Major land cover types	Physical Description
BURN	Burn area***	Forest disturbance by wildfire
CCTA	Clearcutting for timber or agricultural***	Forest disturbance by harvesting for timber and ranching
CCE	Clearcutting for electricity lines***	Forest disturbance by clearcutting to settle down electricity lines
MD	Mixed disturbance***	Forest disturbance by human-induced fire and harvesting at the same place
VGR	Vegetation recovery***	Vegetation recovery after disturbance
GRASS	Bogged larch forests in a wide valley and grassland	Muddy, wetland, willow, floodplain, grassland
MF	Mixed forests in a river valley	Larch mixed with Spruce, willow, grass
OBF	Oak - Daurian birch forests	*Querqus mongolica, Lespedeza bicolor*
BLF	Birch and larch forests	*Larix gmelinii, Betula platyphylla*
SFRV	Spruce forests in a river valley	*Picea ajanensis* (315-700 m a.s.l.) sparsely dispersed near stream
MSF	Mountain spruce forests	*Picea ajanensis* on steep slope (700-1300 m a.s.l.)
DPW	Dwarf pine woodland	*Pinus pumila, Betula lanata* (1100 - 1300 m a.s.l.)
MTV	Mountain tundra vegetation	shrub, sedge, lichen, moss (1100m a.s.l. or up)
TOWN	Settlement	Houses and airports
ROAD	Unpaved road	Roads or ways for transportation without pavement
ROCK	Stream bedrocks	River or Stream bedrocks where no water flows
WATER	Water	Water bodies (e.g. river, lake)

Table 2.2. Red-listed species of IUCN inhabited inside the Reserve.

Common Name (Scientific Name)	
Adlumia asiatica (*Adlumia asiatica* Ohwi)	Golden root (*Rhodiola rosea* L.)
A lady's-slipper orchid (*Cypripedium calceolus* L.)	Lupinaster Eximius (*Lupinaster eximius* (Steph. Ex Ser.) C.Presl),
The Large-flowered Cypripedium (*Cypripedium macranthon* Sw.)	Amur cortusa (*Cortusa amurensis* Fed.)
Red Garden Orchid (*Cypripedium ventricosum* (Sw.) Soó)	Yakutiya ladybells (*Adenophora jacutica* Fed.)
The spotted lady's slipper (*Cypripedium guttatum* Sw.)	Silver aleuritopteris (*Aleuritopteris argentea* (SF Gmel.) Fée)
The white adder's mouth (*Malaxis monophyllos* (L.) Sw.)	Carex conspissata (*Carex conspissata* V. Krecz.)
The hooded Neottianthe (*Neottianthe cucullata* (L.) Schlechter)	Lilium buschianum (*Lilium buschianu)*
The calypso orchid, (*Calypso bulbosa* (L.) Oakes)	The Coral Lily (*Lilium pumilum* Delile)
The ghost orchid (*Epipogium aphyllum* Sw.)	Japanese iris *(Iris laevigata* Fisch, et CA Mey)
Downy clematis *(Atragene macropetala (Ledeb.) Ledeb.)*	Woodland Peony (*Peony obovata Maxim.)*
Large bloom (*Delphinium grandiflorum* L.)	Yellow coralroot (*Corallorrhiza trifida* Chatel.)
Stinking Meadow-rue (*Thalictrum foetidum* L.)	*Hystrix komarovii* (*Hystrix komarovii* (Roshev.) Ohwi)
Meadow rue *(Thalictrum squarrosum* Steph.)	*Asplenium incisum* (*Asplenium incisum* Thunb.)
Five-flavor berry (*Schisandra chinensis* (Turcz.) Baill)	Wall-rue (*Asplenium ruta-muraria* L.).

Table 2.3. Species listed in the Red Data Book of Russia in 2008 inhabited inside the Reserve.

Common Name (Scientific Name)
Adenophora jacutica (*Adenophora jacutica* Fed.)
Golden root (*Rhodiola rosea* L.)
A lady's-slipper orchid (*Cypripedium calceolus* L.)
The Large-flowered Cypripedium (*Cypripedium macranthon* Sw.)
Red Garden Orchid (*Cypripedium ventricosum* (Sw.) Soó)
The hooded Neottianthe (*Neottianthe cucullata* (L.) Schlechter)
The calypso orchid, (*Calypso bulbosa* (L.) Oakes)
The ghost orchid (*Epipogium aphyllum* Sw.)
Woodland Peony (*Peony obovata Maxim.)*

2.2 Data

2.2.1 Field Data

My field visit was taken once in a year; each field investigation took at least 13 days (Figure 2.2; Appendix 1). The month to collect data was August in 2016, 2017, 2018, and 2019. For the field survey, 11 plots (NR1~NR11) located inside the Reserve, 6 plots in the buffer zone area (BZ1-BZ6), and 6 plots outside of the reserve area (ONR1-ONR6) (Table 2.4). Tree species, tree height and diameter at breast height (DBH) data were collected to identify the type of forest cover along with the disturbance intensity. *Larix gmelinii* and *Betula platyphylla* dominated most of the plots. The higher elevation plot was dominated by *Picea ajanensis.* The buffer zone and outside nature reserve plots, however, experienced forest fire and clear-cutting in the past in the meadow valley.

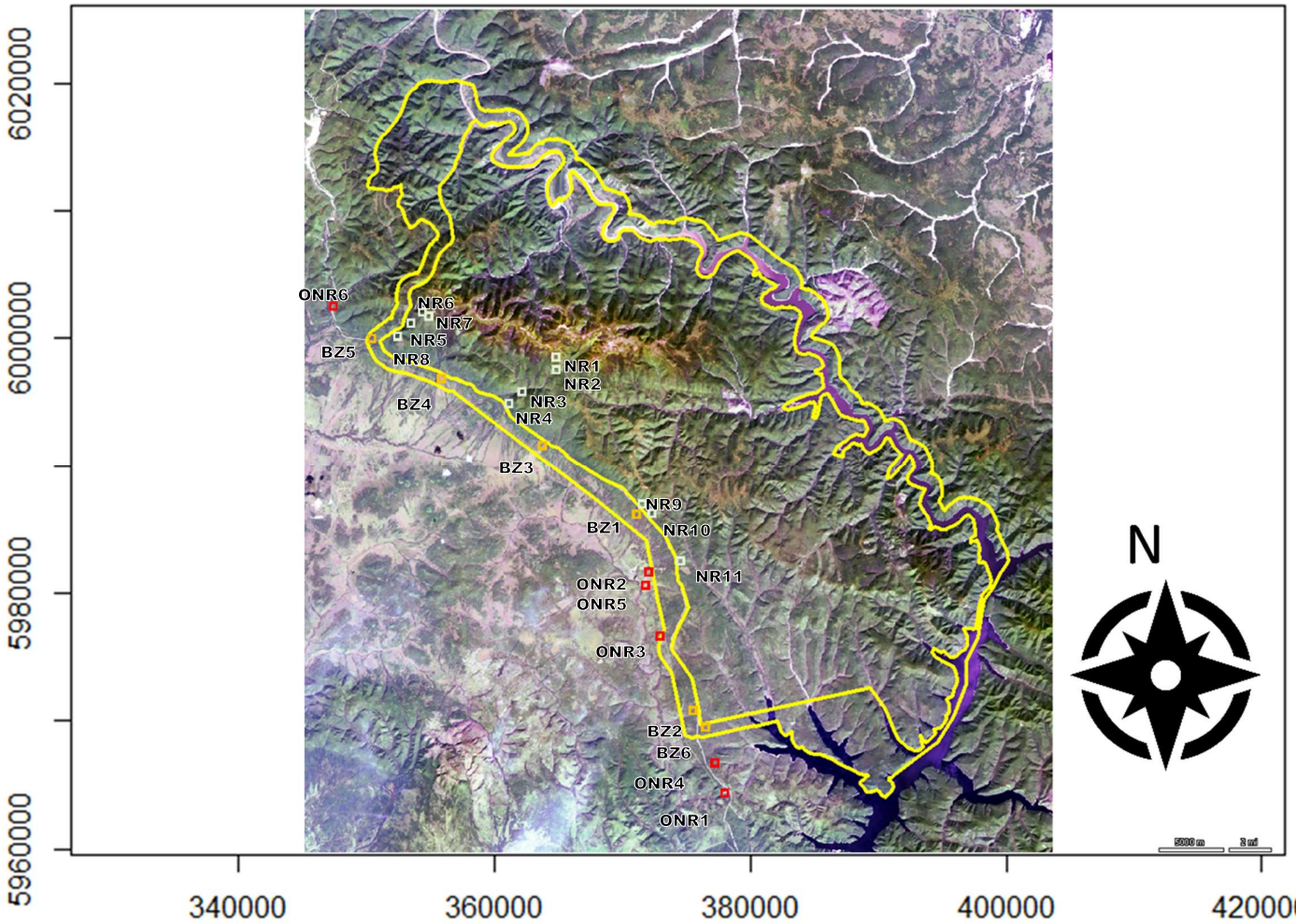

Figure 2.2. 23 Field survey plots; Light green box indicated inside the Reserve plots (NR1-NR11), orange box indicated plots in the buffer zone of the Reserve (BZ1-BZ6), and red box indicated outside the Reserve plots (ONR1-ONR6).

Table 2.4. Field Investigation Plots around the Reserve

Plot name	Date (mm/dd/yyyy)	Latitude	Longitude	Elevation (m)	Slope direction	Slope angle (Degree)	Dominant species (#of trees)	Average DBH of dominant species (cm)	Average height of dominant species (m)	Forest Fire Disturbance Intensity
NR1	8/6/2016	54.1218440	126.932333	1,305.40	195	12	*Picea ajanensis (18)*	21.1	11.2	N/A
NR2	8/7/2016	54.1083570	126.932428	853.04	192	5.5	*Larix gmelinii (13)*	17.5	14.8	N/A
NR3	8/8/2016	54.0913000	126.882125	626.02	335	1	*Larix gmelinii(29), Picea ajanensis (22)*	8.7, 6.3	9.4, 5.7	N/A
NR4	8/8/2016	54.0831370	126.874603	600.15	245	2	*Larix gmelinii (11)*	19.3	18.5	N/A
NR5	8/2/2017	54.1418611	126.758556	716.00	10.5	9.7	*Picea ajanensis (8)*	25.94	16.14	N/A
NR6	8/3/2017	54.1479444	126.779139	1065.00	53	9.4	*Picea ajanensis (26)*	14.18	11.67	N/A
NR7	8/3/2017	54.1473333	126.781278	1073.00	136	11.0	*Pinus pumila (10), Picea ajanensis (4), Larix gmelinii (5)*	3.71, 4.00, 6.39	2.68, 2.78, 4.83	N/A
NR8	8/4/2017	54.1315000	126.739833	622.00	112	4.1	*Betula platyphylla (13)*	14.59	16.54	N/A
NR9	8/5/2017	54.0135833	127.039083	594.00	26	7.7	*Betula platyphylla (5), Larix gmelinii (13)*	15.36, 11.71	17.41, 14.34	N/A
NR10	8/7/2017	54.0135833	127.039083	569.00	78	8.4	*Betula platyphylla (15)*	3.41	4.43	High
NR11	8/8/2017	54.0080555	127.047361	509.00	116	3.2	*Betula platyphylla (13), P. ajanensis (38)*	13.93, 2.18	12.38, 4.38	High
BZ1	8/10/2016	54.0119300	127.037063	555.61	198	34	*Betula platyphylla (36)*	2.5	3.6	High
BZ2	8/7/2017	53.8724722	127.109806	491.00	38	4.9	*Betula platyphylla (23)*	4.57	6.74	Medium
BZ3	8/1/2018	54.0578056	126.920083	545.91	135	1	*Larix gmelinii (12)*	10	9.4	Low
BZ4	8/2/2018	54.1035556	126.796111	561.05	207	2	*Betula platyphylla (4)*	8.2	3.8	Medium
BZ5	8/3/2018	54.1273056	126.704778	559.85	180	4	*Larix gmelinii (7)*	12.5	11.6	N/A
BZ6	8/5/2018	53.8680556	127.121556	458.19	165.5	4.4	*Larix gmelinii (14)*	8.5	11.1	N/A
ONR1	8/10/2016	53.8178850	127.150909	508.97	265	10.1	*Larix gmelinii (4)*	17.3	16.1	High
ONR2	8/5/2017	53.9668333	127.056333	455.00	0	0.0	*Larix gmelinii (4)*	26.36	16.67	High
ONR3	8/7/2017	53.9180556	127.073889	498.00	0	0.0	*Betula platyphylla (6), Larix gmelinii (16)*	10.39, 10.24	12.67, 11.07	High
ONR4	8/8/2017	53.8365556	127.146806	451.00	1	8.0	*Betula platyphylla (16)*	3.72	5.80	High
ONR5	8/1/2018	53.9619722	127.045139	409.40	135	1	*Larix gmelinii (6)*	22.5	16.5	Medium
ONR6	8/5/2018	54.1512778	126.661583	503.61	304	3	*Larix gmelini (7), Picea ajanensis (15)*	15.6, 5.4	18.7, 6.2	Low

2.2.2 Remote Sensing Data

2.2.2.1 Landsat Image Data

Satellite imageries become the advanced tools for scientists to detect the change of environment around the world. All imageries were acquired from the United States Geological Survey (USGS) Earth Resources Observation and Science (EROS) Data Center. The center contained the most comprehensive continuously collection of space-based moderate-resolution data that provide free-access to scientists and non-scientists in all academic disciplines ((USGS 2017) 2017). Landsat has enhanced the number of spectral bands and spatial resolution through time (Table 2.5). The images were downloaded from The USGS Global Visualization Viewer (GloVis) website (http://glovis.usgs.gov/) and USGS EearthExplorer website (https://earthexplorer.usgs.gov/).

Table 2.5. Landsat Satellite Band Designations (USGS 2017).

Landsat-8 OLI & TIRS Sensor (February 11, 2013 - Present)			
Band Number	Description	Wavelength	Resolution
Band 1	Coastal / Aerosol	0.433 to 0.453 µm	30 meter
Band 2	Visible blue	0.450 to 0.515 µm	30 meter
Band 3	Visible green	0.525 to 0.600 µm	30 meter
Band 4	Visible red	0.630 to 0.680 µm	30 meter
Band 5	Near-infrared (NIR)	0.845 to 0.885 µm	30 meter
Band 6	Short-wave infrared (SWIR1)	1.56 to 1.66 µm	30 meter
Band 7	Short-wave infrared (SWIR2)	2.10 to 2.30 µm	60 meter
Band 8	Panchromatic	0.50 to 0.68 µm	15 meter
Band 9	Cirrus	1.36 to 1.39 µm	30 meter
Band 10	Long wavelength infrared	10.3 to 11.3 µm	100 meter
Band 11	Long wavelength infrared	11.5 to 12.5 µm	100 meter
Operational Land Imager (OLI) generates 9 spectral bands (Band 1 to 9) and is onboard Landsat-8. OLI images can discriminates vegetation types, cultural features, biomass and vigor,etc. **Thermal Infrared Sensor (TIRS)** consists of 2 thermal bands with a spatial resolution of 100 meters. TIRS measures Earth's thermal energy particularly useful for tracking how land and water are being used.			

Table 2.5. Landsat Satellite Band Designations (Continued).

Landsat-5 Thematic Mapper (March 1, 1984 - June 5, 2013)			
Band Number	Description	Wavelength	Resolution
Band 1	Visible blue	0.45 to 0.52 µm	30 meter
Band 2	Visible green	0.52 to 0.60 µm	30 meter
Band 3	Visible red	0.63 to 0.69 µm	30 meter
Band 4	Near-infrared (NIR)	0.76 to 0.90 µm	30 meter
Band 5	Short-wave infrared (SWIR1)	1.55 to 1.75 µm	30 meter
Band 6	Thermal	10.4 to 12.3 µm	120 meter
Band 7	Short-wave infrared (SWIR2)	2.08 to 2.35 µm	30 meter
Thematic Mapper (TM) was a high-resolution scanner on Landsat satellites (Landsat 4 and 5). It collected images in visible, near infrared, mid infrared and thermal bands with a spatial resolution of 30 meters.			
Landsat-2 Multispectral Scanner System (January 22, 1975 - February 25, 1982)			
Band Number	Description	Wavelength	Resolution
Band 4	Near-infrared (NIR)	0.5 to 0.6 µm	60 meter
Band 5	Short-wave infrared (SWIR1)	0.6 to 0.7 µm	60 meter
Band 6	Thermal	0.7 to 0.8 µm	60 meter
Band 7	Mid-infrared (SWIR2)	0.8 to 1.1 µm	60 meter
Multispectral Scanner System (MSS) is line scanning systems perpendicular to the orbital track. An oscillating mirror performed cross-track scanning; for each mirror sweep, six lines were scanned simultaneously in each of the 4 spectral bands. The forward motion of the satellite provided the advancement of the scan line along the route.			

The high-quality Landsat images from 1975 to 2019 with less than 10% cloud during the growing season were selected (Tucker 1980; Tucker, Grant, and Dykstra 2004). Due to Scan Line Corrector (SLC) failure of Landsat ETM+ on May 31, 2003, most of the images after this date were discarded; after the screening process, the four most suitable images with appropriate time intervals from Landsat TM and OLI images (WRS2 path 120, row 22) were chosen at first for Chapter 3 and Chapter 4 (Table 2.6).

Table 2.6. List of processed 4 Landsat images used for Chapter 3 and Chapter 4

Path/Row	Date	Sensors	Band Combination for false color composite (R,G,B)
120/22	1988-09-23	Landsat 5 TM	B5, B4, B3
120/22	1999-08-21	Landsat 5 TM	B5, B4, B3
120/22	2010-09-04	Landsat 5 TM	B5, B4, B3
120/22	2016-08-19	Landsat 8 OLI	B6, B5, B4

During the end of 2018 and early 2019, USGS uploaded more images into the archive. I saw the potential to produce more in-depth research on analyzing spectral-values of forest covers and disturbance covers in Chapter 5. The more frequent-time resolution images (Table 2.7) including Landsat MSS image allowed me to evaluate the Reserve's effectiveness and understand disturbance history around the region and its effects from 1975 to 2019. All the Landsat images were extracted into study region as shown in Figure 2.3-2.13. The Shuttle Radar Topography Mission (SRTM) data available in Landsat Level 1 Terrain Corrected (L1T) product which has the resolution of 1 arc-second (approximately 30 meters) was downloaded from USGS Earth Explorer website for topographic correction. The SRTM were resampled using georeferenced of Landsat 8 OLI image to match 30-m resolution. The resampling method was nearest neighbor to cover the study area. Landsat 2 MSS image was also resampled using nearest neighbor method to have the same 30-m resolution as other Landsat images. For the rest of the images, the resolution remained 30m by 30m.

Table 2.7. List of processed 13 Landsat images used for Chapter 5

Path/Row	**Date**	**Sensors**	**Band Combination for false color composite (R,G,B)**
120/22	1975-07-13	Landsat 2 MSS	B5, B6, B4
120/22	1988-09-23	Landsat 5 TM	B5, B4, B3
120/22	1993-09-21	Landsat 5 TM	B5, B4, B3
120/22	1996-08-12	Landsat 5 TM	B5, B4, B3
120/22	1999-08-21	Landsat 5 TM	B5, B4, B3
120/22	2001-08-26	Landsat 5 TM	B5, B4, B3
120/22	2005-06-02	Landsat 5 TM	B5, B4, B3
120/22	2010-09-04	Landsat 5 TM	B5, B4, B3
120/22	2014-06-11	Landsat 5 TM	B5, B4, B3
120/22	2016-08-19	Landsat 8 OLI	B6, B5, B4
120/22	2019-08-28	Landsat 8 OLI	B6, B5, B4

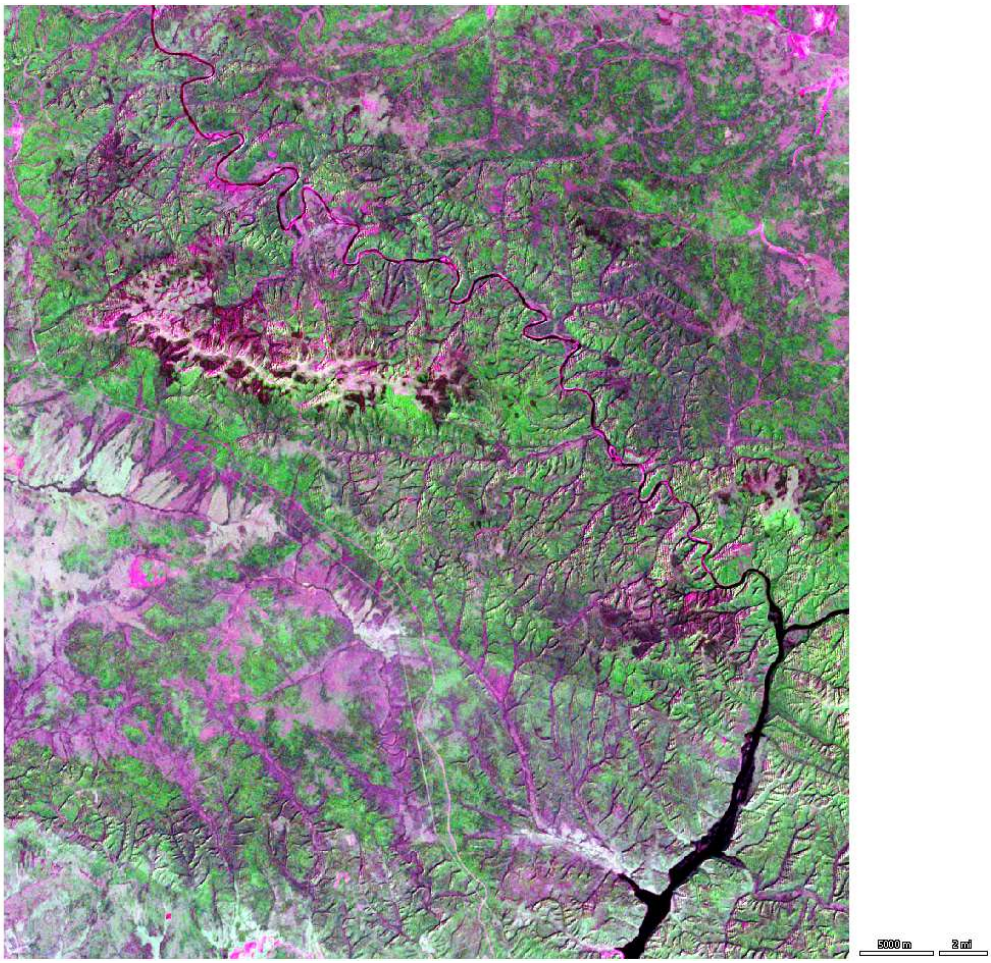

Figure 2.3. Landsat image of the Reserve dated 1975-07-13.

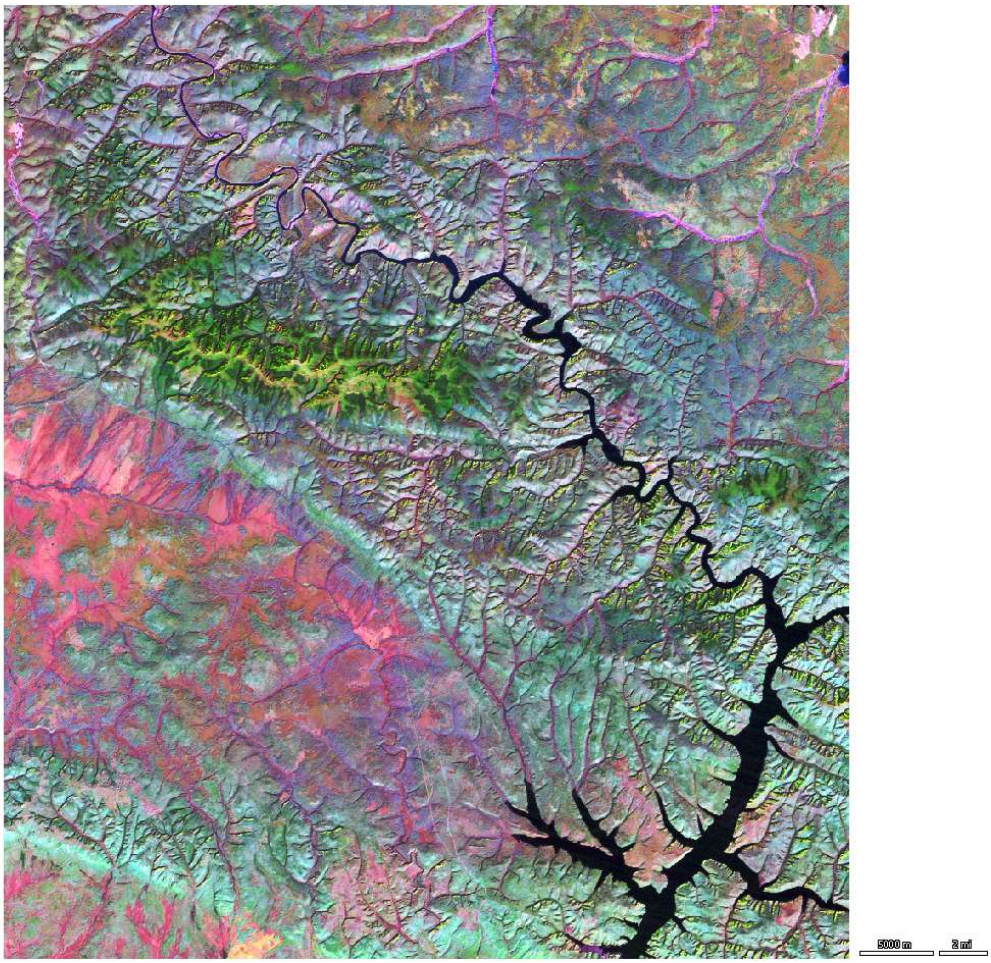

Figure 2.4. Landsat image of the Reserve dated 1988-09-23.

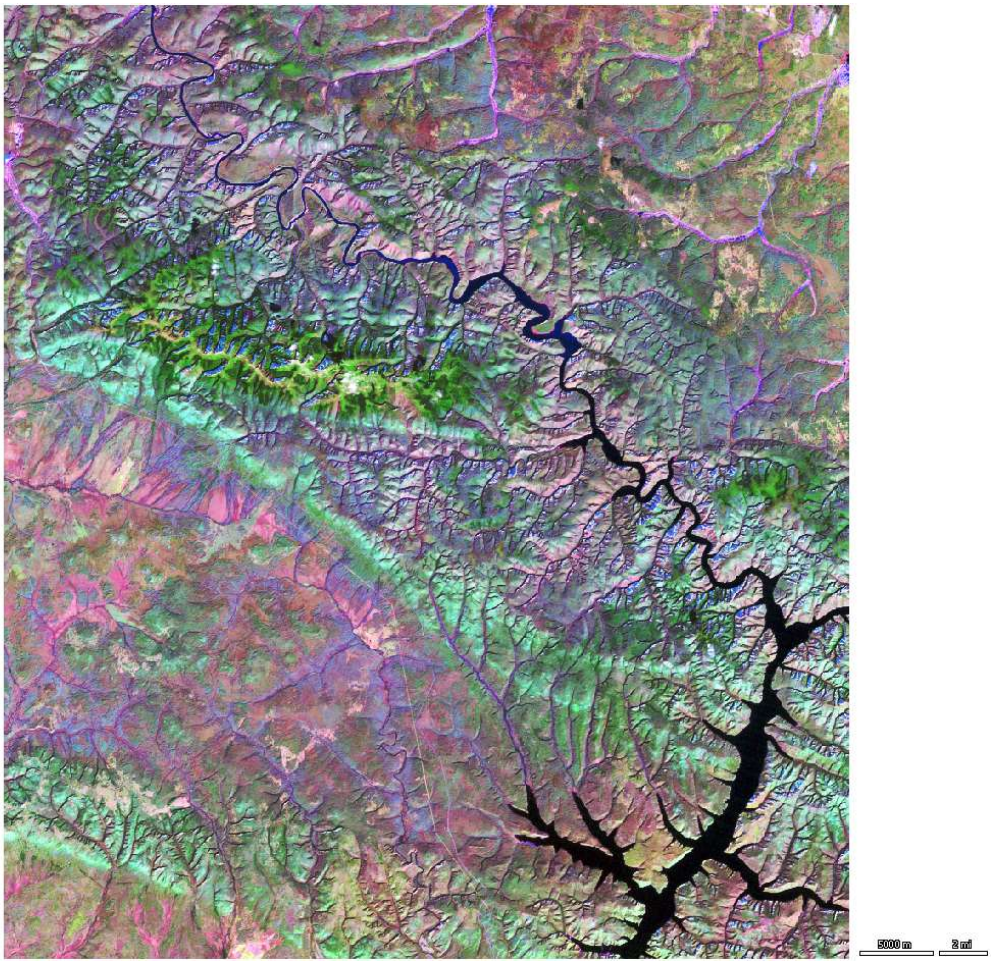

Figure 2.5. Landsat image of the Reserve dated 1993-09-21.

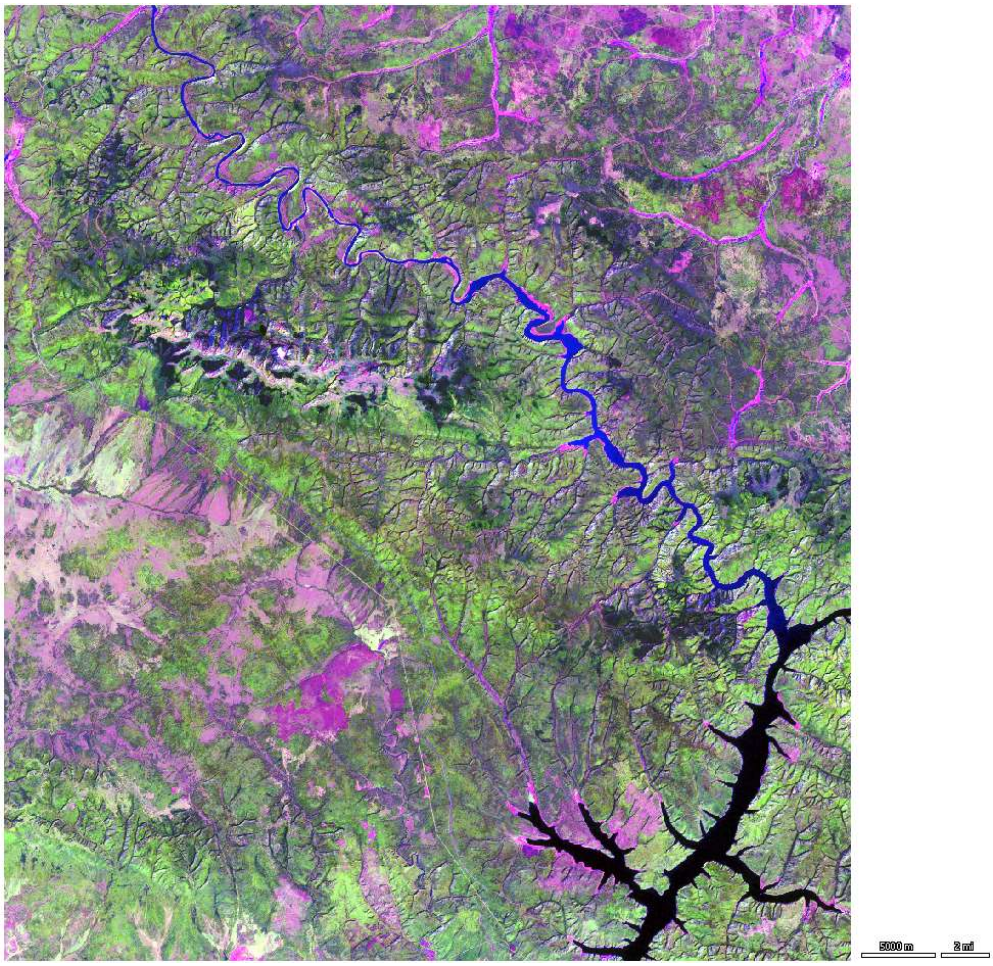

Figure 2.6. Landsat image of the Reserve dated 1996-08-12.

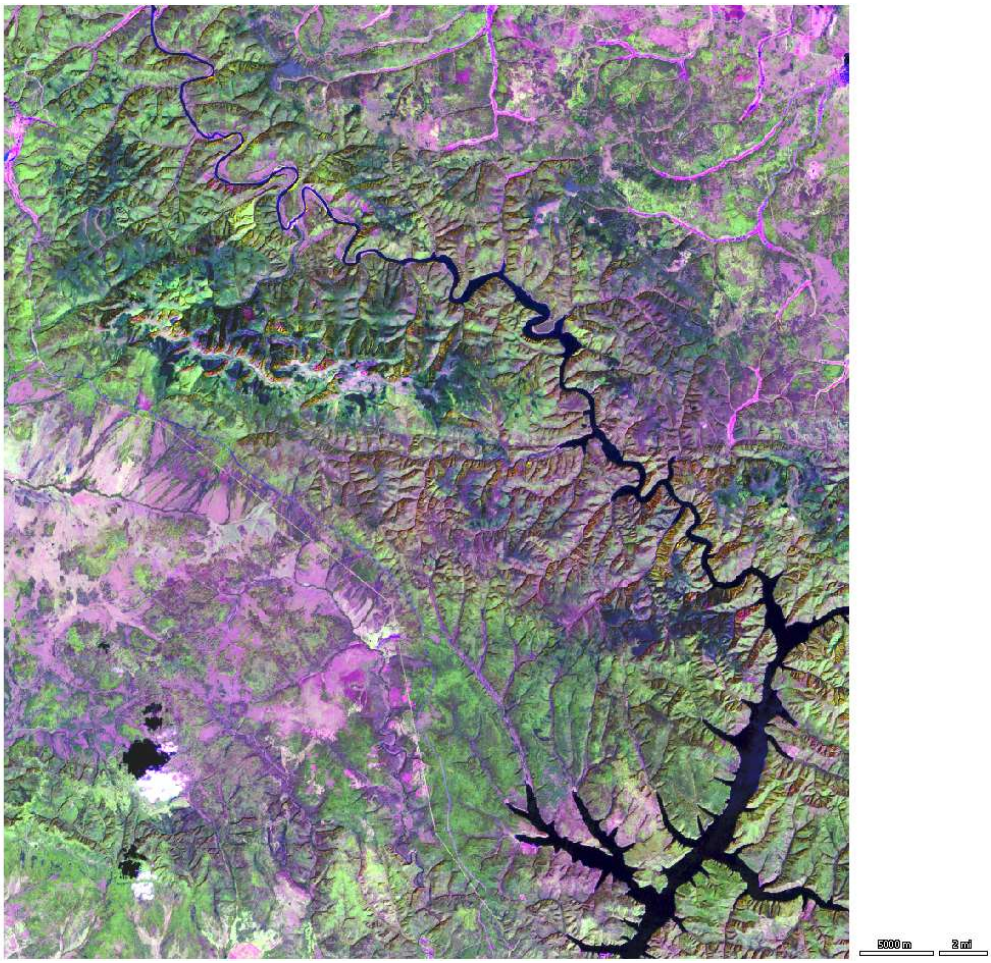

Figure 2.7. Landsat image of the Reserve dated 1999-08-21.

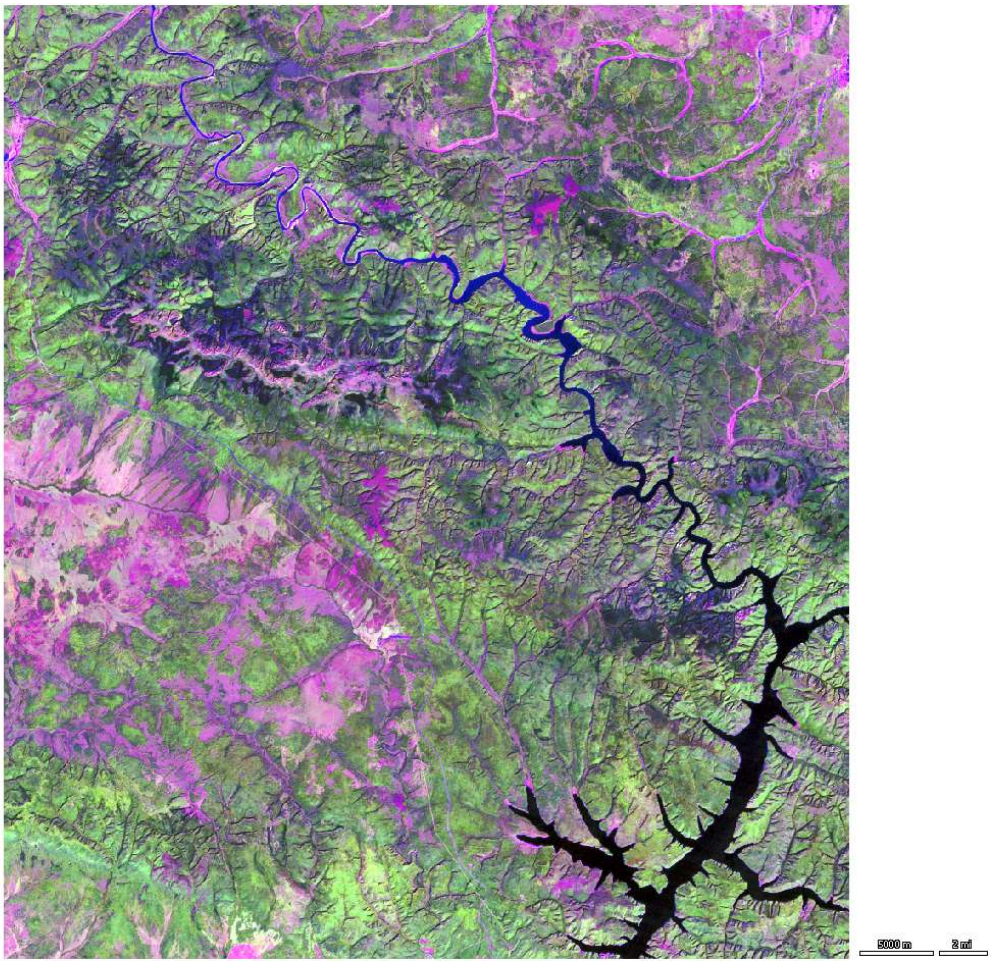

Figure 2.8. Landsat image of the Reserve dated 2001-08-26.

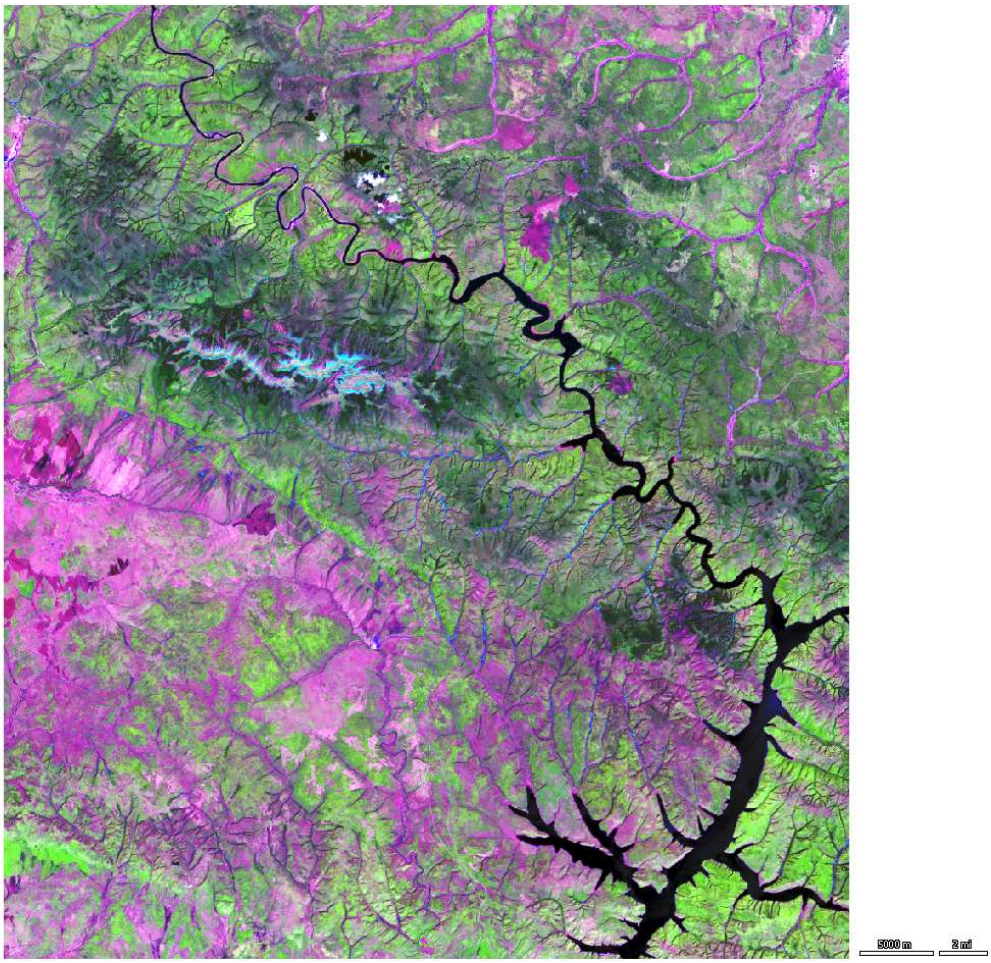

Figure 2.9. Landsat image of the Reserve dated 2005-06-02.

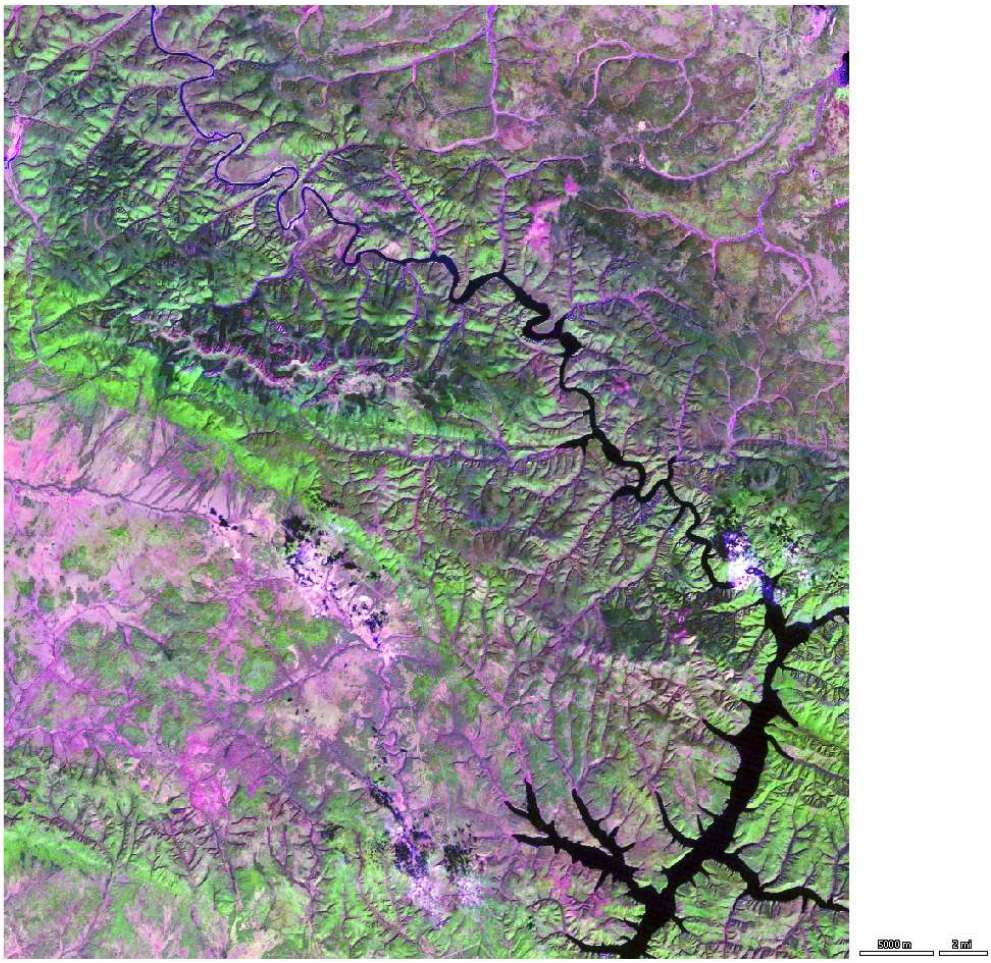

Figure 2.10. Landsat image of the Reserve dated 2010-09-04.

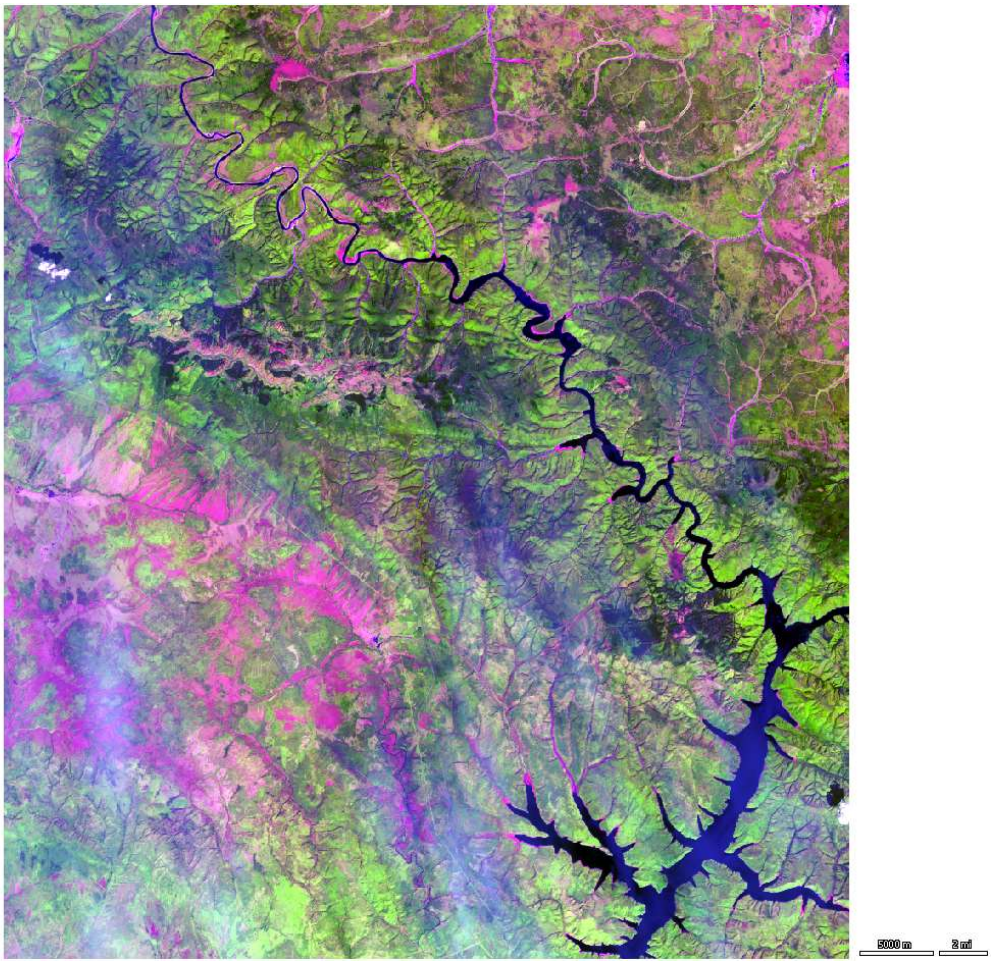

Figure 2.11. Landsat image of the Reserve dated 2014-06-11.

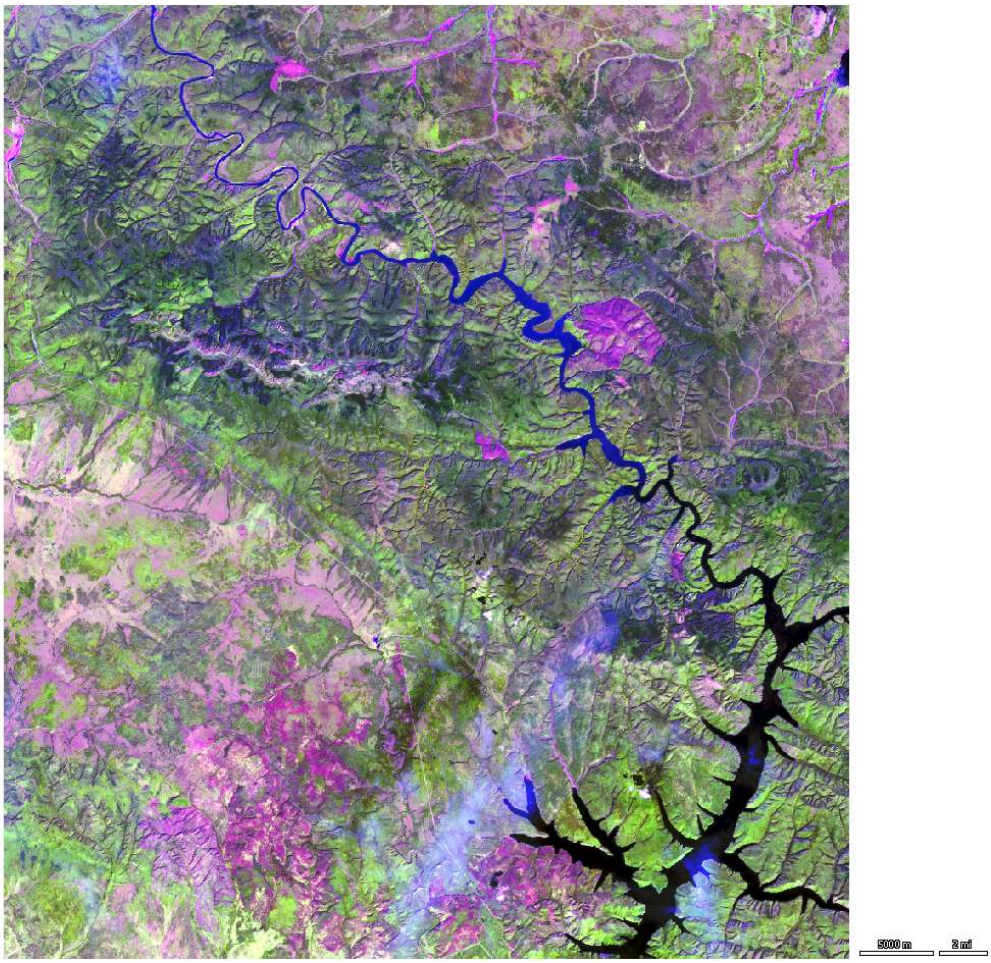

Figure 2.12. Landsat image of the Reserve dated 2016-08-19.

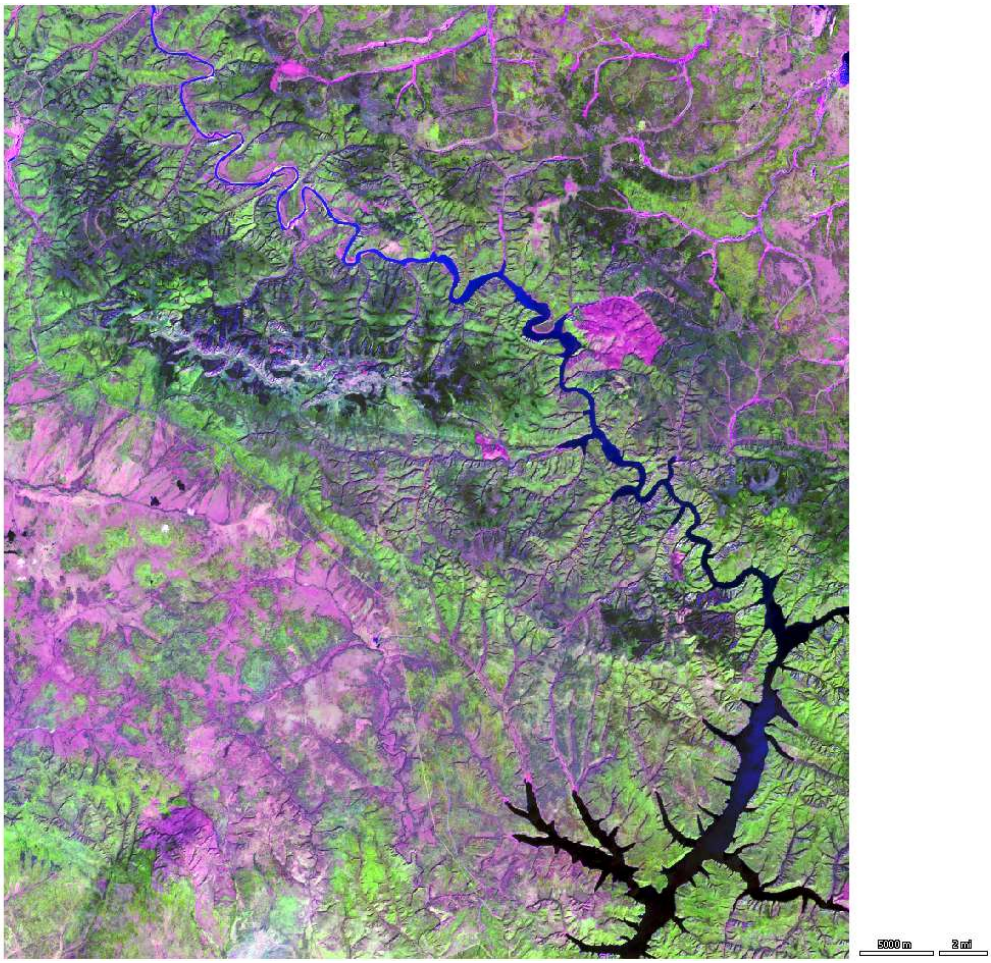

Figure 2.13. Landsat image of the Reserve dated 2019-08-28**.**

2.2.2.2 High-Resolution Data

High resolution image from DigitalGlobe WorldView-2 was acquired (Figure 2.14). The boundary of the image was NW-Lat 54.31678772, NW-Long 126.89402771, SE-Lat 54.08684921, and SW-Long 127.08489990. This image covered an extended area to the northern part of the Reserve beyond my investigation area. This area was inaccessible, so I cannot obtain ground information. High-resolution images allow me to identify the forest cover type in such a remote area of the Reserve (Hansen et al. 2013). Other data were later obtained from the open-access website. Web search engines such as Bing maps owned and operated by Microsoft https://www.bing.com/maps and Google maps and Google Earth program https://maps.google.com/ released tremendous amounts of free-accessed high-resolution images, combinations of DigitalGlobe satellite and their aerial imagery help me cover inaccessible areas (Hansen et al. 2000). However, available images were depended on location and time. Both engines did not provide a full cover of my study area.

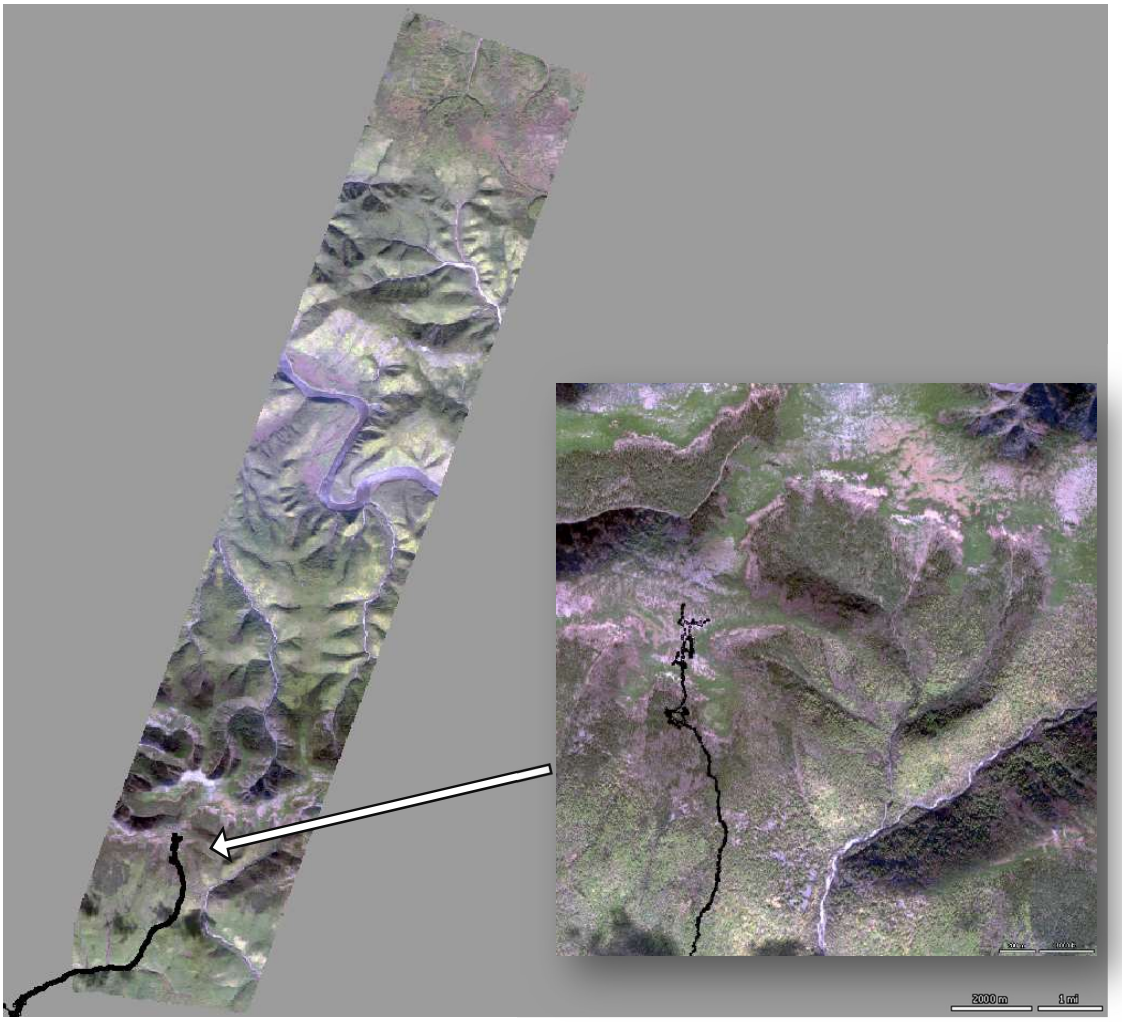

Figure 2.14 High-resolution image from DigitalGlobe WorldView-2 on 2010/09/20 at Zeya State Nature Reserve. The black line indicated the tract of field survey.

2.2.3 Literature and Map Data

Since satellite imagery was taken from a distance and generated output as image data, the procedure was based on ground reflectance value. Experts and official personnel confirm the presence of forest cover and the location of the disturbance. Global Forest Watch www.globalforestwatch.org has also issued new data on land use trend and global forest status (World Resources Institute 2014). Other data provided by Russian scientists includes Dudov 's (2018) vegetation cover map data, Borisova and Veklich 2013's (2013) oak forest plot information, overview photos of the coastal forest near artificial lake, Zeya reservoir, and Zeya State Nature Reserve wildfire layouts. The information was used to address the problems in the latter classification system. All fires officially reported by the reserve office from 1980 to 2015 were included in the historical wildfire layouts of the Zeya State Nature Reserve. Routine observation by satellite has covered reserve territory since 2005. Forest fire information, yet, was rarely gathered by aerial observation. According to the Reserve office personal, many fires would occur from lightning and burned for several days, particularly in the central part of the Reserve, and could vanish after the rainfall. Consequently, there were many missing flames. This situation resulted in some mismatches from other historical fire data sources (Chen et al. 2016).

2.3 Pre-processing of Remote Sensing Data

I used TNTmips software version 2019 (MicroImages, USA) to extracted image into the region of interest. MSS images, which has pixel size of 60m x 60m, were resampled using nearest neighbor method with Resample and Reproject function to match other Landsat images (30m resolution). The value of each cell in the resampled raster is calculated by merely copying the value from the nearest input cell. After that, all images were processed with Image/Radiometric Correction which provides functions to calibrate the image, correct the dark object and shadow, and correct the complex topography that favors in different sunlight angle

using Digital Elevation Model (DEM) (Figure 2.15). The most suitable input parameter values for radiometric correction process were considered to provide the best image for all images were “Green” for Skylight Band and “0.80” for Skylight Fraction. The output image was radiance value with the pixel size of 30m x 30m. The cloud and shadows were masked (Figure 2.16). The process removed unnecessary colored pixels polluted by cloud and cloud shadow (Potapov, Turubanova, and Hansen 2011). These corrections allowed more accurate assessment of ground surface properties and improve forest cover and result accuracy in boreal regions (Potapov et al. 2008). The corrected images; hence, were used to conduct research experiments in a later chapter.

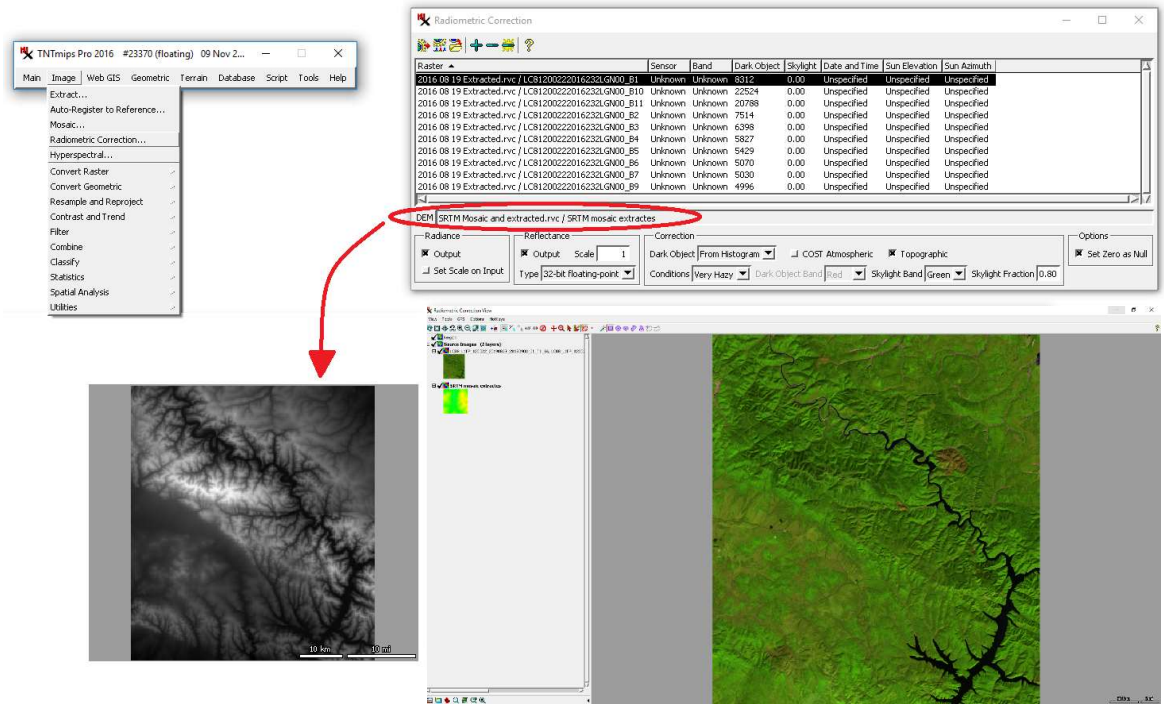

Figure 2.15. Radiometric correction function in TNTmips software.

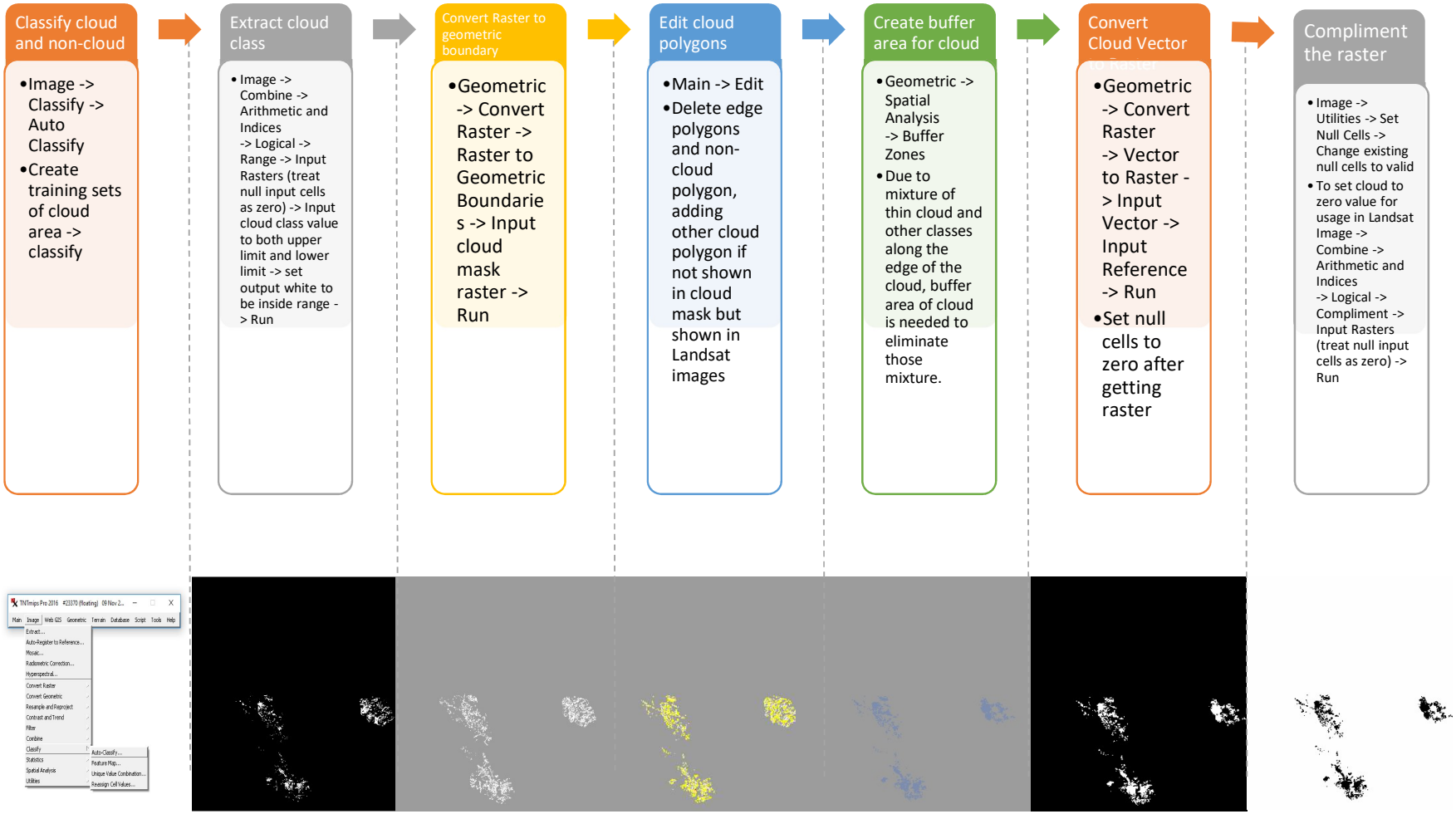

Figure 2.16. Flow chart of the cloud masking process in TNTmips2016.

Chapter III

Long-Time Interval Satellite Image Analysis on Forest-Cover Changes and Disturbances around Protected Area, Zeya State Nature Reserve in the Russian Far East

3.1. Introduction

Boreal forests are considered the largest ecoregion on Earth. This particular area is well-known for its productivity and diverse forest types which is home to many endangered species. About 20% of the world's boreal forests are located in Eastern Siberia and the Russian Far East affected by natural disturbances and human activities (Astrup et al. 2018). Deforestation and degradation are expected to expand in the Central Siberia (Loboda et al. 2012), the Eastern Siberia, and the Russian Far East (Dong Chen et al. 2016). In recent decades, unprecedented large-scale fire events have caused air pollution, smog blankets, ecosystem degradation, and biodiversity loss (Astrup et al. 2018; Dong Chen et al. 2016). The increasing temperature of and the windy weather may intensify the forest fire on the mountain top after lightning occurred. There were significant positive correlations between lightning and wetter precipitation and the advent of forest fires during the summer and fall seasons (Zhao, Liu, and Shu 2020). More than 70% of forest fire in Russia are caused by human activities, 11% by lightning, 10% by agricultural prescribed burning (A. I. Bedritsky, V. G. Blinov, and D. A. Gershinkova 2008; Bockel et al. 2014). Road building and bridge construction were expanded in Siberia and the Russian Far East, which has a tendency to cause the area more flammable when the weather is dry and warm. Mining and prescribed burning are also the causes of huge fire area in the 2015 Russia wildfire event and 2003 Siberian Taiga Fires event. The fire was out of control, causing as much as ten million hectares from West Siberia to the Russian Far East (Viacheslav I. Kharuk et al. 2021). Scientists have linked the loss of forest cover in fires to human activity and global climate change, but as some remote regions in the Russian Far

East are still unexplored, there are still lack of many data on the information of land-cover characteristics and forest dynamics (Cohen and Goward 2004).

Several nature reserves have been designated in the Russian Far East, to protect the landscape and conservation efforts against land conversion (Wendland et al. 2015; Bartalev et al. 2014). Although these remote places have a little human occupation, lack of monitoring makes them susceptible to landscape alteration, such as clearcutting for timber, agricultural expansion for ranching, mining, and road building (Kareiva et al. 2007). Keeping the forest landscape stable and maintaining forest succession after disturbance is necessary to protect species diversity and climate regulation. Boreal forests are famous for their annual fire cycle (Dong Chen and Loboda 2018). However, some disturbed areas have not recovered to the old-growth forest, and many old-growth forests have turned into secondary forests and grassland. This modern forest dynamic increases the risk of reducing the function of the forest ecosystem, raising the risk of global climatic disturbance (Achard et al. 2006).

The inaccessible area and remote locations mean that forest changes and disturbance history have not been well studied (Wendland et al. 2015). Studying areas requires advanced technologies such as remote sensing. Using remote sensing to detect the disturbance history is essential for evaluating the effectiveness of site protection measures (Wendland et al. 2015). For example, satellite image analysis demonstrated that the Russian Far East forests were greatly affected by Siberian Taiga Fires in 2003, which destroyed nearly 3 million ha of forest, the most considerable loss in the Russian Far East's history (Loboda et al. 2012; Achard et al. 2006; Peterson et al. 2009). Satellite imagery is routinely used to calculate the normalized difference vegetation index (NDVI) and the normalized burn ratio (NBR), and the normalized difference water index (NDWI) which were used to detect vegetation health, fire severity, and water (Fiore et al. 2020; Ju and Masek 2016). Such data can be useful for landscape management (Amiro et al. 2006; Dong Chen et al. 2016). As commercial satellite images are

costly, the use of freely available data, such as Landsat images, is a popular alternative for ecologists and environmentalists (Loboda et al. 2012; D. Chen et al. 2017; Vyacheslav I. Kharuk et al. 2010). However, the images have disadvantages for studying forest cover in the Russian Far East due to frequent cloudiness and short seasons, limiting the number of high-quality images available (Potapov et al. 2008). Two year images could be overlaid to increase reliability. Such a two-image classification can yield higher accuracy than standard single-image classification, overcoming limited image availability (He et al. 2018). However, the potentially long time interval between successive images reduces the accuracy of detecting forest disturbances, resulting in underestimation of disturbance (Potapov, Turubanova, and Hansen 2011). A disturbed area might have recovered to typical vegetation in the later image and can no longer be treated as disturbed area (Loboda et al. 2012; Bright et al. 2019). Therefore, to adequately evaluate disturbance, it is necessary to consider changes of the forest types or successional forest type direction.

Here I determined forest-cover change and disturbance in a protected region of the Russian Far East to help managers prioritize conservation efforts on protecting flora and fauna and managing fuel above ground to prevent severed fire (M. G. Turner 2010; W. Turner et al. 2003; Wulder and Coops 2014; Anderson-Teixeira 2018). I present the maps of forest-cover change between 1988 and 2016, in this vulnerable ecosystem, based on remote-sensing data, to show the following: (1) how forest cover and disturbance differ among inside the protected area, the buffer zone, and outside the protected area. The buffer zone indicated the area that runs along the boundary of the Reserve that limited some level of human activities but not highly restricted as the Reserve and enhance the protection of biodiversity of the reserve. The next is (2) how vegetation indices can be used to overcome disadvantages of long-interval image analysis to show forest successional stages after disturbance; and the last is (3) how effective the Reserve

is in terms of preventing fire disturbance and protecting forest based on the area of forest successional directions inside, the buffer zone, and outside of the reserve.

3.2. Materials and Methods

3.2.1. Study Area

The study area is located in Zeya State Nature Reserve, Amur Oblast, Far Eastern Russia (53°58′–54°07′ N, 126°52′–127°22′ E; Chapter 2; Figure 2.1). The reserve, with a total area of 99,430 ha, was established on 3 October 1963, at the eastern end of the Tukuringra Ridge. Within the reserve, 40% of the area has an elevation of up to 700 m a.s.l., 35% of 700 to 1000 m, 18% of 1000 to 1300 m, and 7% of over 1300 m. The average temperature is −28.8 °C in January and +19.7 °C in July. The average annual precipitation is 515.2 mm. The prevailing winds are northeasterly, most commonly (75%) at 1.2 to 2.2 m/s. The Reserve are considered home to more than thousands of species, including 1111 species of plants, 2001 species of invertebrates, and 225 species of vertebrates. The biodiversity in the Reserve is richer than other protected area in the Russian Far East. More than 35 species of fauna and flora are listed on the Red Book of Russia, and 10 species of bird and 1 species of mammal are on the International Union for Conservation of Nature (IUCN) Red List (Zeya State Nature Reserve 2020).

More than 90% of the Reserve is covered by 7 major different forest types, with the most dominant be the *Betula platyphylla* and *Larix gmelinii* species (80% of the Reserve and *Picea ajanensis* species (10% of the reserve). According to Dudov's (Dudov 2018) spatial map of vegetation, the mountain tundra belts, located at elevations of >1200 m, are dominated by alpine dry heath species, such as *Vaccinium uliginosum* L., *Arctous alpina* (L.) Niedenzu, and *Betula exilis* Sukacz., edged by the dark green shrub-like tree *Pinus pumila* (Pall.) Regal. *Picea ajanensis* (Lindl. et Gord.) Fisch. ex Carr. grows at two elevations, high on the mountains and sometimes mixed with larch along river valleys. *Larix gmelinii* (Rupr.) Kuzen and *Betula*

divaricata Pall. spread across the mountain in various habitats and end at the mountain tundra belt (1200 m). Vegetation under the canopy of larch forests includes *Vaccinium vitis-idaea* L., *Ledum palustre* L., *Rhododendron dauricum* L., and green mosses. Grasses and willows grow in the river valleys and floodplains at lower elevations. *Quercus mongolica* Fisch. et Ledeb. grows in the southeastern part of the Reserve along the northern slopes. *Tilia amurensis* Rupr., *Lespedeza bicolor* Turcz., and *Corylus heterophylla* Fisch. ex Trautv. grow under the canopy of oak and black birch forests. Other plants along the river valleys include *Dasiphora fruticosa* (L.) Rydb., *Syringa amurensis* Rupr., *Calamagrostis* spp., and *Carex* spp. Meadows and grasslands are scattered in several places, such as fire-disturbed areas and floodplains. Marshes occupy only a small area inside the reserve, mostly in flat areas and on gentle slopes with northern exposure. In 2003, the region experienced a large-scale fire (around 700 km^2) that caused extensive damage to forests both inside and outside the reserve.

The Reserve established a buffer zone along the edge of the reserve, extending more than 5 km distance from the border of the Reserve to the road on the eastern side and to the electricity line on the southern side and to the river on the western and northern sides. The area has reduced some degree of human activities but is not quite restrictive as inside the reserve. The buffer-zone area strengthens the conservation of biodiversity, providing protection shield to the reserve's fauna and flora and only allowed limited intense use of natural resources. There is some monitoring at the buffer zone area to track human disturbance and infrastructure developments, like roads and bridge construction. Outside areas of the Reserve beyond the buffer zone line owned by the federal government is seldom controlled or monitored by government officials. Rare surveillance may put the region at risk of forest destruction and landscape changes. The Reserve interior was well protected from human disturbance, with no settlements or clearcutting activity within it. This situation has shown its effectiveness in protecting natural resources and ecosystems. However, many human-induced disturbances

were still found nearby. The flat terrain and unprotected status outside the Reserve make large forests vulnerable to human disturbance activity (Schroeder et al. 2011). Clearcutting occurred more in the buffer zone during the most recent period because of easier accessibility and a new mining camp. In recent years, most forest fires have occurred in the clearcutting area, raising the question of whether the timber harvesters or the miners caused the fire and whether it was accidental or natural. For example, many areas of mixed disturbance located next to the mining area and the nearby electricity line in 2010–2016. An increasing fire frequency resulting from changes in species composition that favor the regrowth of deciduous forests prone to fire (Smith et al. 2016; Sommerfeld et al. 2018) usually occurs in small-scale clearcutting or selective logging areas (Schroeder et al. 2011).

3.2.2. Data and References

I used two datasets in this study: satellite images of the Reserve during summer, for classification; and field data plus maps and literature, along with the high-resolution image and photographs, as references. The dataset for classification included Landsat satellite imagery, and 30 m Shuttle Radar Topography Mission (SRTM) data were acquired from the US Geological Survey's Earth Resources Observation (USGS) (USGS 2017). I selected Landsat images with <10% cloud cover during the growing season (1 June to 30 September). After screening, I chose only four most suitable images based on cloud-free and relatively within the same season and appropriate time-interval, acquired in 1988, 1999, 2010, and 2016, from the Landsat Thematic Mapper (TM) and Operational Land Imager (OLI) imagery (Table 1). The images were preprocessed, using radiometric calibration, atmospheric correction made with COST model(Chavez 1996), and topographic correction made with SRTM as Digital Elevation Model (DEM) with TNTmips 2017 software (MicroImages, Raymond, NE, USA).

Table 3.1. List of processed Landsat images.

Path/Row	Date	Sensor	Band Combination for False Color Composite (R,G,B)
120/22	23 September 1988	Landsat 5 TM	B5, B4, B3
120/22	21 August 1999	Landsat 5 TM	B5, B4, B3
120/22	04 September 2010	Landsat 5 TM	B5, B4, B3
120/22	19 August 2016	Landsat 8 OLI	B6, B5, B4

TM, Thematic Mapper; OLI, Operational Land Imager.

To preprocess the SRTM images, I used the TNTmips2017 Radiometric Correction, the most suitable parameters that provide the best images on all four dates were a scale of 1 for reflectance, “dark object from histogram”, and “very hazy” with a skylight fraction of 0.80 for correction. These parameters provided similar ranges of reflectance values between sunny and shadowy areas. After the reflectance images of all the full Landsat scenes were produced, they were extracted into regions of interest that covered the entire reserve and some areas outside it.

The reference dataset used as training and validating samples to evaluate classification accuracies, I investigated the area inside and outside the Reserve during the summer season, August 2016 to 2018, and collected measurement data. I established twenty-three plots in total:

eleven plots (NR1–NR11) inside the reserve, six plots in the buffer zone (BZ1–BZ6), and six plots outside the Reserve (ONR1–ONR6), each covering approximately 100 m^2 (Figure 3.1). In each plot, I recorded tree species, tree height, and diameter at breast height, to identify forest cover. The photos and evidences of burn scars and cut woods helped identify the disturbance type in the area. Most of the plots were dominated by *L. gmelinii* and *Betula platyphylla*, and the higher elevation plots were dominated by *P. ajanensis*. Several plots, however, had experienced forest fire and clearcutting in the past.

Besides the field investigation information, other references included drawing maps, vegetation maps, high-resolution images, and photographs. For drawing fire maps, the reserve-management-office specialists observed and recorded the burned area that occurred from the 1990s to 2010 and hand-drawn the boundaries of the burned area on the Reserve map. The vegetation map had been published in 2016, in Russian, by Dudov (Dudov 2018), using satellite images as a based map. The author collected information in the field and produced the classified vegetation map of the reserve, consisting of 45 forest classes in total. The mountainous topography and inaccessibility of the northern part of the Reserve made it difficult for me to collect data there, so I used a high-resolution image from Digital Globe WorldView-2, taken on 20 September 2010, covering around 20 km^2, to investigate the inaccessible area at the northern border of the Reserve and check whether there is any evidence of forest burning or clearcutting area. I also obtained photographic evidence and evidence from experts and scientists who previously conducted experiments inside the reserve. The high-resolution images from global online mapping services, such as Google Earth imageries, Bing Maps, and Google Maps, also allowed me to monitor the change of the landscape and used it as one of the references to identify of forest cover and disturbance outside of the Reserve area.

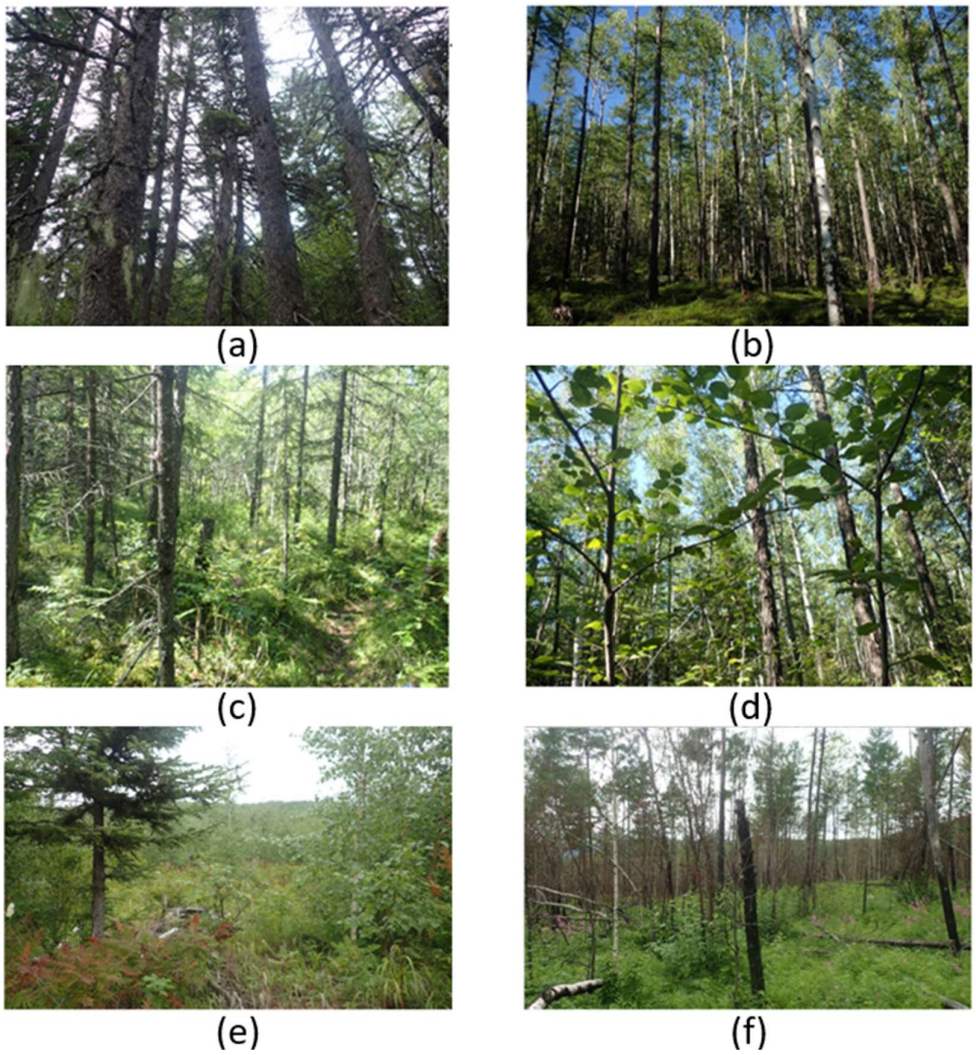

Figure 3.1. Overview examples of forest plots in the field: (**a**) plot NR1, located below the tundra belt, at 1305 m a.s.l., and dominated by mountain spruce forests; (**b**) plot NR2, located along the trail, at 853 m a.s.l., dominated by larch; (**c**) plot NR3, located at 626 m a.s.l., along the river valley, with the dominant species being larch and spruce in the river valley; (**d**) plot NR4, located near the road, with dominant trees including birch and larch; (**e**) plot BZ1 buffer zone plot, which experienced both massive forest fire and clearcutting in 2003 and 2007, and is now recovered by grass and shrub and birch; (**f**) plot ONR1, outside reserve plot, experienced with frequent annual burning from wildfires, the latest of which occurred in July. The photos were taken on August 8, 2016 (Khatancharoen 2016; personal observation).

3.2.3. Classification

For image-classification processing (Figure 3.2), image datasets were first classified by object-based segmentation, a multi-scale object-oriented procedure that divides an image into small regions called “objects”, using eCognition v. 9.0 software (Trimble Geospatial, Sunnyvale, CA, USA). This study introduced a two-year overlaid image classification technique. In my object-based classification process, I inserted 12 layers of 6 bands (R, G, B, NIR, SWIR1, and SWIR2) from two Landsat dates (pre- and post- year images, e.g., 1988 and 1999) and a layer from the SRTM data in the workspace. All 13 band images were then segmented into objects, using a multiresolution segmentation algorithm with a scale of 10 for the most appropriate scale parameter (Hirata and Takahashi 2010). I also gave image layer weights of 2 for NIR layer to weigh vegetation cover more. The other parameters remained defaults (0.1 for shape and 0.5 for compactness) (Başay and Ersan 2015). The multiresolution segmentation algorithm provided ability to divide the pixels with similar spectral values into polygons. This technique lowers the numbers of heterogeneity polygon areas (Drăguţ, Tiede, and Levick 2010).

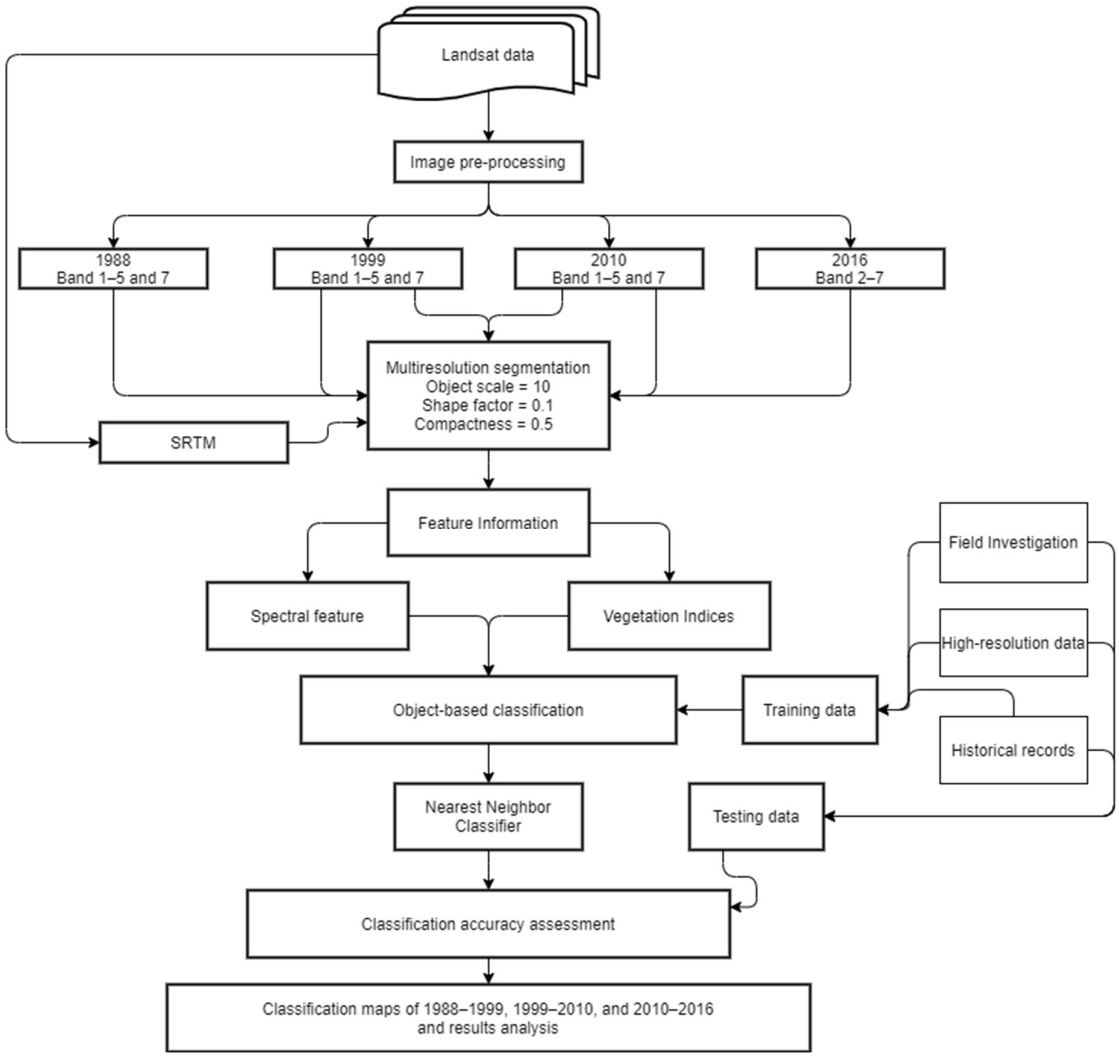

Figure 3.2. Flowchart for object-based classification based on Landsat images.

Image datasets were first classified by object-based segmentation, a multi-scale object-oriented procedure that divides pixels with a similar range of spectral reflectance into regions called 'objects' in eCognition v. 9.0 software (Trimble Geospatial, Sunnyvale, CA, USA). The reference data were used as training and validation datasets. I classified forest cover change in three periods, namely 1988–1999, 1999–2010, and 2010–2016. Three vegetation indices (NDVI, NDWI [normalized difference water index], and NBR) and band values (RED, NIR [near-infrared], SWIR1 [short-wave infrared band 1], and SWIR2) of the Landsat images were used as

classification variables (Tucker 1980). The NDVI was used to detect live green vegetation(Gao 1996) to separate forest type into different classes. It was calculated as:

$$NDVI = (NIR - RED) / (NIR + RED). \quad (3.1)$$

The NDWI was used to detect surface waters in wetlands (Chu, Guo, and Takeda 2016) and to distinguish wetland from valley grassland. It was calculated as:

$$NDWI = (NIR - SWIR1) / (NIR + SWIR1). \quad (3.2)$$

The NBR was used to estimate pre- and post-fire area (Bright et al. 2019). It was calculated as:

$$NBR = (NIR - SWIR2) / (NIR + SWIR2). \quad (3.3)$$

I also calculated the change of the NDVI and NBR between years. The change of NBR between two years allowed me to locate the burn area in my study area, while the change of NDVI can give me a hint as to the location of deforested areas.

For the classification process, the study employed the nearest neighbors (NNs) algorithm. The core concept of the non-parametric machine learning NN algorithm method was that if the training objects and the neighboring objects in feature space belonged to the same class, then the objects would be identified as that class (Franco-Lopez, Ek, and Bauer 2001). It was appropriated for my study because many objects had spectral values across multiple categories. The objects unfitted to the class would be identified as unclassified objects on the classification layer. I also used the interactive algorithm, such as the thresholding algorithm and assigning algorithm, for the post-classification to assign the unidentified and mismatch class objects to the proper class based on spectral values and indices. During the classification process in eCognition, first, I inserted the class hierarchy of 17 land-use classes. I selected training objects that represented each class well and assigned classes to the objects based on the criteria in Table 1. I checked the area on the layers and selected the polygons that match the physical description

of each land-cover type, based on the Zeya State Nature Reserve vegetation map, field investigation, and high-resolution images used as training samples. After creating training samples for each image, NDVI and NDWI were calculated in the software, to add sufficient information for object features, which included 12 band values, four spectral indices, and the SRTM. In each period classification, I applied the standardized nearest neighbor (SNN) function (Sw et al. 2008) with the object features altogether with additional parameters that were already predefined in the software, including brightness, relative borders, shape index, and area index. The function allowed me to input specific characteristic information to the training objects, so that the classification would classify the objects based on similar information as the training objects. The classification function used NN algorithm and produced raster layer results of the 17 classes and unclassified class (Table 3.2). After classification, several misclassified or unclassified isolated objects may exist, so I corrected them by using a basic classification algorithm that includes a class-reassignment algorithm, to adjust misclassified objects based on elevation range, expert's explanation, and reference data (Appendix 2).

The thresholding algorithm allowed me to reassign misclassified class to the aiming class based on the condition I set. First, I corrected the unclassified class to WATER class, using a thresholding algorithm, by setting the mean NIR value to be less than 80. Due to the mislocation of MTV class and GRASS class, I reassigned MTV class of <1100 m a.s.l. as GASS, and GRASS class of > = 1100 m a.s.l., as MTV, by referring to SRTM elevation layer. Moreover, mislocated MSF class in the lower valley of <700 m a.s.l. was reassigned to SFRV class. These reassignment was executed by "assigned class" algorithm. On the other hand, a few unclassified objects and human-related disturbance classes misidentified inside the Reserve were reassigned to the proper classes by their properties and physical characteristics or similarity to the nearest class inside the reserve, by executing "selected object" algorithm. This

interactive algorithm allowed me to reassign misclassified class to the desired class to only the objects I selected. Two-year overlaid images were finally classified to obtain the results of one period of the forest-cover-change maps. I performed the same classification algorithms for three periods (1988–1999, 1999–2010, and 2010–2016). A total of three maps of three periods were generated as the final classification maps.

Table 3.2. Classification criteria for object-based segmentation classification

Class Name	**Major forest types**	**Physical Description**	**Color in Landsat Images (False color)**
BURN	Burn area***	Forest disturbance by wildfire	Red and pink
CCTA	Clearcutting for timber or agricultural***	Forest disturbance by harvesting for timber and ranching	Yellow and red in geometric shape
CCE	Clearcutting for electricity lines***	Forest disturbance by clearcutting to settle down electricity lines	Long-straight lines with bright color
MD	Mixed disturbance***	Forest disturbance by human-induced fire and harvesting at the same place	Red and pink in geometric shape
VGR	Vegetation recovery***	Vegetation recovery after disturbance	Bright pink patches
GRASS	Bogged larch forests in a wide valley and grassland	Muddy, wetland, willow, floodplain	light pinkish with smoot light green
MF	Mixed forests in a river valley	Larch mixed with Spruce, willow, grass	Sparse light and dark green
OBF	Oak - Daurian birch forests	*Querqus mongolica, Lespedeza bicolor*	Very bright green

BLF	Birch and larch forests	*Larix gmelinii, Betula platyphylla*	Normal green
SFRV	Spruce forests in a river valley	*Picea ajanensis* (315-700 m a.s.l.) sparsely dispersed near stream	Dark green
MSF	Mountain spruce forests	*Picea ajanensis* on steep slope (700-1300 m a.s.l.)	Very dark green
DPW	Dwarf pine woodland	*Pinus pumila, Betula lanata* (1100 - 1300 m a.s.l.)	Smoot light green
MTV	Mountain tundra vegetation	shrub, sedge, lichen, moss	White
TOWN	Settlement	Houses and airports	Red to pink color
ROAD	Unpaved road	Roads or ways for transportation without pavement	Grey color in long-straight lines
ROCK	Stream bedrocks	River or Stream bedrocks where no water flows	Very reddish color
WATER	Water	Water bodies (e.g. river, lake)	Dark blue
CLOUD	Cloud****	Smog, cloud and cloud shadows	White and black color
NOTE: * Forest cover change class detected after verifying existence between the two year. ****Cloud cover change class was masked out in forest cover change maps and analysis**			

3.2.4. Accuracy Assessment

I randomly selected new sample “objects” or polygons to assess classification accuracy within the study area. To avoid appearing on a similar location as a training area and cloud and shadow effects, the “objects” located in such area were excluded, and then the total numbers of “objects” for validating process were 2121 for 1988–1999, 2321 for 1999–2010, and 2541

for 2010–2016. Those new sample objects were treated as validating objects and selected independently from training sample objects. The validating objects were identified based on references, including ground-truth plots, drawing fire map, vegetation maps of 2016, high-resolution image, and experts' knowledge to evaluate the classification performance, using the "Accuracy Assessment" function in eCognition. I inserted the vegetation map 2016 raster layer and high-resolution image to eCognition. I selected validating objects based on reference layers and also refer to drawing a fire map. For classes outside of the Reserve which were inaccessible, I referred to a high-resolution image of 2010, employed from Digital Globe World View-2, Google Maps, and Bing Maps, along with field photographs (Figure 3.3) and staffs' knowledge, to identify the ground-truth forest cover. The validating objects were then converted to the Training and Test Area (TTA) Mask, to compare with the classification layer. Finally, classification accuracy was assessed, using "Error Matrix Based on TTA". The outputs included user's accuracy, the number of correctly classified objects in that class divided by the total number of that class's objects on the classified maps, producer's accuracy, the number of correctly classified objects in that class divided by the total number of reference objects for that class, the overall accuracy, the total number of correctly classified objects divided by the total number of reference objects, and Kappa index of agreement (KIA) that measured the interrater reliability.

CLASS	Landsat Image	Classification Layer	High-resolution Image	Field Photograph
BURN	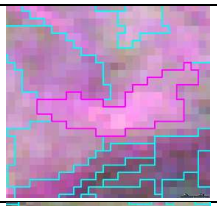	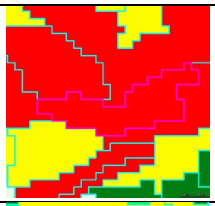	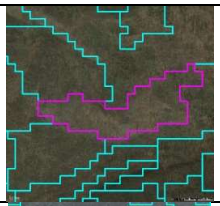	
CCTA	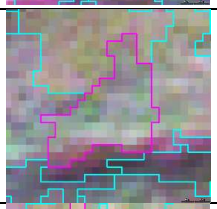	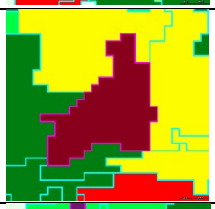	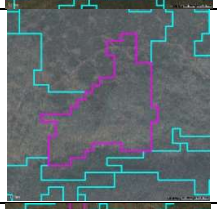	
CCE	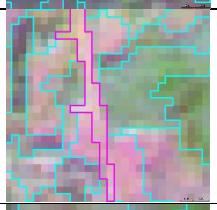	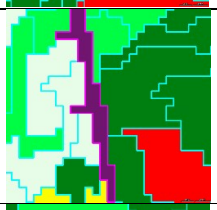	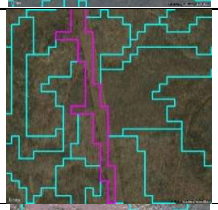	
MD	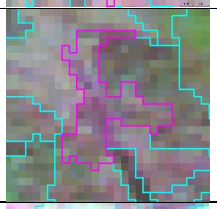	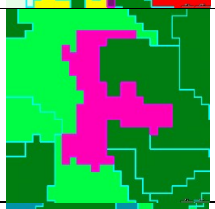	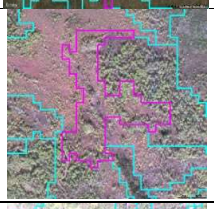	
VGR	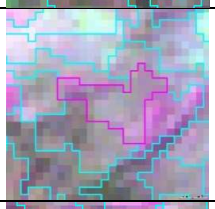	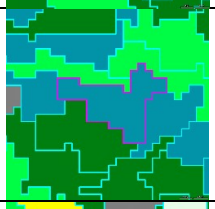	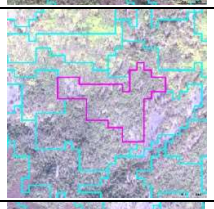	
GRASS	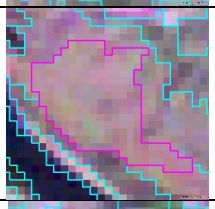	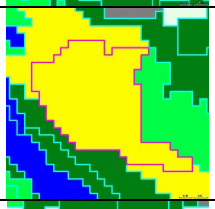	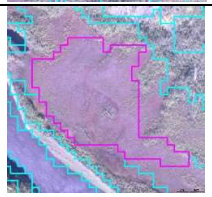	
MF	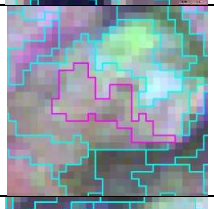	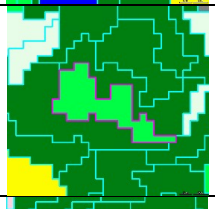	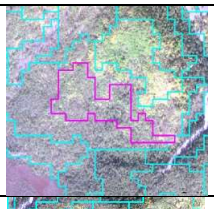	
OBF	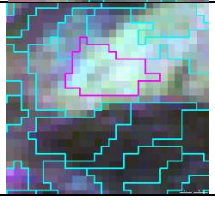	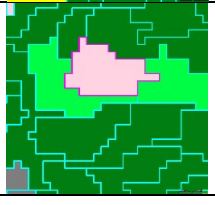	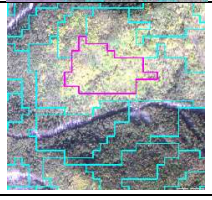	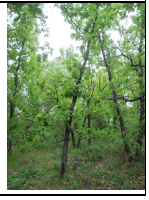

Figure 3.3. continued

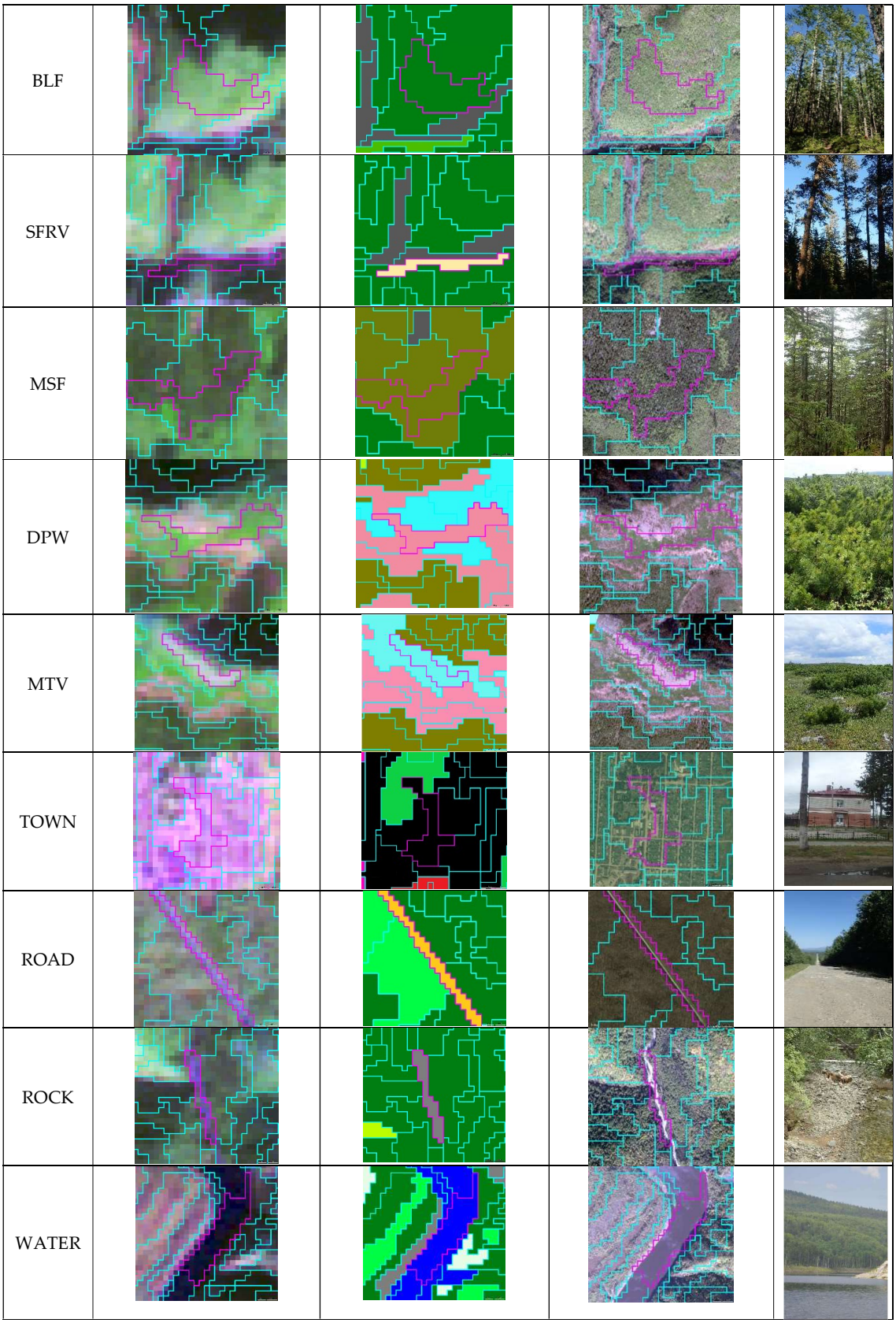

Figure 3.3. Examples of comparison of Landsat image data, classification result, and reference data (high-resolution image and field photographs) for 17 classes.

3.2.5. Forest-Cover Change and Disturbance Analysis

I generated forest-cover-change maps based on the 17 classes in each of the three periods. Delineating three zones—inside the reserve, a buffer (an area that runs along the boundary of the Reserve which limited some level of human activities but not highly restricted as the Reserve and enhance the protection of biodiversity of the reserve), and outside the reserve—helped me analyze the forest-cover change and disturbance areas. The buffer zones added security to the reserve's biodiversity and ecosystem. The Reserve established the buffer zone border to avoid heavy usage of natural resources. To understand the dynamics of forest and disturbance around the reserve, I separate the buffer zone area from the outside area to monitor the disturbance patterns and trend near the border of the reserve. The area was extracted by using the polygons of inside, buffer zone, and outside the Reserve for forest-cover change and disturbance analysis. I calculated the areas of all the classes and created a matrix of area changes among the three periods and the three zones. I focused on six classes (BURN, VGR, GRASS, MF, OBF, and BLF) for analysis. These classes represented typical forest successional stages after disturbance in large areas inside the reserve, buffer zone, and outside the reserve. I excluded four classes (SFRV, MSF, DPW, and MTV) because those vegetation types were at higher elevations, had small area, and were rarely disturbed. I analyzed the mean values of NDVI and NBR of the six successional stages to assess forest succession. The lowest average value of NDVI and NBR class was considered the first stage while the higher average value class was considered the next stage and so on. The broad-leave forests typically dominated the land before needle-leave forest, thus I arranged BLF as the last stage of forest succession. After I assessed forest succession, I created a matrix of the percentage of area changes of successional stages to show their directions in the three zones.

Finally, I compared inter-annual fires to check the more precise dates of fire in the study region, using the MCD64A1 product (Giglio et al. 2015, 64) from Moderate Resolution

Imaging Spectroradiometer (MODIS) satellite (ORNL DAAC 2018) (Figure 3.4). As MODIS started orbiting after 2000, it was possible to compare only two periods (1999–2010 and 2010–2016) in this research. The MODIS sensor has 36 spectral bands to monitor earth and water surface conditions, spatial resolutions of 250 m, 500 m, and 1 km, and temporal coverage of 1 or 2 days (Justice et al. 1998). I selected the MCD64A1 product because it was specifically developed for burned area detection and has 500 m spatial and 1 month temporal resolutions (Roy et al. 2005). This helped me better understand how the fire cycle impacted the forest cover in my study area.

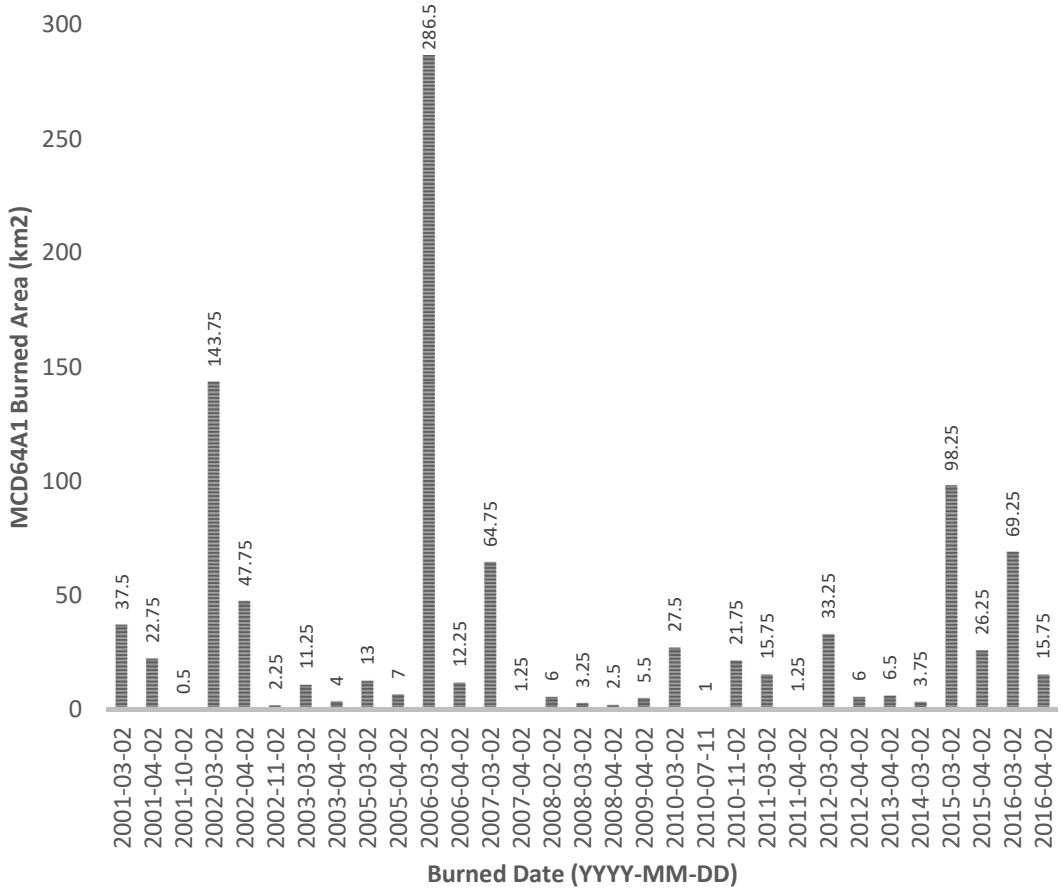

Figure 3.4. The Reserve burned area in each date registered by the MCD64A1 product.

3.3. Results

3.3.1. Classification Maps

The object-based classification produced three changed maps from three periods (1988–1999, 1999–2010, and 2010–2016). The maps indicated "change classes" and "stable classes" (Figure 3.5). "Changed classes" referred to the disturbance and recovery classes for which a large change was detected during classification, while "stable classes" referred to classes for which a large change was not detected between pre- and post-year images, during classification; this included, forest, rock, water, permanent road, and settlement classes. These classified maps were the first change maps ever produced in the study area. This is also the first time I detected large burned area across the river at the northern border, outside the reserve, during 1999–2010 and 2010–2016. Most of the burned area lay to the southern, outside the reserve, near grassland. I found that, in the period 1988–1999, the burned area was small and hardly detected, but when compared to the period 1999–2010 and 2010–2016, large burned areas were detected across the southern parts of the reserve. By combining sequential images, I found that the classification had high overall accuracy for all three periods: 91.6% for 1988–1999, 90.9% for 1999–2010, and 94.3% for 2010–2016 (Table 3.3). For 1988–1999, the producer's accuracy was low in most disturbance classes: 64.3% in mixed disturbance, 69.4% in burned area, 58.9% in clearcutting for timber or agriculture, and 70.0% in clearcutting for electricity line. The user's accuracy for mixed disturbance class was 40.9%. This means that, even though 64.3% of mixed disturbance area from the ground-truth was correctly identified as mixed disturbance, only 40.9% of the mixed disturbance area on the classified map was actually mixed disturbance. For 1999–2010, the user's accuracy was low in mixed disturbance (66.7%), burned area (40.9%), and vegetation recovery (57.4%). For 2010–2016, accuracy was very high except for clearcutting for timber or agriculture, with a user's accuracy of only 60.0%.

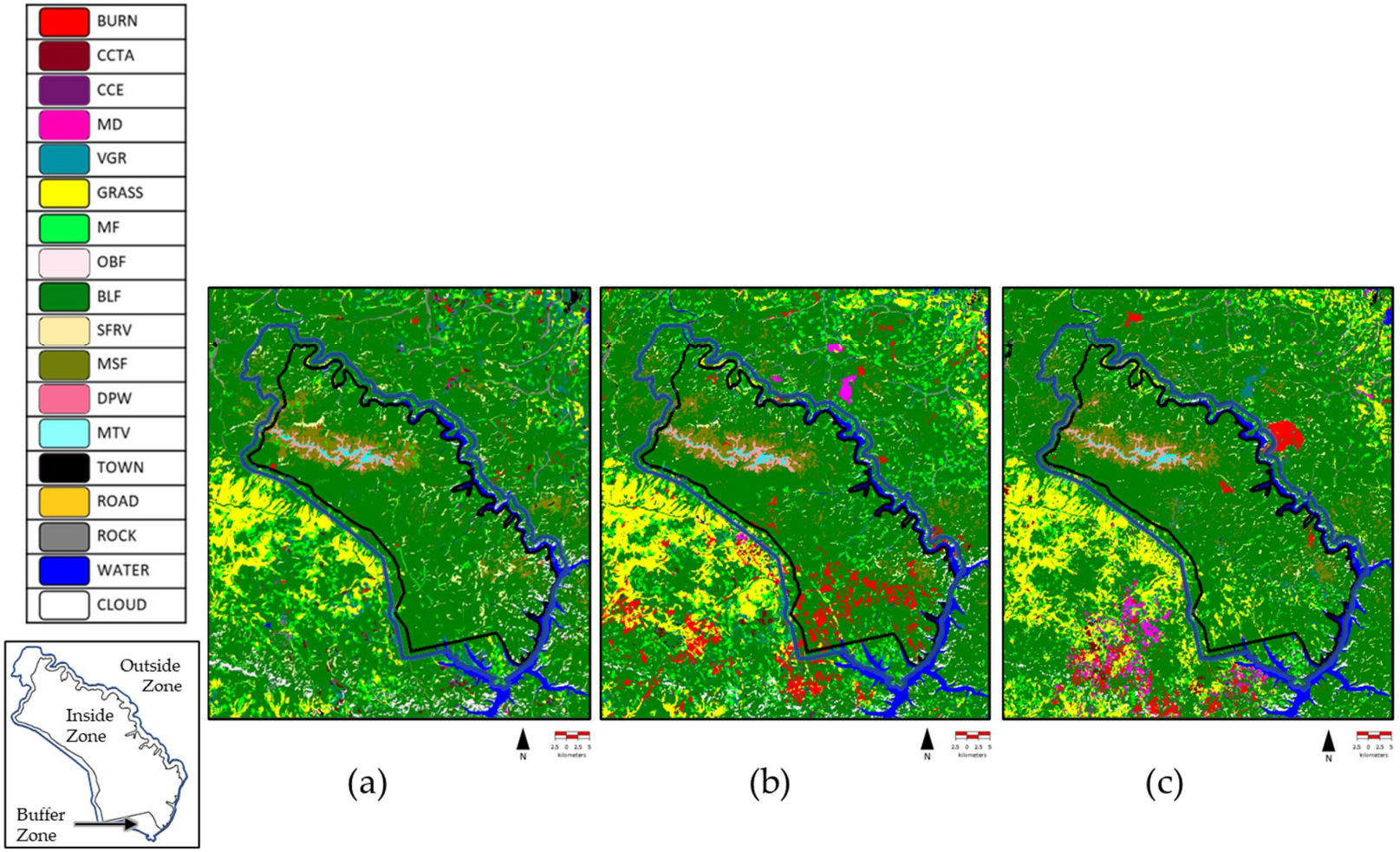

Figure 3.5. Object-based segmentation classification results (a) forest cover change map of 1988-1999, (b) forest cover change map of 1999-2010 and (c) forest cover change map of 2010-2016.

Some of the forest areas in the southern parts experienced burning and two or more clearcuttings during 1988–2016. The burned area increased more than 3.48% of total area from the period of 1988–1999 to 1999–2010, but it decreased −2.02% from the period of 1999–2010 to 2010–2016, covering ~137 km^2 (Figure 3.6; Table 3.4). Most of the burned area lay around the southern region inside the Reserve during 1999–2010 (Figure 3.5; Table 3.4). The grassland area decreased inside and increased outside the reserve, after the first period. The total grassland area increased around 2.15% from the period of 1988–1999 to 1999–2010. Mixed disturbance was the only class that increased continuously, by about 0.20% from the period of 1988–1999 to 1999–2010, and 1.10% from the period of 1999–2010 to 2010–2016. Birch and larch forests lost ~42 km^2 to vegetation recovery and lost ~212 km^2 to mixed forests in 1999–2010, the largest conversion (Table 3.5). Other significant conversions of >50 km^2 included birch and larch forests to grassland (69.35 km^2), mixed forests to birch and larch forests (100.43 km^2), and spruce forests in river valley to birch and larch forests (68.56 km^2). In 2010–2016, most of the disturbance occurred in mixed forest areas, which lost ~19 km^2 to burned area, and ~18 km^2 became vegetation recovery (Table 3.6).

Table 3.3. Producer's accuracy and user's accuracy for 1988–1999, 1999–2010, and 2010–2016.

Class	1988–1999		1999–2010		2010–2016	
	Producer	**User**	**Producer**	**User**	**Producer**	**User**
BURN	69.44%	89.29%	65.85%	40.91%	84.31%	93.48%
CCTA	58.93%	86.84%	85.71%	85.71%	100.00%	60.00%
CCE	70.00%	100.00%	86.67%	100.00%	87.50%	87.50%
MD	64.29%	40.91%	80.00%	66.67%	84.62%	100.00%
VGR	78.82%	78.82%	100.00%	57.39%	88.42%	95.45%
GRASS	95.26%	95.94%	88.06%	99.76%	87.88%	80.56%
MF	77.30%	84.56%	97.42%	72.60%	92.59%	75.76%
OBF	100.00%	100.00%	95.00%	95.00%	100.00%	100.00%
BLF	98.67%	90.24%	98.35%	90.99%	97.39%	95.51%
SFRV	94.25%	98.80%	78.95%	100.00%	100.00%	76.92%
MSF	96.26%	94.74%	94.30%	91.46%	86.71%	93.75%
DPW	85.71%	91.14%	88.51%	89.53%	96.30%	81.25%
MTV	92.86%	88.64%	90.91%	85.11%	77.55%	92.68%
TOWN	87.91%	97.56%	85.96%	80.33%	80.00%	100.00%
ROAD	93.75%	88.24%	85.71%	94.74%	100.00%	90.91%
ROCK	91.41%	93.60%	77.97%	94.85%	76.47%	100.00%
WATER	100.00%	100.00%	100.00%	93.52%	100.00%	100.00%
Overall Accuracy	91.61%		90.90%		94.33%	
Kappa index of agreement (KIA)	90.10%		87.86%		92.68%	

Table 3.4. Area (km^2) of class covers in first (1988–1999), second (1999–2010), and third (2010–2016) periods.

Class	Area (km^2)		
	1988–1999	**1999–2010**	**2010–2016**
BURN	15.4134	136.9125	67.6089
CCTA	20.0142	8.1333	6.5934
CCE	4.2867	3.6063	9.4788
MD	3.1158	10.1043	49.734
VGR	105.9642	97.9578	45.4932
GRASS	248.5971	316.1943	340.9686
MF	224.7192	318.0006	209.2185
OBF	70.4358	52.1739	46.4472
BLF	2666.847	2468.893	2598.881
SFRV	72.0909	31.7277	65.6172
MSF	131.1309	115.5024	126.2691
DPW	21.1194	24.8724	23.58
MTV	7.1253	6.7365	8.1981
TOWN	5.2515	2.9889	4.5891
ROAD	5.6367	4.2255	7.2792
ROCK	41.5503	29.7927	23.7357
WATER	114.6123	128.7387	123.948

Table 3.5. Area changes in different vegetation classes during 1999–2010 compared to 1988–1999. Green color gradient indicates upgrading process of vegetation succession. Red color gradient indicates degrading process of vegetation succession.

1988-1999 Total Area (km^2)	1999-2010 Total Area (km^2)																
CLASS	**BURN**	**CCTA**	**CCE**	**MD**	**VGR**	**GRASS**	**MF**	**OBF**	**BLF**	**SFRV**	**MSF**	**DPW**	**MTV**	**TOWN**	**ROAD**	**ROCK**	**WATER**
BURN	0.1062	0	0.018	0.2511	2.3697	1.287	2.2455	0.0099	6.5349	0.0855	0.108	0	0	0	0.0009	0.117	0.2637
CCTA	0.8541	0.0243	0.0585	0.549	4.9005	2.4156	2.7657	0.1035	8.1018	0.0009	0	0	0	0.0207	0.0171	0.0621	0.1404
CCE	0.2529	0.0576	0.4545	0	0.369	1.7667	0.3483	0	0.8874	0	0	0	0	0	0	0.1098	0
MD	0.1224	0	0	0.3429	0.9891	0.2286	0.2754	0	1.0674	0.0216	0	0	0	0.0135	0.0549	0	0
VGR	1.3518	0.2097	0.1332	0.7785	15.9309	28.6947	22.3056	1.3779	27.0648	0.0018	0.0684	0	0	0.0018	0.1773	0.828	1.2411
GRASS	5.4918	0.6957	0.5247	0.1719	7.4547	165.535	15.6564	1.7838	27.4311	0	0.1035	0.0117	0.0162	0.009	0.0585	1.5723	0.0594
MF	9.9081	0.9963	0.3105	0.8379	12.8349	42.399	41.4657	2.3688	100.433	0.1701	3.1077	0.1791	0	0.0477	0.0504	1.5795	1.0134
OBF	2.2635	0.1098	0.1422	0	2.2104	1.9692	8.244	22.7376	36.2295	0.072	0	0	0	0	0	0.4185	3.4065
BLF	108.887	5.9805	1.3239	6.9669	41.8617	69.345	212.485	23.6709	2134.61	15.0183	25.884	1.2267	0.0234	0.1179	0.7434	8.9937	7.8048
SFRV	5.3388	0.0063	0	0.0054	0.3789	0.1611	1.1736	0.036	68.5566	14.877	1.0179	0	0	0	0.0054	0.5553	2.0421
MSF	1.6326	0	0.0009	0.1962	0.0378	0.0072	0.0216	0	49.8411	0.8802	81.4131	3.1941	0.2457	0	0	0	0.0504
DPW	0.0063	0	0	0	0	0	0	0	1.6884	0	3.0789	17.8938	1.2717	0	0	0	0
MTV	0.0513	0	0	0	0	0	0	0	0.0666	0	0.7173	2.367	5.1795	0	0	0	0
TOWN	0.045	0.0045	0.0009	0	1.5696	0.6417	0.6381	0.0027	0.1953	0	0	0	0	2.025	0.1017	0.0333	0.0018
ROAD	0.207	0	0.0756	0.0009	0.2043	0.0297	0.4527	0.0009	1.4382	0	0	0	0	0.0099	1.9512	0.2718	0.1188
ROCK	0.387	0.0486	0.5634	0.0036	6.831	1.7064	9.8712	0.0693	2.8935	0.0072	0.0027	0	0	0.7434	1.0593	14.9274	1.1826
WATER	0.0072	0	0	0	0.0153	0.0072	0.0522	0.0126	1.8558	0.5931	0.0009	0	0	0	0.0054	0.324	111.414

Table 3.6. Area changes in different vegetation classes during 2010–2016 compared to 1999–2010. Green color gradient indicates upgrading process of vegetation succession. Red color gradient indicates degrading process of vegetation succession.

	2010-2016 Total Area (km^2)																	
	CLASS	BURN	CCTA	CCE	MD	VGR	GRASS	MF	OBF	BLF	SFRV	MSF	DPW	MTV	TOWN	ROAD	ROCK	WATER
1999-2010 Total Area (km^2)	BURN	1.5741	3.1644	0.7056	3.1167	13.8816	40.9257	18.5418	0.2961	50.6457	0.2178	0.8946	0.0072	0.0144	0.9306	0.4734	1.3941	0.1287
	CCTA	0.4293	0.0423	0.1998	0.7407	0.6291	1.6587	1.0746	0.0261	3.2418	0	0	0	0	0	0.0549	0.0351	0.0009
	CCE	0.0855	0	0.6102	0.0225	0.0063	0.495	0.5301	0.0324	1.6236	0	0.0216	0	0	0	0.1611	0.018	0
	MD	0.0171	0	0.063	0	5.769	1.4517	0.7101	0	1.6353	0.0063	0.4266	0	0	0.0045	0.0162	0.0045	0
	VGR	1.2447	0.027	0.72	3.2652	3.6819	18.7506	17.991	1.422	49.1004	0.009	0.036	0	0	0.279	0.2727	1.0341	0.1134
	GRASS	0.5427	3.0384	1.6668	2.3949	10.9485	216.296	36.4806	0.5967	41.7294	0.0027	0.0414	0	0	0.2637	0.4329	1.4157	0.2925
	MF	7.8813	0.0342	1.2555	8.7705	2.5983	24.3063	37.7244	5.8869	225.44	0.1746	0.2871	0	0	0.1512	0.8577	2.3004	0.3213
	OBF	3.2958	0	0.0801	0.3537	0.0027	0.6687	2.3517	15.6384	29.5704	0.0207	0	0	0	0	0.0405	0.0135	0.1377
	BLF	52.7517	0.1881	3.9762	30.969	12.6198	51.0975	98.775	14.769	2130.01	27.0972	34.6779	1.1691	0.0009	0.2952	3.1635	4.5486	2.6685
	SFRV	1.1511	0	0	0.0045	0.0162	0.0684	0.0072	0.0054	15.7005	13.3038	1.0008	0	0	0	0.0153	0.018	0.4365
	MSF	0.486	0	0	0	0.7344	0.423	0	0	33.0786	0.8559	76.9401	2.5776	0.3474	0	0.0009	0.0585	0
	DPW	0	0	0	0	0.0009	0.0288	0	0	2.3616	0	5.1831	15.7635	1.5048	0	0	0.0297	0
	MTV	0	0	0	0	0.0189	0.0342	0	0	0.0027	0	0.3474	1.2429	5.0742	0	0	0.0162	0
	TOWN	0	0.0153	0	0.0036	0.0882	0.4734	0.0099	0	0.2826	0	0	0	0	1.773	0.0873	0.2556	0
	ROAD	0	0.0126	0.0405	0.0117	0	0.3717	0.4122	0.0036	1.287	0	0	0	0	0.0135	1.8405	0.144	0.0882
	ROCK	0.0378	0.0657	0.1647	0.0306	0.2601	4.1427	1.0809	0.144	8.0064	0.045	0	0	0	0.8262	0.4779	12.8556	1.6398
	WATER	0.1278	0.0045	0.0369	0.0504	0.0324	1.5831	0.1755	0.2511	5.7564	1.7397	0.0225	0	0	0.0441	0.2484	0.1728	118.429

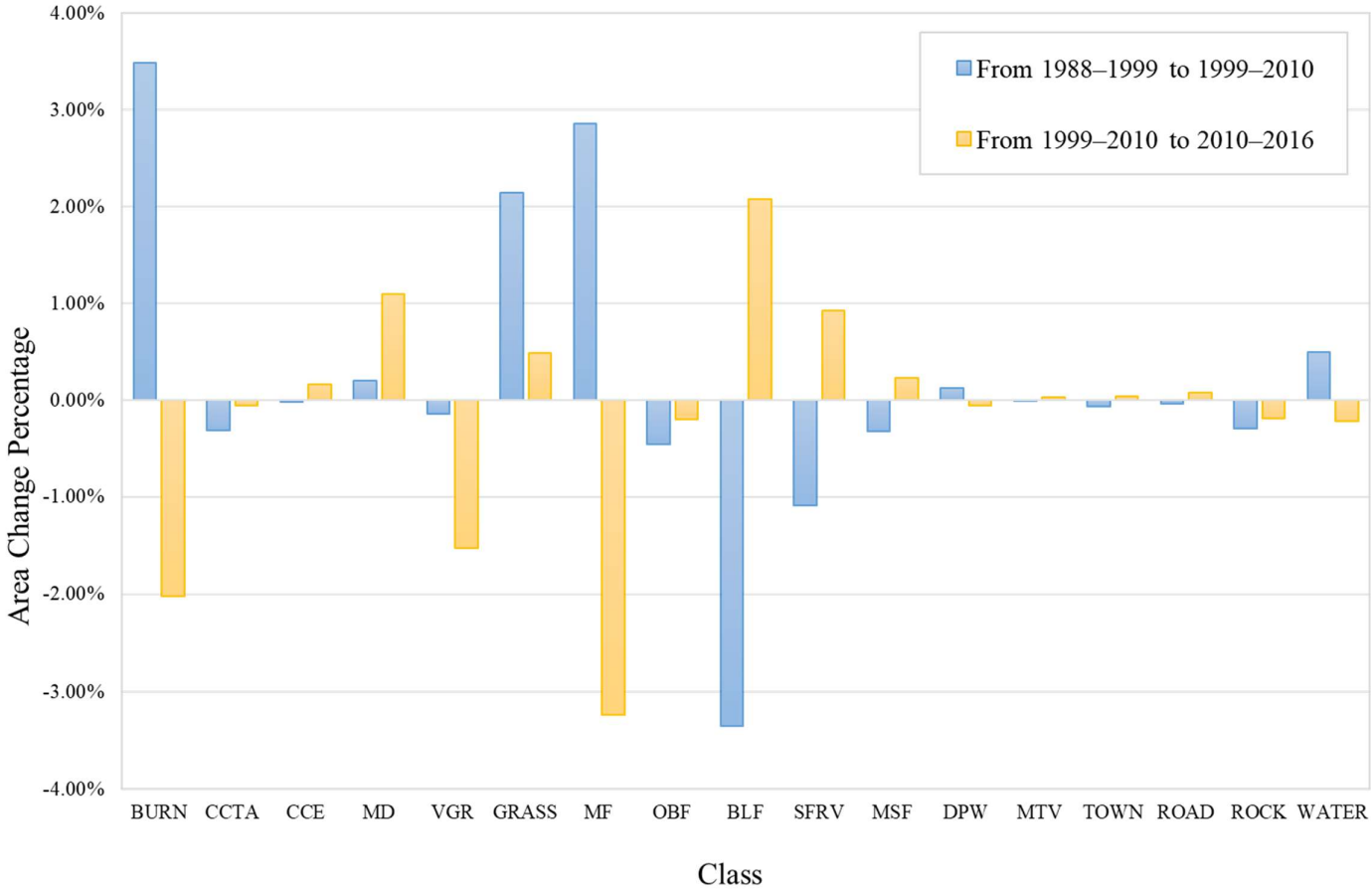

Figure 3.6. Area change percentage of class covers from the period of 1988–1999 to 1999–2010 and from the period of 1999–2010 to 2010–2016.

Some of the burned area areas in 1999–2010 repeatedly occurred during 2010–2016 (1.57 km^2), and some converted to mixed disturbance (3.12 km^2). Vegetation recovery area was unexpectedly low, at only 45 km^2 during 2010–2016. The largest conversion was mixed forests to birch and larch forests (225.44 km^2). The most surprising finding was the change of 51 km^2 of the burned area to birch and larch forests. Major disturbances increased from the period of 1988–1999 to 2010–2016, especially outside the reserve, and both burned areas and mixed disturbance occupied larger areas (Figure 3.7). The burned area contained a large percentage increase from the period of 1988–1999 to 1999–2010 for all zones, inside (5.36%), the buffer zone (1.86%), and outside (2.93%) of the reserve, while it decreased in all zones, from the period of 1999–2010 to 2010–2016 (Figure 3.8). Clearcutting area for timber or agriculture and mixed disturbance only occurred in the buffer zone and outside of the reserve. Clearcutting for timber or agriculture increased the area by more than 0.18% in the buffer zone from the period of 1988–1999 to 1999–2010. For the outside of the reserve, mixed disturbance appeared to expand the area more than 0.31% from the period of 1988–1999 to 1999–2010, and 1.69% from the period of 1999–2010 to 2010–2016.

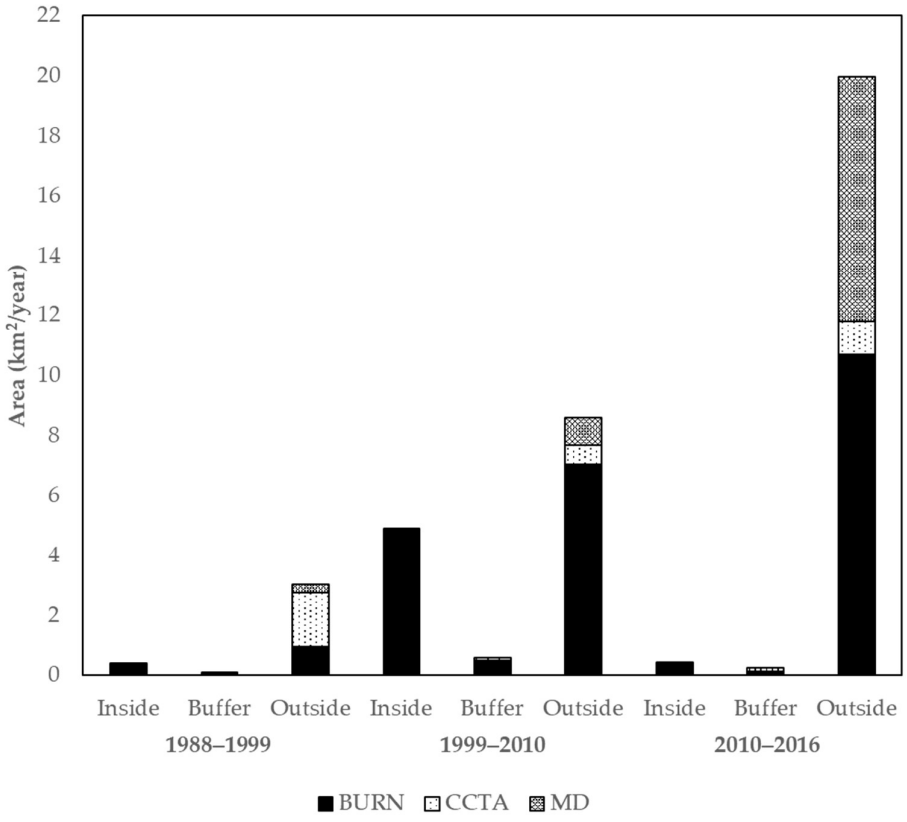

Figure 3.7. The area of major disturbance classes, per year, in inside, buffer zone, and outside of the reserve, during 1988–1999, 1999–2010, and 2010–2016.

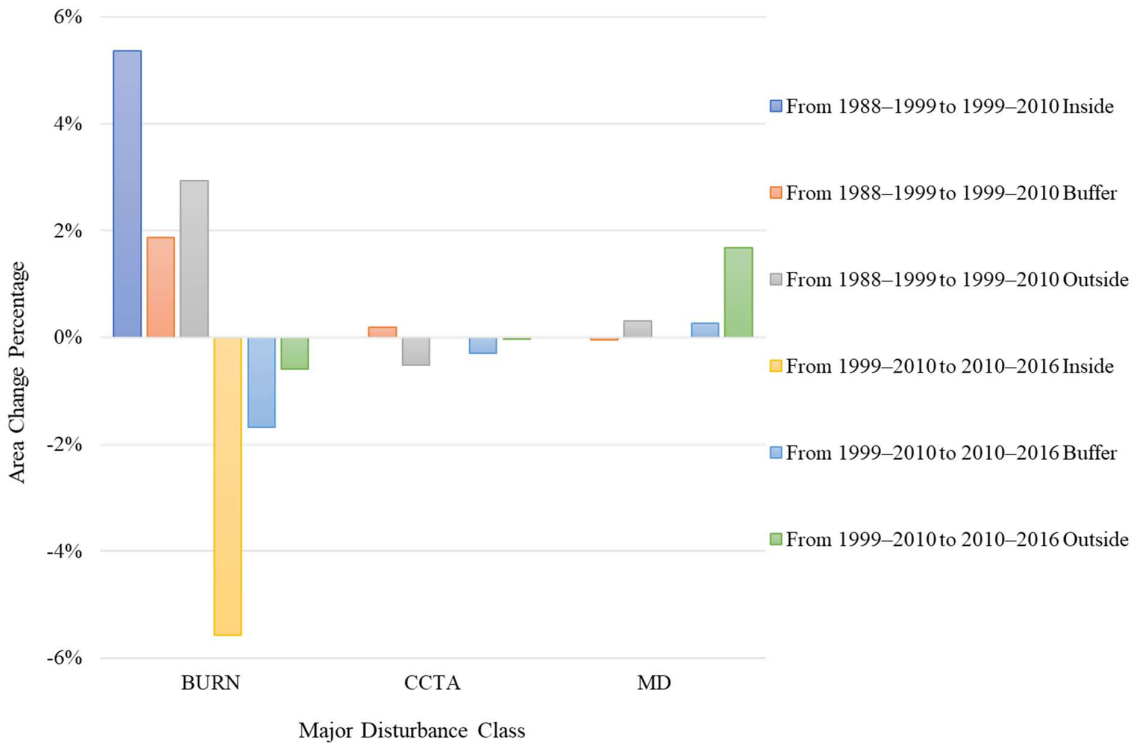

Figure 3.8. Area-change percentage of major disturbances inside, buffer zone, and outside the reserve, from the period of 1988–1999 to 1999–2010, and from the period of 1999–2010 to 2010–2016.

3.3.2. Determination of NDVI and NBR of Successional Stages

Mean NDVI and NBR values were lowest in burned area in 1999 and 2016 and tended to decrease during the study period. Most values were lower outside the Reserve than inside and in the buffer zone. Higher values mean a gain in vegetation coverage. The characteristic values of NDVI in the growing season for this geoclimatic region ranged from 0.3 to 0.8 for NDVI of birch and larch forests (Tei et al. 2019; Suzuki et al. 2011; V. I. Kharuk et al. 2013). Birch and larch forests, oak–Daurian birch forests, mixed forests, and vegetation recovery had higher NDVI and NBR values than grassland and burned area (Figure 3.9). The leftward and downward shifts of NDVI vs. NBR lines over time indicated that vegetation coverage decreased owing to disturbance. Birch and larch forests dominated the landscape, with larger NDVI and NBR, and with means between those of mixed forests and oak–Daurian birch forests. Oak–Daurian birch forests had higher mean values than the other five successional classes. The large-scale fire in 2003 occurred in many places with different degrees of severity. The long period (1999–2010) created a spatial mixture of vegetation coverage, so the mean NDVI and NBR values of the burned area areas varied between inside and outside the reserve. However, based on box plots of NDVI and NBR (Figures 3.10–3.13), some of burned area and vegetation recovery areas had already recovered to a similar index value as grassland or higher. I then determined the ranking of the six successional classes after burn disturbance from first to last as burned area, vegetation recovery, grassland, mixed forest, oak–Daurian birch forests, and birch and larch forests based on the field investigation information. Thus, after a forest fire, areas enter the vegetation recovery stage before grassland develops. The growth of broadleaf and conifer seedlings creates a mixed of short grass and some trees. Broadleaf oaks or birch fully occupy the areas a few years later. If the areas are far from water bodies, larch will finally outcompete them and dominate.

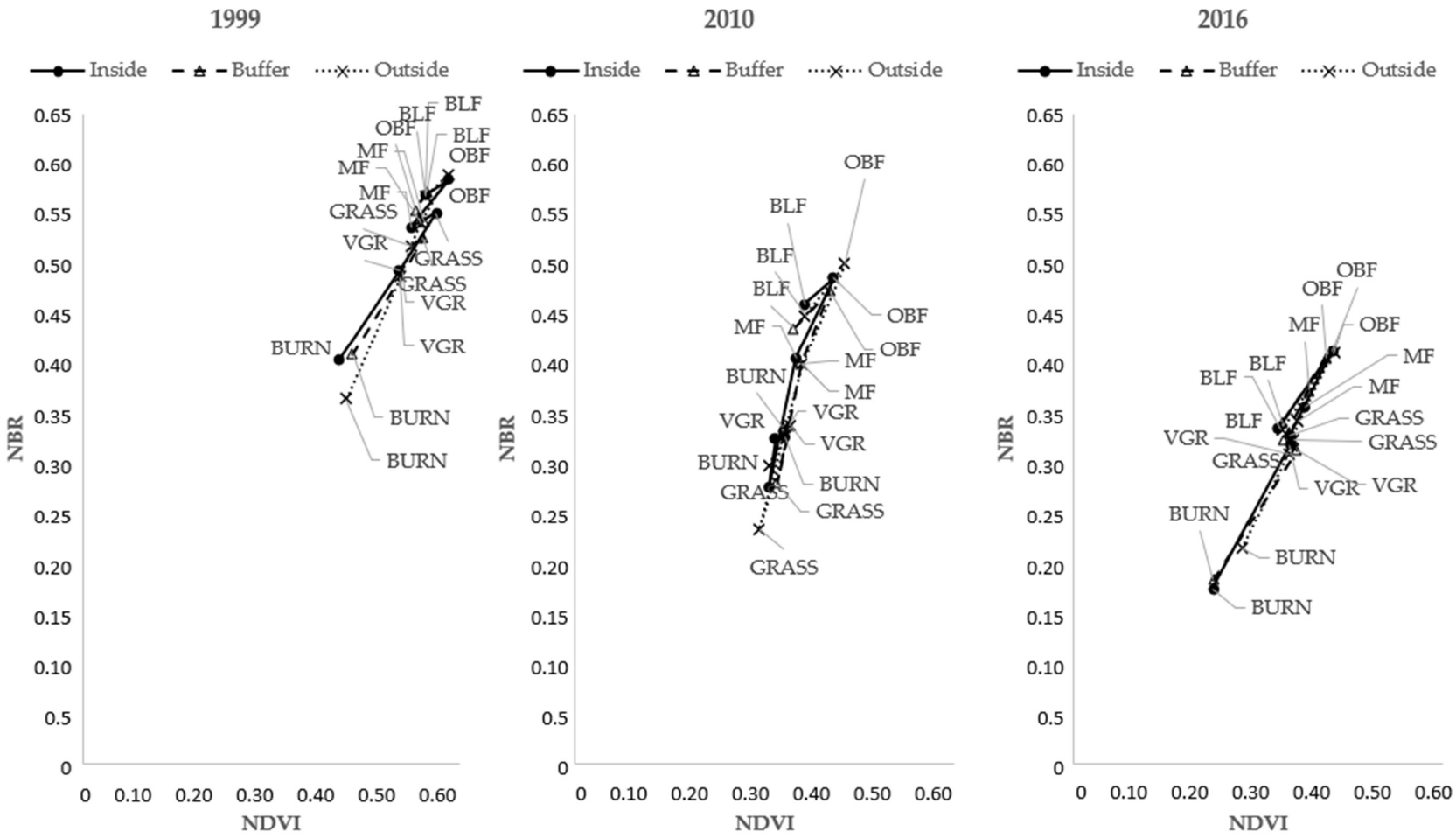

Figure 3.9. NDVI versus NBR inside, buffer zone, and outside of the Reserve in 1999, 2010, 2016.

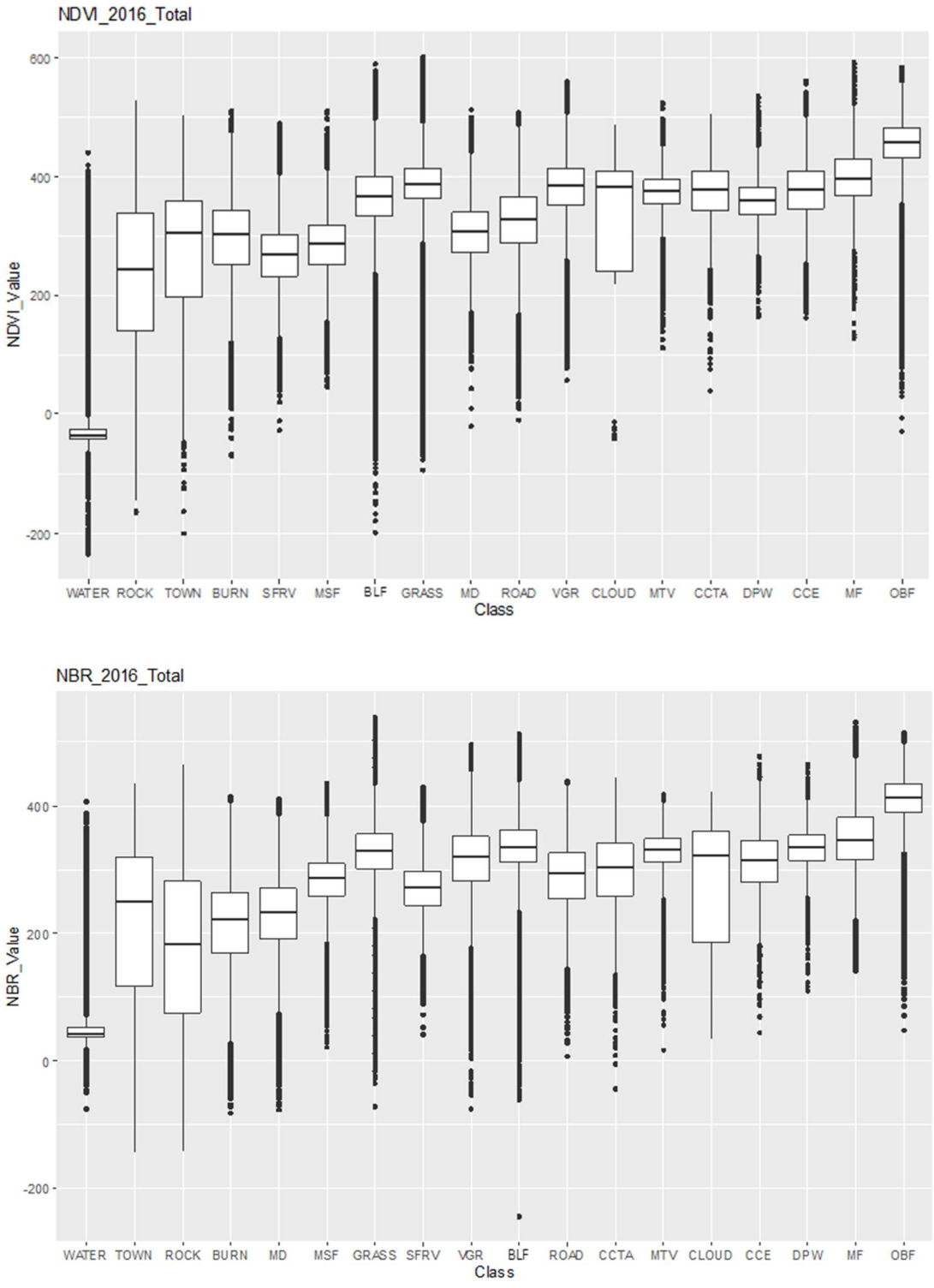

Figure 3.10. Box plot of (a) normalized difference vegetation index (NDVI) and (b) normalized burn ratio index (NBR) values for total area of the Reserve for each class in 2016. Middle line in box represents the median; lower box bounds the first quartile; upper box bounds the 3rd quartile. Whiskers represent the 95% confidence interval of the mean.

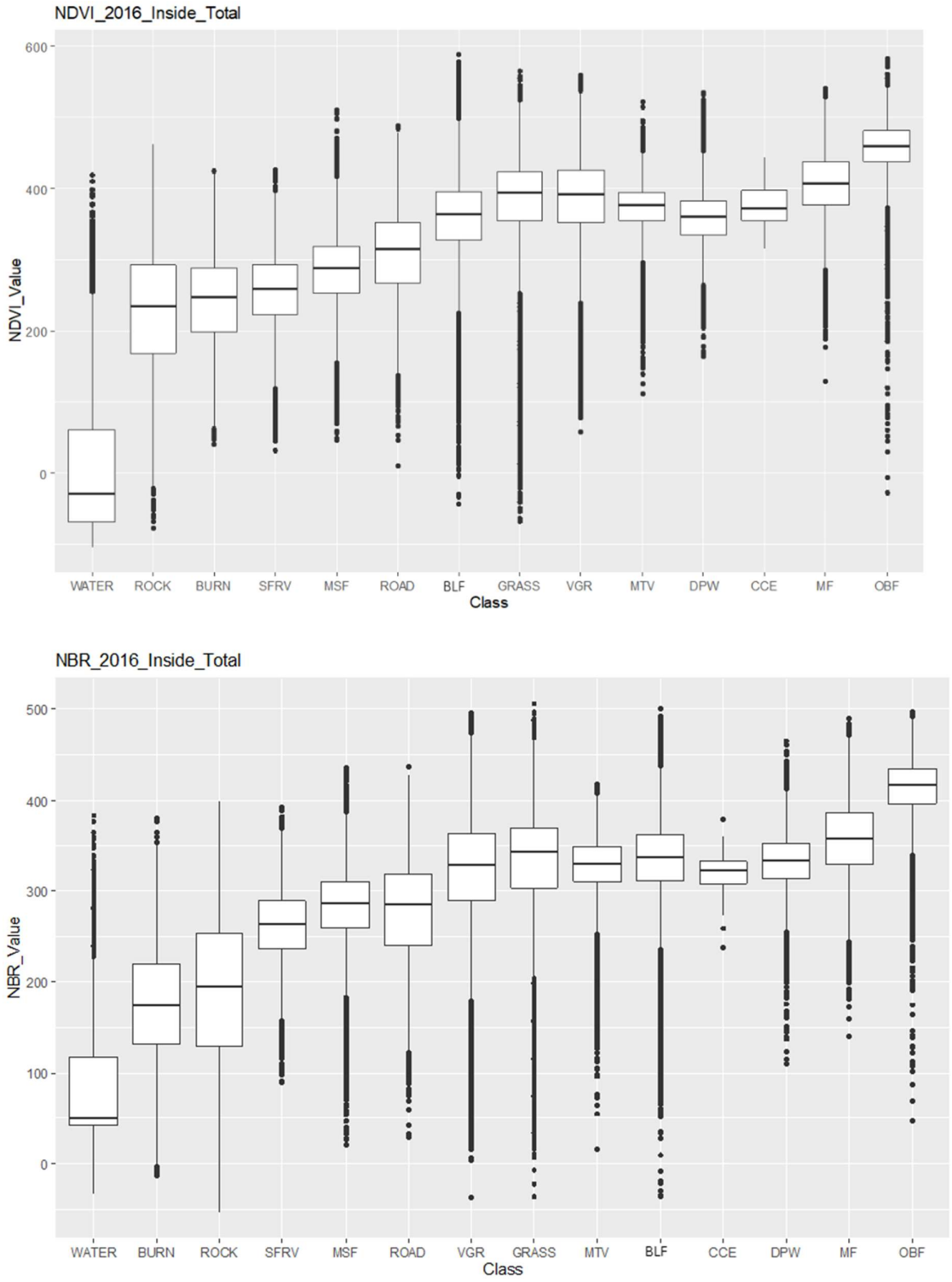

Figure 3.11. Box plot of (a) normalized difference vegetation index (NDVI) and (b) normalized burn ratio index (NBR) values in inside area of the Reserve for each class in 2016. Middle line in box represents the median; lower box bounds the first quartile; upper box bounds the 3rd quartile. Whiskers represent the 95% confidence interval of the mean.

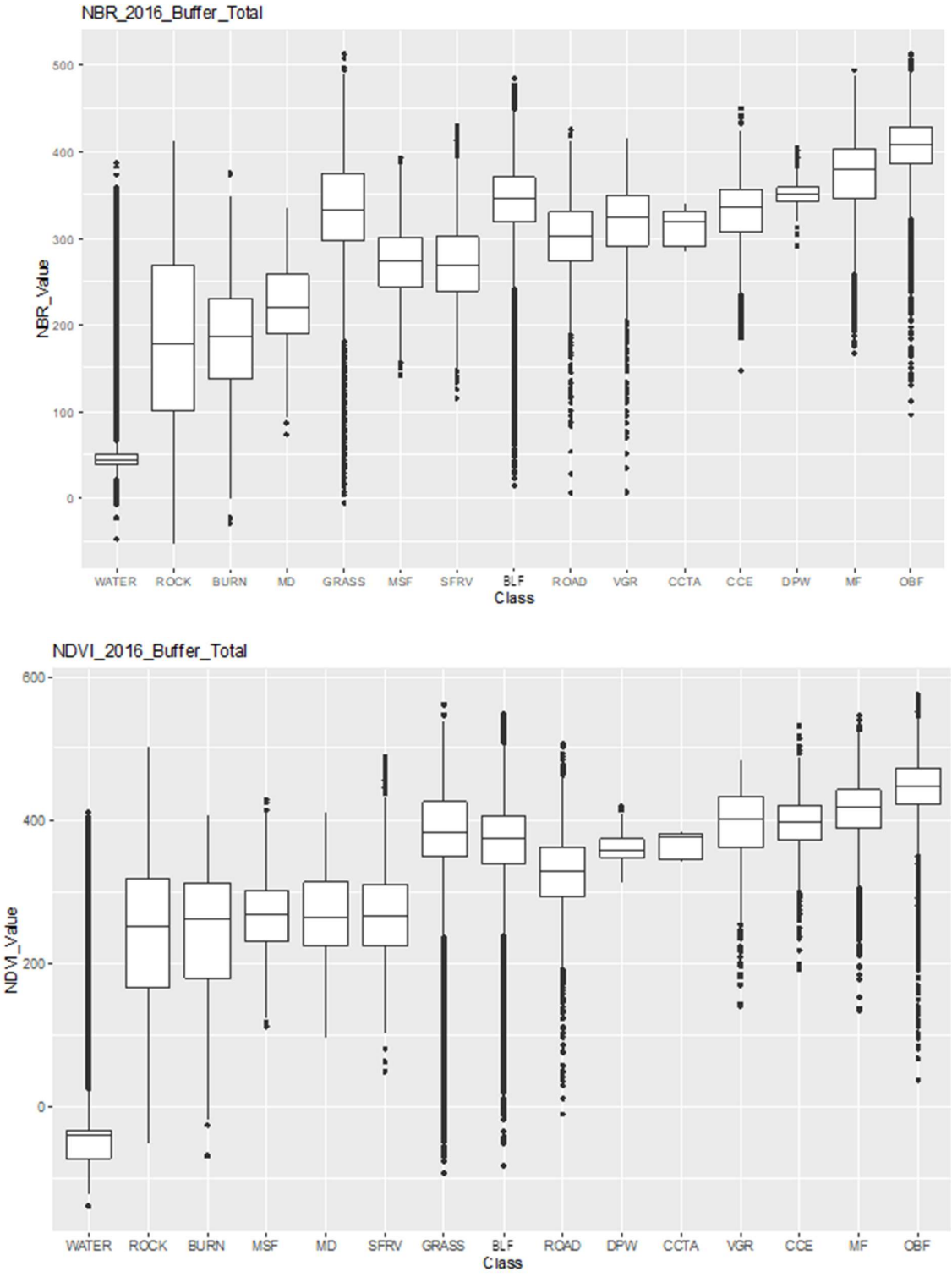

Figure 3.12. Box plot of (a) normalized difference vegetation index (NDVI) and (b) normalized burn ratio index (NBR) values in buffer zone area of the Reserve for each class in 2016. Middle line in box represents the median; lower box bounds the first quartile; upper box bounds the 3rd quartile. Whiskers represent the 95% confidence interval of the mean.

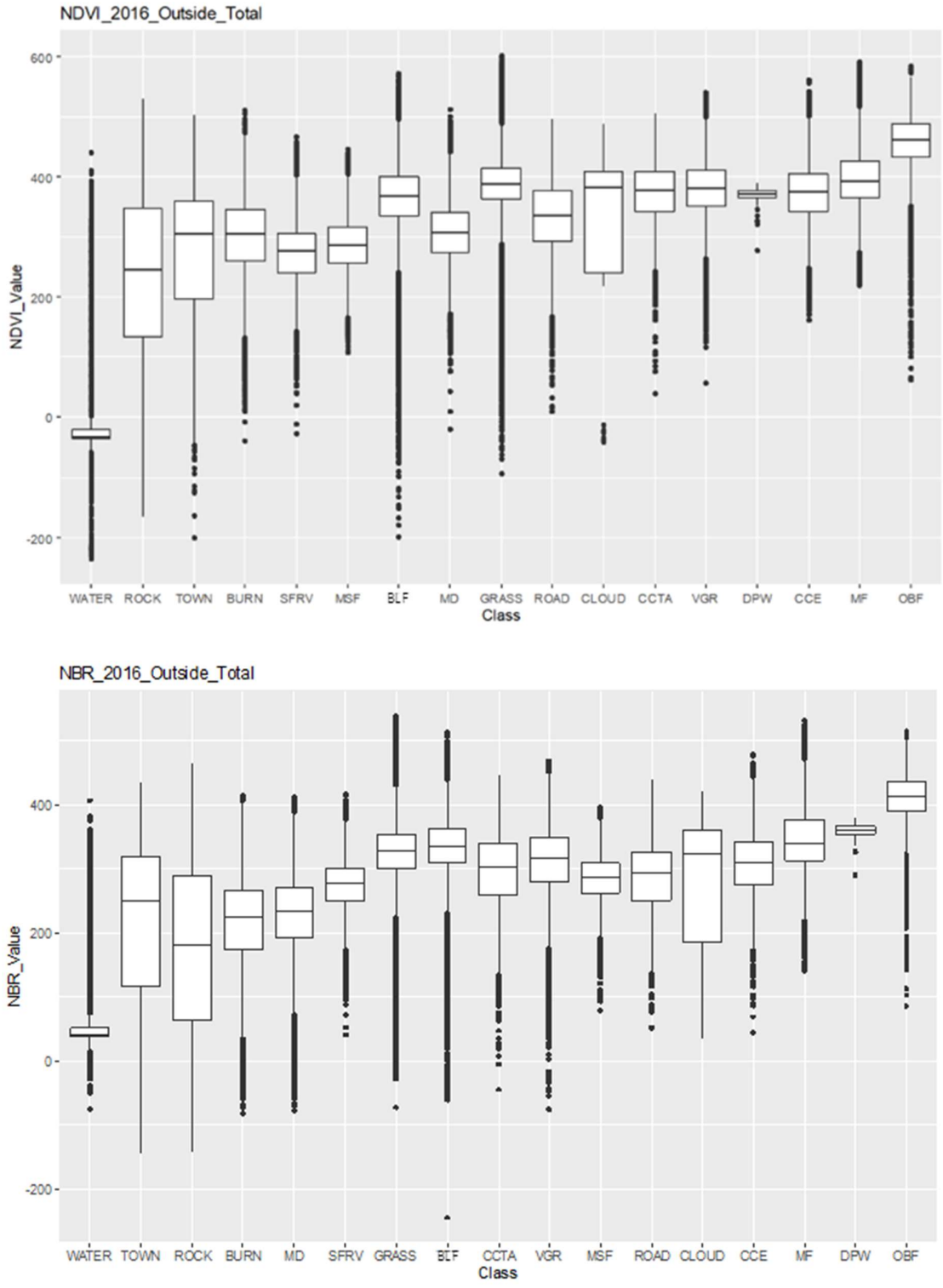

Figure 3.13. Box plot of (a) normalized difference vegetation index (NDVI) and (b) normalized burn ratio index (NBR) in outside area of the Reserve for each class in 2016. Middle line in box represents the median; lower box bounds the first quartile; upper box bounds the 3rd quartile. Whiskers represent the 95% confidence interval of the mean.

3.3.3. Effectiveness of the Reserve

The change matrices show the direction of forest successional change (Figure 3.14): upper right indicates higher stability, meaning forward succession, while lower left indicates lower stability, meaning backward succession. Green color gradient represented the forward successional stages and red color gradient represented the backward successional stages. The darker color means the higher percentages of an area moving toward that direction. Inside had higher ratios of each class moving forwards than the buffer, and outside of the reserve. On the contrast, outside had higher ratios moving backwards successional stages than inside the reserve. From the period 1999–2010 to 2010–2016, inside of the Reserve was well protected, with all the classes moving backward successional stages were less than 5%. From the period of 1999–2010 to 2010–2016, 40.20 km^2 of mixed forests outside converted to grassland, the largest ratio (22%) of backwards succession, indicating significant forest area loss to fire (Table 3.7). During the same time, 11.5% of mixed forest area in the buffer zone was converted to grassland while the inside of the Reserve showed the smallest area of mixed forest-grassland conversion. More than 10% of mixed forests, oak–Daurian birch forests and birch and larch forests in the buffer zone and outside of the Reserve moved at least one class backward on the forest successional stage from the first period to the second period.

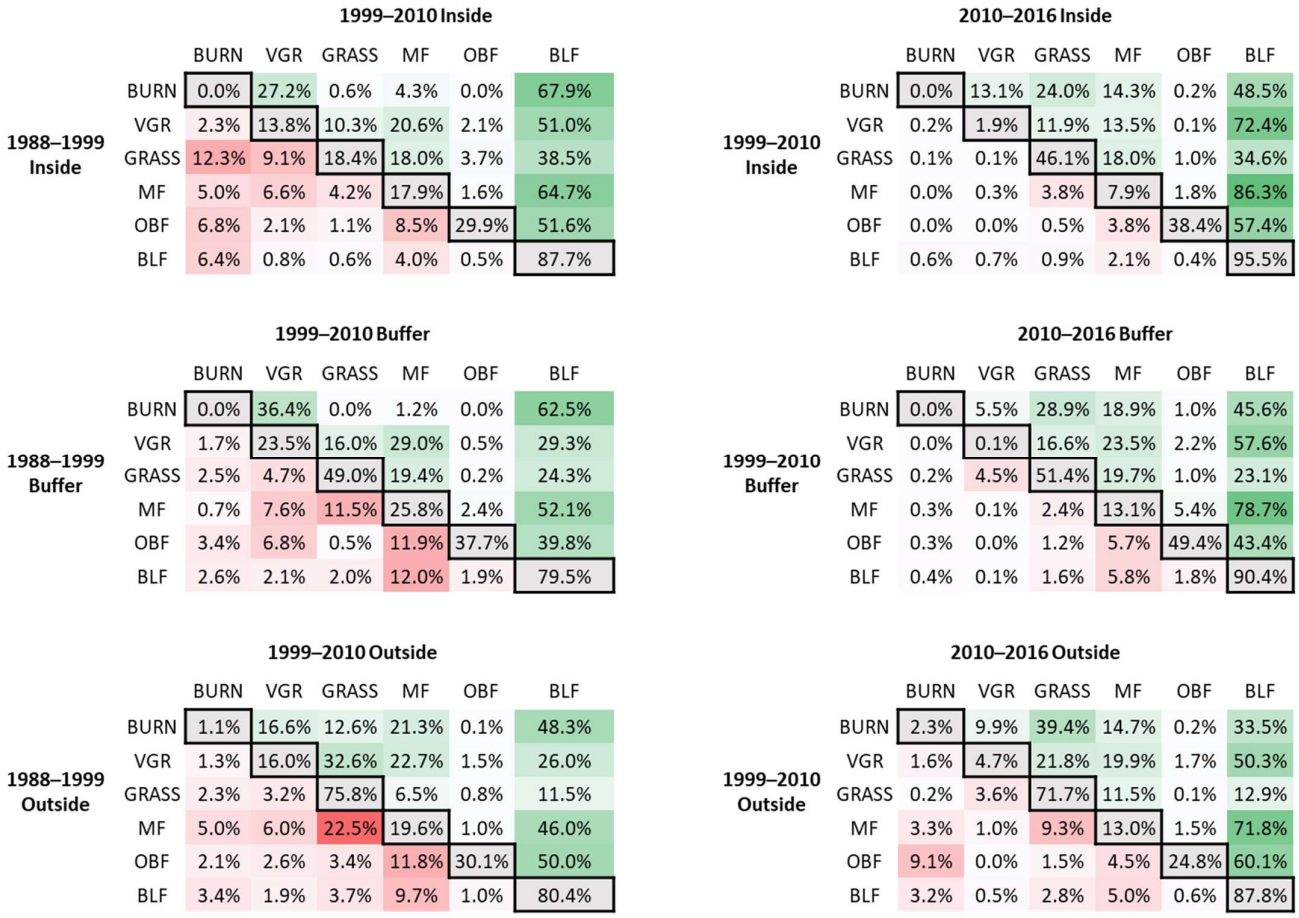

Figure 3.14. Percentage of area changes of forest successional stage classes green color gradient represented the forward successional stages, red color gradient represented the backward successional stages. The darker color means the higher percentages of an area moving toward that direction.

Table 3.7. The change matrix of successional stages of class cover area (km^2) in different periods and different zones of the Reserve.

	1999–2010 Inside								2010–2016 Inside							
		BURN	VGR	GRASS	MF	OBF	BLF	Total			BURN	VGR	GRASS	MF	OBF	BLF	Total
1988–1999 Inside	BURN	0	0.6147	0.0144	0.0981	0	1.5354	2.2626	1999–2010 Inside	BURN	0.0153	6.8742	12.6018	7.5231	0.1062	25.4916	52.6122
	VGR	0.1521	0.8955	0.6687	1.3356	0.1341	3.3102	6.4962		VGR	0.0189	0.1836	1.1826	1.3401	0.009	7.164	9.8982
	GRASS	0.4275	0.3186	0.639	0.6264	0.1305	1.3401	3.4821		GRASS	0.0054	0.0081	2.8089	1.098	0.0639	2.106	6.0903
	MF	0.9063	1.1862	0.7506	3.2112	0.2934	11.6217	17.9694		MF	0	0.0909	1.3518	2.8458	0.6372	30.9636	35.8893
	OBF	0.9171	0.2763	0.1485	1.1376	3.9978	6.9138	13.3911		OBF	0	0	0.0396	0.3249	3.2994	4.9284	8.5923
	BLF	47.2599	6.2649	4.2039	29.3067	4.0581	648.4518	739.5453		BLF	3.9078	4.6998	6.0525	14.3442	2.4588	665.5131	696.9762

	1999–2010 Buffer								2010–2016 Buffer							
		BURN	VGR	GRASS	MF	OBF	BLF	Total			BURN	VGR	GRASS	MF	OBF	BLF	Total
1988–1999 Buffer	BURN	0	0.0828	0	0.0027	0	0.1422	0.2277	1999–2010 Buffer	BURN	0.0009	0.2925	1.5273	0.9981	0.0531	2.4048	5.2767
	VGR	0.1386	1.9062	1.2942	2.3553	0.0405	2.376	8.1108		VGR	0	0.0054	1.2735	1.7973	0.1692	4.4163	7.6617
	GRASS	0.1539	0.2889	3.0375	1.2042	0.0126	1.5048	6.2019		GRASS	0.0216	0.4185	4.7646	1.8234	0.0972	2.1429	9.2682
	MF	0.0882	0.9531	1.4481	3.2409	0.2961	6.5565	12.5829		MF	0.0999	0.0234	0.7029	3.852	1.5759	23.0715	29.3256
	OBF	0.2763	0.5598	0.0378	0.9828	3.1032	3.2805	8.2404		OBF	0.0216	0	0.0828	0.3942	3.4254	3.0042	6.9282
	BLF	4.6467	3.7332	3.6207	21.8178	3.5451	144.639	182.0025		BLF	0.5688	0.1251	2.5506	9.351	2.8863	146.0259	161.5077

	1999–2010 Outside								2010–2016 Outside							
		BURN	VGR	GRASS	MF	OBF	BLF	Total			BURN	VGR	GRASS	MF	OBF	BLF	Total
1988–1999 Outside	BURN	0.1062	1.6722	1.2726	2.1447	0.0099	4.8573	10.0629	1999–2010 Outside	BURN	1.5579	6.7149	26.7966	10.0206	0.1368	22.7493	67.9761
	VGR	1.0611	13.1292	26.7318	18.6147	1.2033	21.3786	82.1187		VGR	1.2258	3.4929	16.2945	14.8536	1.2438	37.5201	74.6307
	GRASS	4.9104	6.8472	161.8587	13.8258	1.6407	24.5862	213.669		GRASS	0.5157	10.5219	208.7226	33.5592	0.4356	37.4805	291.2355
	MF	8.9136	10.6956	40.2003	35.0136	1.7793	82.2546	178.857		MF	7.7814	2.484	22.2516	31.0266	3.6738	171.405	238.6224
	OBF	1.0701	1.3743	1.7829	6.1236	15.6366	26.0352	52.0227		OBF	3.2742	0.0027	0.5463	1.6326	8.9136	21.6378	36.0072
	BLF	56.9799	31.8636	61.5204	161.3601	16.0677	1341.517	1669.308		BLF	48.2751	7.7949	42.4944	75.0798	9.4239	1318.469	1501.537

3.3.4. Analysis of MODIS Data

Figure 3.15 shows the annual distribution of the MCD64A1 product's burned areas over the Reserve for a whole year and the monthly distribution of burned areas detected from 2000 to 2016. The fire season usually occurred from March to May. These three months contained the largest burned areas per month. Approximately 50% of the total burned areas detected in my study area were aggregated in 2002, 2003, 2008, and 2015. On the contrary, 2000 and 2009 had no registrations of burned areas.

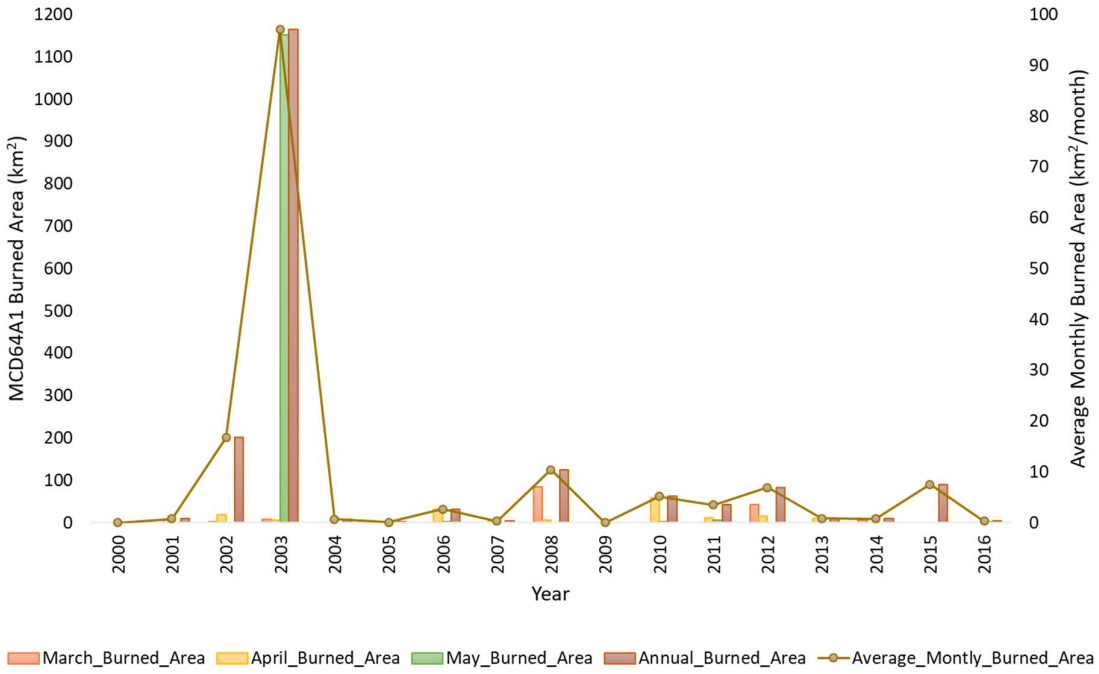

Figure 3.15. The burned area in the study area (March, April, May, and whole year only) obtained by the MCD64A1 product.

3.4. Discussion

3.4.1. Forest Cover Change and Disturbance

This study is the first to assess fire disturbance and forest-cover change in the Zeya State Nature Reserve at the landscape scale. I used remote-sensing data to compensate for the lack of data in this remote region. Although ground-truth data were insufficient for accurate classification, my results show a high accuracy of classification maps. To analyze forest dynamics from long-time interval Landsat images, I used mean NDVI and NBR values to extract forest successional stages. The vegetation recovered through successional stages of grasses, shrubs, broadleaf and conifer trees, oak–birch forest, and birch and larch forests after severe fires (Figure 3.16). The results of the classification maps showed that several classes had both low producer's accuracy and low user's accuracy. The low producer's accuracy of the disturbance classes (burned area, clearcutting for timber or agricultural, and mixed disturbance) in the 1988–1999 map was due to the limited ground-truth information in the historical data. The low user's accuracy for burned area, mixed disturbance, and vegetation recovery in the 1999–2010 map was due to limitations in distinguishing spectral values due to the massive burned class being possibly adjacent to or including clearcutting area (Escuin, Navarro, and Fernández 2008). More high-resolution images are needed to monitor whether the tree canopy has been cut down in the disturbance classes. The sufficient data that can separate burned area and mixed disturbance will further improve the accuracy of classification.

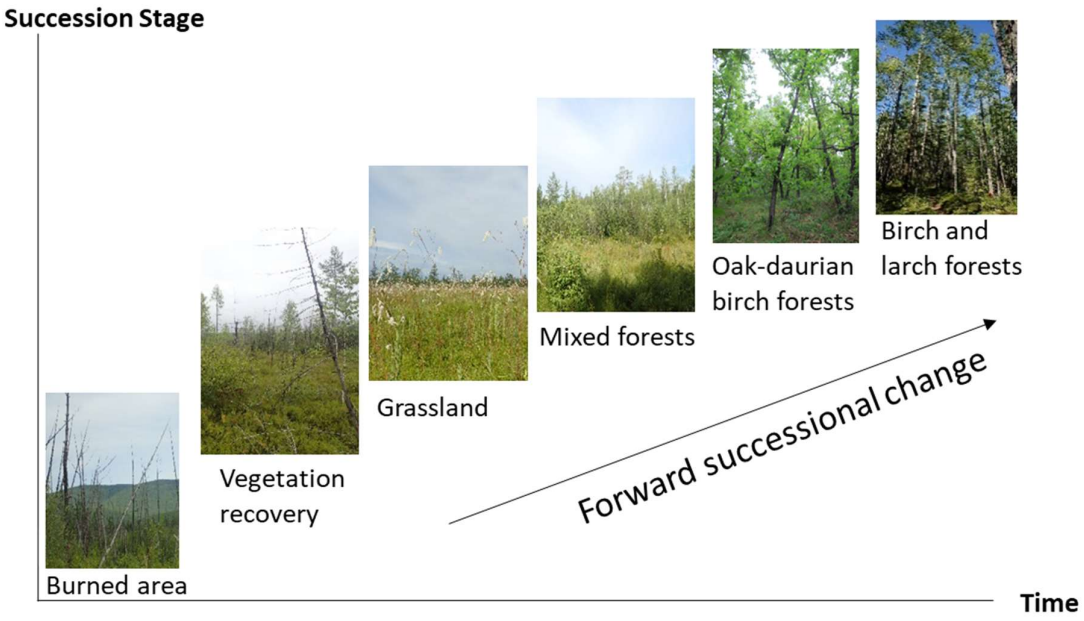

Figure 3.16. Typical forest successional gradient after forest fire disturbance on Zeya State Nature Reserve.

3.4.2. NDVI and NBR of Successional Stages

The large-scale conversion of a mature forest to a lower successional stage is rarely observed in nature. Low-intensity, short-interval disturbances in the late 1980s to early 1990s reverted larch and birch forests to earlier ecological stages (Fernández-Nogueira and Corbelle-Rico 2018). Clear-cut areas outside the Reserve were associated with forest fires in recent years, challenging the separation of types of disturbances with similar severity. Vegetation indices helped determine the forest and disturbance types (Escuin, Navarro, and Fernández 2008). However, I found a similar range of mean NDVI and NBR values for grassland and burned area, owing to rapid understory vegetation recovery (Smith et al. 2016). Intense disturbances created a massive loss of the forest canopy and understory vegetation, which showed up as lower vegetation areas on the Landsat images (Ju and Masek 2016). The decrease in NBR mean values during all three periods might be linked to the long-term effects of human activities on the ecosystem (Fiore et al. 2020). In the future, I will research the potential of

using other difference satellites, such as Russian, Japanese, Chinese or Indian satellites to cover the gaps due to cloud coverage. my study also contained enormous diversity of land features, from flat terrain to steep hills. Other satellite sensors, such as, the Sentinel-1 and Sentinel-2 data, could help me generate images with high temporal resolution for differentiating small agricultural areas and grassland (Kpienbaareh et al. 2021). The synthetic aperture radar (SAR) have been widely used to detect clearcutting in the tropical forest (Ruiz-Ramos et al. 2020), however, my study did not involve such a method. I will also apply SAR-based change detection approach to monitor clearcutting evidences in my study area in the future.

As I assumed some forest areas can suffer repeated fires, the recovery from which varies, while other places might only experience fire once and recover rapidly. Some heavily disturbed areas can only restore to the recovery stage of grass and mixed forest (Chen and Loboda 2018) while others with fewer and less intense fires might have a higher possibility of recovering back to the original forest stage (Bright et al. 2019). For simple succession, such as recovery stage and grass, the whole process might finish within a year. On the other hand, the large severe fire area in mature forests might require longer recoveries. Birch and larch forests and oak forests might take years to recover. From 2010 to 2016, grassland, vegetation recovery, and mixed forests did not differ much in NBR compared with BLF and OBF, which had lower NBR values than 1999–2010. This might be due to much slower recovery than grassland (Dong Chen et al. 2016) or because the fire occurred near the post-year image.

3.4.3. Effectiveness of the Reserve and MODIS Data

MODIS showed supporting evidence that major fire damage occurred in the early years in the 1999–2010 period and later in the 2010–2016 period. This temporal variation in fire occurrence within a period can impact the recovery stage detected at the end of the period (Dong Chen et al. 2016; Bright et al. 2019). The years 2015 and 2016, which were the final years of the classified map 2010–2016, included larger recent fires than the years 2009 and

2010, which had small fires. A large-scale fire settled in the year 2003, so the recovery process of some classes in the 1999–2010 period might have had higher NBR and NDVI values than the 2010–2016 period. Even though this analysis did not involve forest succession process based on local climate (temperature and rainfall) and soil type, I recommend that future work consider those factors. My approach overcame the gaps inherent in long-interval image analysis.

The findings of MODIS revealed that large areas of burning during 2002, 2008, 2012 and 2015. The findings matched the recorded fire map for all years except 2008. The southwest of the Reserve had a fire in 2002, while the northern border of the Reserve had a fire in two areas in 2012. In 2015, due to extreme temperatures and high winds, Russian wildfires have caused large damage around the reserve. The fire was initially set to clear grass but it was out of control, causing vast areas of forest loss from Trans Baikal to the Far East of Russia. Historical documents failed to capture the burned area inside the Reserve during 2008, my approach by using MODIS showed that the satellite could capture forest fire in an inaccessible location. I also found that the burned area from the records in 2000 and 2011 was absent from the MODIS data and the Landsat image, the location is yet to be explored, and in the future I will look for further confirmation from other satellite images. The overall study period showed the effects of strong enforcement of the protection of the reserve. Even though forest fires occurred inside the reserve, from 1999 to 2010, other human-made disturbances were low. The buffer zone around the Reserve and the area outside the Reserve faced more deforestation and burning, which pose threats to the area inside the reserve. Thus, more restrictions should be established to avoid unpredicted consequences. The buffer zone perhaps experienced more disturbances due to infrequent monitoring and the difficulty of preventing large fires. Difficulties in assessing such terrain also restrict enforcement. Forest fires and clearcutting were concentrated near the Reserve boundary because of timber activities along the roads and flat terrain.

Even though remote-sensing data are useful in detecting burned areas, I found three limitations of the object-based segmentation classification. First, the Landsat surface reflectance's pixel values were similar for clearcutting objects and neighboring objects that represented burned areas. Differentiating between mixed disturbance and burned areas on Landsat images is difficult (Schroeder et al. 2011). Due to the extensive cloud cover and early vegetation regrowth, it was also difficult to identify fire scars and clearcutting area (Cocke, Fulé, and Crouse 2005). Second, the time-resolution of my study was not fine enough to detect precise disturbance events and vegetation recovery. The early recovery of grasses and shrubs (secondary succession stage) after a disturbance has been overlooked during long periods and has instead been interpreted as grassland. Third, areas burned from 1988 to 1999 and clear-cut for agriculture from 2010 to 2016 were minimal (Schroeder et al. 2011).

Our results suggest the need for more frequent observation and the incorporation of environmental factors. Sufficient ground-truth data of historical disturbance—not only large-scale fires but also small fires and clearcutting—would enhance classification accuracy. Analyzing large areas in short time intervals is difficult, costly, and laborious. Instead, using long-interval Landsat images is possible if I consider the successional stage as supporting information. This would allow me to recognize how fast the understory vegetation has recovered and the effectiveness of reserves at protecting fauna and flora (Bragina et al. 2015). For example, mountain tundra vegetation and other alpine ecosystems are well protected from human disturbance, but they are vulnerable to climate change(Makoto et al. 2016). Therefore, knowing how forest covers change over time inside and outside protected areas, especially in inaccessible locations, can improve forest conservation and management [9,55,57]. Information on forest fires, timber harvesting, and other anthropogenic activities around reserves, along with the help of remote-sensing techniques, can support park protection (Wendland et al. 2015; Chistyakova and Leonova 2003; Degteva et al. 2015; Wade et al. 2020).

3.5. Conclusions

Using open-access satellite data is essential for detecting forest disturbance and forest-cover change. Applying object-based segmentation classification, using overlaid images from different years, also increased the accuracy and consistency among forest-cover-change maps. The analysis of successional stages based on NDVI and NBR values provided important insights into forest-cover-change patterns inside the Zeya State Nature Reserve, in the buffer zone, and outside the reserve, from the periods of 1988–1999, 1999–2010, and 2010–2016. Severe burning from the periods 1999–2010 and 2010–2016 revealed the critical role of fire in forest dynamics. Most areas burned outside the Reserve were associated with clearcutting, indicating that anthropogenic factors influenced forest fire and forest-cover change. Even though the Reserve is protected effectively, I found a reduction of both vegetation indices in burned areas, so there is no guarantee that forest-cover change and disturbance patterns outside the Reserve will not affect the forest dynamics inside it.

The direction of forest successional stages is based on disturbance severity. Some forest areas did not return to their climax class. The dominant birch and larch forests were found to be linked with burned areas. If the consequences of disturbances are not predictable, the risk of losing biological diversity and ecological function is high. There is an urgent need for multiple-spatial-scale studies of how forest fires have behaved recently. Data on fire frequency, intensity, and severity can identify susceptible areas.

This study supported the assumption that fires are becoming more frequent in boreal forest and have been more extensive in recent years, affecting forest-cover patterns and trends. Unexpected weather events, increasing demand for timber along the Russia–China border, and increases in legal and illegal logging activity could alter the boreal forest ecosystem. Thus, a better understanding of recent forest fires and forest-cover changes in remote areas is needed to develop better ways to preserve biological diversity and ecosystem services. My research

has yielded data on forest disturbances in remote areas that other researchers can use to improve forest management and conservation plans for large-scale protected areas.

I encourage further studies using vegetation indices to determine ecological succession after disturbances to overcome the disadvantages of long-time-series analyses. Such methods can reduce the effort needed to monitor global forest trends. I also recommend that future studies focus on forest disturbances and forest-cover patterns in other protected areas, so that I can understand the effectiveness of forest conservation there as well.

Chapter IV

Analysis of Disturbances and Environmental Factors and Climatic Data between Inside, Buffer, and Outside of Zeya State Nature Reserve, Russia

Summary

This study proposed to use patch-wise method and the maximum entropy approach to combat the challenges of disturbance monitoring in large area. The results suggested that patch analysis provided opportunity for scientists to understand the frequency and the massiveness of the disturbance events occurred through time. MaxEnt also provided a useful tool when dealing with disturbance presence-only data and allowed the researchers to understand the importance of environmental and climatic data that influenced the distribution of disturbances. The technique acquired essential information without vast field-based information gathering. Specifically, in a setting of environmental and climatic variables, this study provided vulnerable area information based on an open-source Landsat data and freely-analyzing software to understand the distribution of disturbances around protected area.

Chapter 4 uncovered the importance of measuring the contribution and effects of environmental and climatic variables that influenced the changing of disturbance distribution. The Reserve needed updated information and integrative works of many protected area across the Russia Far East to understand the disturbances pattern. The study recommends future research to explore on other disturbance types and other forest ecosystems such that to improve world's forest conservation and planning. The findings inspired further investigations to also look at the fire cycles that might be the effect of climate change across the regions.

Chapter V

Effectiveness of a Protected Area, Measured by the Change in Vegetation Indices of Forest Covers and Disturbances in the Inside, Buffer, and Outside Zones of Zeya State Nature Reserve, Russia

Summary

Changes in human habitats, increasing infrastructure, and climate changes may contribute to unpredictable consequences. On the basis of dNDVI and dNBR, this study raised a concern that although the Reserve is effective in terms of protection and the restriction of human activity inside the Reserve, the outside and buffer zones were exposed to severe disturbances, resulting in the large loss of forest area. This study found potential uses for the relationship between dNDVI and dNBR, in recognizing the difference in stableness between forest and disturbance classes. The magnitude of change of dNDVI and dNBR could be a strong measurement tool to analyze spatial heterogeneity. The results demonstrated that forest classes were more stable than disturbance classes based on dNDVI and dNBR. Although many inside the Reserve classes showed a relatively lower *S* value than that of the buffer or outside zones, I found no significant difference between zones when using the ANOVA test. However, the results seemed to have a certain trend toward significance difference interpretation. I could interpret that the inside of the Reserve is generally more stable than the buffer zone and the outsideThe expansion of monitoring and the stronger enforcement of illegal cutting along the roads and mining along the river near the Reserve's border are hence suggested, to reduce the risk of losing the edge forest inside the Reserve.

Chapter VI

General Discussion and Conclusion

In the Russian Far East, the remote boreal forests faced unsurprising threats from deforestation to degradation from human activities(Potapov et al. 2008; Chen and Loboda 2018). The decades of clearcutting for timber and forest fire impacted the change of forest ecosystem and its structure. The strong demand of timber worldwide, especially high demand of imports by China on housing development implies illicit harvesting or bogus licenses in logging operations (Peterson et al. 2009). The landscape environment can only be preserved by the stabilization of a protected status of the Reserve and the restoration of ecosystem within it (Degteva et al. 2015; Chistyakova and Leonova 2003; Elbakidze et al. 2013; Wendland et al. 2015). In order to maintain the conservation efforts of the Reserve, it demanded advancement of technology that can remotely observe information from the distance. The knowledge obtained from remote sensing data evolved sciences in remote forests in the region (Potapov et al. 2008; Bartalev et al. 2014; Chen and Loboda 2018; Chen et al. 2016; Chu, Guo, and Takeda 2016). This thesis focused on how to evaluate the effectiveness of the protected area in the Russian Far East by giving the application of remote sensing to answer the objectives of the introductory chapter.

6.1. Monitor Forest Cover Change and Disturbances and Effectiveness of Protected Area by Using Long-Time Interval Satellite Image Analysis

This thesis is the first study that monitored the forest cover changes and disturbances occurred around the Reserve. It introduced new techniques to evaluate the forest cover changes and disturbances and accessing the effectiveness of the Reserve. The Reserve, Zeya State Nature Reserve had been used as the study area in this thesis. This is also first time producing both long-time interval and short time interval classification maps which helped me to understand more of forest dynamics around the Reserve region and how the protection status

helped maintain the forest ecosystem in the region. The performance of classification maps did not just explain the location of each forest types and disturbances, but also telling the importance of losing forest classes in each different zone that contain different conservational status. This thesis created the possibility for other researchers to utilize the information and develop conservation management plan to protect biodiversity and resource use in other areas. The adoption and application of the methodologies also expanded the scope of forestry and conservation studies and other disciplines.

The chapter 3 highlighted how forest cover and disturbances in the protected area, such as logging and fire problems, using two-year overlaid image classification by classifying two long-time interval images at the same time. Because there were only four suitable satellite images available in the study area, I found that during master thesis, the single year image classification provided low accuracy results and unstable in class area. The two-overlaid-image classification then being considered. The classification results showed high accuracy, thus this method provided the solution with the long-time image available and to deal with how disturbance it shaped the ecosystem within the region. The outstanding results showed that 2-year overlaid long-time interval images stabilized the class to monitor the changes. During 1988-1999, clearcutting had the highest impact on forest around the Reserve because human needed the woods for house and city expansion near the reservoir (Peterson et al. 2009; Dubinin et al. 2010). The availability of the water resources allowed human settlement to expand and more infrastructure has been developed (Peterson et al. 2009). Historical forest fire had caused a massive die-off of larch and birch forest both outside and inside the Reserve (Chen and Loboda 2018; Chen et al. 2018). Several oak forest near rivers and spruce forest upon the mountain also had lost. Several studies found less demand for timber harvesting during the late 1990s and early 2000s as a result of abandonment of agriculture and people moving toward capital city in which made the population around the Reserve to be lower than previous years

(Dubinin et al. 2010; Peterson et al. 2009). The trend of population moving out of town is still continuing (Federal State Statistic Service n.d.). The prohibition codes of large area of clearcutting and more restricted in forest resource uses introduced in 2000 was also another effect that lowered the events of clearcutting (Peterson et al. 2009). However, in the recent decades, the mixed disturbance areas were found to expand and caused more damage to the forest cover. Human-induced fire played a major role and was found to have an association with the clearcutting activities around the Reserve (Dudov 2018). Most of the fires outside of the Reserve was unnatural and usually presented adjacent to the clearcutting area, roadway and electricity lines. This made researchers fully aware of the potential impact on forest loss nearby the human transportation path and infrastructure (Peterson et al. 2009; Barber et al. 2014; Freitas, Hawbaker, and Metzger 2010).

Maintenance and monitoring activities in the buffer and outside the Reserve is low. This could be attributed to an inability to track and detect major forest fires on a daily basis. Burned areas outside the reserve were found to primarily correlated with clearcutting for post-2010 disturbance and along a road. Due to the increased accessibility and recently developed mining camp, clearcutting for agriculture has taken place over a more recent time (Dubinin et al. 2010; Bergen et al. 2020; Kondrashov 2004). The details of landscape changes and forest fire in these areas have not been well researched in the past because of low accessibility. I found that the classification results provided information about many unrecorded forest fires spreading outside the Reserve. The transportation routes of gold, mining materials, and logs provided resource movement information (Peterson et al. 2009). The tracking of such movement in this region needed to be paid attention and should have given a closer look to check how resource were used, so that the government officials and the Reserve's staffs can improve conservation management plan. Knowledge on forest fire, wood cutting and other environmental factors

around the reserve would also be considered to determine appropriate areas to be labeled as protection status (Newell and Henry 2016).

6.2. The Distribution of Disturbances around the Protected Area in Relation to Environmental and Climatic Factors

The impacts of environmental factors were hardly identified and the scientific community still rarely understood the effects of human activities (Beck and Goetz 2011; Lasslop and Kloster 2017; Jacquelyn K. Shuman et al. 2017; Jacquelyn Kremper Shuman, Shugart, and O'halloran 2011). Chapter 4 looked for possible causes that can harm and negatively affect the forest structure around the protected area. The Zeya State Nature Reserve has a rich biodiversity and a diverse ecology in its natural climate. In recent decades, the reserve has been subjected to face anthropogenic dangers including forest fires and clearcuttings, along with selective logging and mining (Dudov 2018; Potapov et al. 2008). I found the patch size of each disturbance had a growing trend. The results expected an increasing forest fires in the future. The growing region for farmland had converted several of forest area. The findings in this thesis have shown that over modern years, forest fire have become more frequently disturbed in larger size. Road was found to be very important since most of disturbance were located nearby road. Burning patch that associated with clearcutting sites often overlooked by distant observation from satellite images. BingMap.com comprised of many several high-resolution image that showed dirt tracks all around valley and rivers in the northern region (Figure 6.1). Landsat could not detect such kind of information due to its low resolution (Bergen et al. 2020). This raised awareness of how much forest have been lost to human-related disturbance factors.

Topography also indicated the possibility that attracted forest cover changes and disturbance (Freitas, Hawbaker, and Metzger 2010). The elevation and the Reserve's zones (inside, buffer zone, and outside) were considered as important changers in landscape dynamics in this thesis. The improvements in infrastructure or the possibility to construct new roads in

the lower elevation definitely impacted the dynamic of forest change around the Reserve. (Wear and Bolstad 1998). Roads showed strong relation to the clearcutting and the forest fire in which impact forest dynamics (Freitas, Hawbaker, and Metzger 2010; Barber et al. 2014; Uvsh et al. 2020).

In the first time period (1988-1999), clearcutting expanded to lower elevation area less than 600 m a.s.l. In the second time period (1999-2010), forest fire occurred heavily nearby roads and some present in the Reserve, while vegetation recovery occurred more in sites with steep slope and far from roads and settlements in the study area. Last period (2010-2016), human disturbance found to be mixed between clearcutting and burning at the same location. Most of these disturbances located nearby roads and electricity line and some located at the northern region nearby river. In these cases, the human infrastructure was an indication that human disturbances had an impact on forest loss in the study area.

Roads, elevation, and slope are relatively important landscape elements (Freitas, Hawbaker, and Metzger 2010). Due to increase of human transportation and access, these factors facilitated the growth of deforestation action (Uvsh et al. 2020). The forests did not recover large enough because of extensive land use changes (Potapov et al. 2017). A new illegal logging along the roads outside of the Reserve could cause significant forest cover changes in future if monitoring and enforcement on illegal logging are not effective. The protection of the Reserve alone did not prevent side effects of human intervention around its boundary. Forest cover change and disturbances around the Reserve has been associated with topographic factors and road. Steep slope and inaccessibility generally limited the change in forest landscape, many changed areas were located at easy access areas, either by roads or river (Potapov, Turubanova, and Hansen 2011; Peterson et al. 2009; Uvsh et al. 2020). For the first time in the study area, I found variations among patch numbers and patch areas in different disturbance types when considered the distance from road and water and the topographic properties. The roads were

expanded in lower elevation area which had low degree of slope angle, which probably allowed clearcutting associated with burning to expand and thereby losing forest areas.

The topographic properties and roads were not only drivers of forest dynamics. Climate change was another impact in recent years that showed forest fire to be much larger and more frequent (Jacquelyn Kremper Shuman, Shugart, and O'halloran 2011; Jacquelyn K. Shuman et al. 2017; Bonan, Pollard, and Thompson 1992; de Groot, Flannigan, and Cantin 2013; Randerson et al. 2006). Even though, this study did not ensure the direct causality between climate variation and increase of disturbance, nevertheless, the findings showed strong relation in term of warming temperature in the area that experienced human disturbance in the during historical fire year (1999-2010) and recent period (2010-2016). Remote areas in the north of the Reserve where large disturbance present could be used to evaluate the landscape changes caused by a climate change. The forest fire indicated that warmer temperature during summer attracted human activity and then instituted a new disturbance in the forest (Zhao, Liu, and Shu 2020). The study found that inside the Reserve, where human disturbance was not present, had a large fire exhibited on the mountain slope. The disturbances were most likely side affected by warmer temperature and wetter years as showed in the MaxEnt model results. The increasing maximum temperature of warmest month and increasing of precipitation of wettest month predicted to be the large contribution forest fire in those mountain areas inside the Reserve during 1999-2010. Mixed disturbance also contributed large by increasing annual precipitation in the southern part of the Reserve. This study did not contain evidence of the cause of fire inside the Reserve due to inaccessibility on the mountain top. According to the study by Zhao, Liu, and Shu (2020), there was significant positive correlations of lightning fires and wetter precipitation to ignited the forest fire during summer and fall season.

This thesis showed disturbance locations differed between inside and outside of the Reserve. The different climatic variables also played important role that establish fire in

different zone. In the Reserve, forest fire occurred on the top of the mountain with high elevation and steeper slope. These areas often face strong wind and high precipitation. While the outside of the Reserve, the disturbance by human occurred in the areas of lower elevation and flat slope, facing different temperature and precipitation. However, this study did not take wind direction and wind current into consideration. The aboveground fuel also was not considered. However, navigating the effects of wind and fuel was essential to predict the relationship between climatic data and disturbances (Wu et al. 2018; Jacquelyn Kremper Shuman, Shugart, and O'halloran 2011; Chen et al. 2018). The positive correlation between the occurrence of large fire and temperature variables suggested that the side effects of climate change can alter the forest cover and disturbance intensity (Chen and Loboda 2018).

The future human activities around the Reserve also contributed to the fluctuation of climate pattern (Ryzhkova et al. 2020). And the climate pattern, such as warmer temperature wetter season can consequence the unpredictable amount of forest fire. Therefore, it is likely that feedback mechanisms increased regional fire cycle (de Groot, Flannigan, and Cantin 2013; Jacquelyn K. Shuman et al. 2017; Chen and Loboda 2018). This thesis showed that forest fires in the late-era can be potentially of higher severity and are more difficult to control. An increase in human activities around the Reserve might have contributed to additional fire at the clearcutting edge. The study suggested the temperature and wetness in recent decades allowed human-induced fire to spread over the whole region. The results also suggested that climate drove the increase in fire activity during 1999-2010, and human disturbances, were of importance to causing its even further in 2010-2016. There is still a challenge to partition between which forest fire is human-caused and which is natural. However, this thesis can argue that inside the Reserve did not contain human-related disturbance impact since the protected area is considered the most restricted category that prohibit recreational activity inside the Reserve. Thus, the investigation for historical fires along with environmental records on

different zone needed to be explored whether climate change in the region is human-driven or not (Lasslop and Kloster 2017). The outside area of the Reserve, on the other hand, showed promising result that during the historic fire years (1999-2010), human disturbance effects had been strongly linked to the climate change.

6.3. Stableness of the Forest and Disturbance Covers around Protected Area Short-Time Interval Satellite Image Analysis

The study found a way to maximize the potential of analysis by using short-time interval images. The newly updated images were available in the USGS in the beginning of 2019. This allowed me to utilize more images and understand the effect of human disturbances and forest cover change around the Reserve. The earliest satellite image available was dated back to 1975, before the Zeya dam was established. Only a small river was seen in the image, in the eastern side of the region. This showed that before the dam construction, the region was full of dense forests. Even though classification maps of frequent images (Chapter 5; Table 5.5) produced lower accuracies compared to long-time interval overlaid images (Chapter 3; Table 3.1), the results were still reliable and promising. The maps showed the change of forests after dam construction completed.

This is the first study to evaluate the change of forest before and after Zeya dam construction in the region. The dam construction changed forest area into lake more than 210 km^2 from 1975 to 1988. Majority of forested area included spruce forests and oak-birch forests. In the vicinity of the Reserve, agriculture had grown during before the year 2000 (Dubinin et al. 2010; Peterson et al. 2009). As a consequence of higher agricultural demands, population development has led to rising disturbances inside the forest (Kareiva et al. 2007). Urbanization of villages near water sources, coupled with enhanced transit mobility, has been noted in several areas of Amur region (Mishina 2015). The findings provided evidence to strengthen decision-making and environmental preparation for forest conservation. Clearcutting issues

have consequences for reducing the protected ecosystem function, loss of floodplain areas and rising soil degradation which allowing more burning in the later years (Jacquelyn Kremper Shuman, Shugart, and O'halloran 2011; Loranty et al. 2016; Bright et al. 2019). The differences of spectral characteristics from Landsat images were used in the classifying processes. The thesis used vegetation indices in order to evaluate the stableness of forest class and disturbance class in each zone of the Reserve. The findings of the chapter 5 looked at trend of the land cover classes around the Reserve that no study have been achieved. This thesis is also the first pioneer to navigate the differences of stableness between the forest classes and disturbances classes and how the spectral characteristics of NDVI and NBR changed between inside, buffer, and outside of the Reserve.

The uses of Landsat indices (NDVI and NBR) produced essential parameters to distinguish the forest and disturbance classes (Escuin, Navarro, and Fernández 2008). Both indices declined substantially since 2000 in most of the classes, based on research finding. The variance of dNDVI and dNBR inside the Reserve was less than the variance of the outside area of the Reserve. The estimation of variance of the difference between pre- and post-index value identify regions that experience transitions and shifts in vegetation areas (Dubinin et al. 2010). I raised concerns that warmer temperature consequences may be buffered in the lower valley. Human disturbances also destroyed the natural vegetation around the Reserve, which is highly vulnerable to fire (Jacquelyn K. Shuman et al. 2017; Lasslop and Kloster 2017). The consequences might unexpectedly shift the index values in the last 20 years. The area of birch and larch forest and vegetation recovery area has been diminished rapidly, resulting large variance outside the Reserve. For resource management, it is important to define and map change spatial distribution (Chu, Guo, and Takeda 2016). I recommend using variances of dNDVI and dNBR as potential indices to monitor the trend of vegetative and disturbance areas between inside, buffer zone, and outside of the Reserve.

When the study evaluated the stableness, the research found variation of stableness between different zone of the Reserve. Inside the Reserve contained more stable classes. The buffer zone of the Reserve represented dramatically loss of grassland, oaks, birch and larch, and mixed forest. While outside of the Reserve found birch and larch to be most vulnerable to disturbances. Due to the remote and inaccessible areas, I cannot measure the intensity of disturbance in those places. The intensity affected the change of spectral characteristics (Chen and Loboda 2018). However, the prediction can be made that if large vegetation index change was observed with small areas of class, meaning high intensity of disturbance/recovery occurred in that area. And if small change of vegetation index occurred in large area of that class, it means low intensity of disturbance/recovery occurrence was observed. The Reserve management strategies will help recognize and prioritize vulnerable areas for future conservation efforts (Barber et al. 2014; Bragina et al. 2015; Wendland et al. 2015). The results also recommend further study on other vegetation indices to evaluate the stableness of forest and disturbance classes. This offers a wide field of knowledge on natural resources conservation in forest cover transition (Bragina et al. 2015).

High-resolution could enhance the ability to detect small areas of disturbance (Hansen et al. 2013). A long-term forest conservation plan could be built to mitigate forest declines (Wendland et al. 2015; Newell and Henry 2016; Degteva et al. 2015). The protection of forest cover of inside, buffer, and outside of protected area in the Russian Far East is needed. The forest restoration inside of the Reserve reflected the key factors and impacts of environmental support and biodiversity (Anderson-Teixeira 2018; Biswal et al. 2013; Marcot et al. 1997). Hence, expanding to the buffer zone, and outside region may contribute to the healthy forest ecosystem and prevent the risk of future fires (Biswal et al. 2013). I recommend the scientists to use two-year-overlaid image classification method if a few Landsat images were available throughout the long time period.

The future works carry out using this dissertation will benefit from an examination of forest cover around protected area that affected by human disturbances in long-term studies. The impact of human disturbances will have a long-term effect (Lasslop and Kloster 2017). Thus, forests are in danger to various changes. In the past decades, forest fire and human disturbances have been identified around the Reserve (Dudov 2018). Several study suggested that a compromise was important between forestry sector that worked on fire safety activity and local citizens to create the fire protection plan to maintain biodiversity in the areas (Newell and Henry 2016; Wendland et al. 2015; Degteva et al. 2015; Fiorino and Ostergren 2011). The outside area, where mixed disturbance that associated with fire is the main area of forest loss. Even though, the findings demonstrated that fires were an important factor affecting the forests across the region, however, human disturbances were still leading causes of forest loss outside the Reserve. Conservation management of the Reserve and similar protected areas in the Russian Far East should, therefore, acknowledge the role of fire and human disturbances that affecting the forest of inside, buffer, and outside of the Reserve (Wade et al. 2020; Newell and Henry 2016). Most of forest is more likely, however to be preserved and regenerated away than other landscape types. It would be good to look at how human activities will change and how future climate change and human disturbance could influence future forest dynamics and how effective conservation efforts and restorations strategies are inside, buffer, and outside of the Reserve (Biswal et al. 2013; Wendland et al. 2015). I suggested that human activities outside of the Reserve near the border should be prohibited to preserve the forest around the edge of the Reserve. Fire suppression activities are also needed to preserve fire as a driver of forest dynamics in the Reserve ecosystem since boreal forest ecosystem depend on the fire cycle (Matsypura, Prokopyev, and Zahar 2018). To maintain fire-depended ecosystem, the forestry sectors can collaborate with scientists to use prescribed burning technique near the human activity areas to help forest regeneration (Matsypura, Prokopyev, and Zahar 2018). Burning

will also reduce the dangers of large-scale fire-replacement by reducing the volume and continuity of fuel (Chen and Loboda 2018; Matsypura, Prokopyev, and Zahar 2018).

6.4. General Conclusion

Remote boreal forests in the Russian Far East have experienced unsurprising challenges from erosion to destruction from human action. Changes in vegetation distribution and ecosystem function often influence forest cover changes in the area. However, there were difficulties and limitation to study and observe forest cover changes and disturbances around the Reserve. Most forests occur in isolated locations that are vulnerable to alternation. The remote forests of the Reserve have become a challenging topic due to their large scale and due to the reality that clearcutting is taking place in far places. There is now technology to be able to view the remote forest from the distance.

This research monitor forest cover changes and disturbances that have arisen across the Reserve. The implementation of the technique from this work allowed other disciplines to broaden the goal of their study. The thesis provided new knowledge that encouraged other researchers to use the data to establish conservation management strategies for other regions. There are 3 primarily aims of this thesis – 1. using long-time interval classification maps to evaluate forest dynamics inside, buffer zone and outside the reserve, also with limited Landsat data, 2. analysis of the relationship between the change of forest and disturbance classes and environmental variables, such as distance from road, distance from water, elevation and slope, and climatic factors like temperature and precipitation, 3. using vegetation indices from short-time interval classification maps to track stableness of the forest inside, buffer zone, and outside of the Reserve to help monitor efficacy of the Reserve in terms of avoiding drastic alteration of the landscape.

Based on long-time classification maps, the maps demonstrated overall high accuracy in all three periods. The maps were really helpful to the future where the field investigation cannot

be completely done and also cost-effective. The aim was to work with minimal accessible images and an economical manner. The clearcutting had the greatest effect on the forest during the period 1988-1999. Forest fire triggered a major loss of larch and birch forests both outside and inside the Reserve between 1999-2010. And in the last decades of 2010-2016, mixed disturbance areas have been observed to damage the most to the forest cover. Human-induced fire has played a significant role and has been shown to be correlated with clearcutting around the Reserve. The analysis showed that, based on two-year overlays technique, this can improve the forest and disturbance monitoring around the Reserve. The forest inside the Reserve are found to be more stable than the forest area outside the Reserve. Furthermore, outside the Reserve, there were more disturbed areas than inside and buffer zone of the Reserve.

Since no research have been undertaken to clarify the interaction between environmental factors and forest change and disturbance across the Reserve. This study demonstrated how classes in different zone of the Reserve differed and what factors were important. Elevation and the Reserve's zones (inside, buffer zone, and outside) played a very important role in the allocation of forest and disturbance classes. The high altitude inside the Reserve comprises of few disturbances and more areas of dwarf-pine, spruce and mountain tundra vegetation's, while the low altitude, grassland, birch and larch trees, along with different types of disturbances, in particular human-related disturbances, were present. Focusing on disturbance classes, burned areas outside the Reserve were mainly associated with clear-cutting after 2010 and they found to occur near by the road. There was also an increasing area in the disturbance. In recent years, forest fire has been more widely disturbed on a broader of the Reserve and is situated near the road. It is anticipated that this study would continue to strengthen the conservation management strategy at the boundary of the protected area. Current illegal logging along roads outside the Reserve could trigger major forest cover changes in the future if surveillance and enforcement of illegal logging are not successful. For the first time, the study observed specific pattern

between patch numbers and patch areas in three disturbance classes. The larger disturbance patch size occurred few number of patch, while the smaller disturbance patch size occurred many. For environmental factors, roads were found to locate at a lower elevation area with a narrow slope, which would presumably encourage disturbances to occurred and thereby destroy forest cover. The analysis showed that inside the Reserve, where there was no human disturbance present, there was a still a big fire on the hillside. Various climatic factors are predicted to play an important part in setting fire inside the Reserve. The positive association between the distribution of major fire and temperature variable indicated that the side effects of climate change may modify the forest cover and propose disturbance events. The research did not take into account wind direction and wind current. The aboveground fuel was also not considered. However, navigating the impact of wind and fuel was necessary to forecast the relationship between climate data and major disturbance inside the Reserve. The results revealed a clear association in terms of temperature warming in the region where human disturbance happened during the historical fire year (1999-2010) and the recent period (2010-2016). The study indicated that temperature and humidity in recent decades may potentially cause fires to spread inside the Reserve from the outside. Results have indicated that temperature contributed to a rise in fire frequency between 1999-2010, and that human disturbance were of interest to further trigger in 2010-2016.

This thesis assessed forest cover change in short-time interval images including image before and after Zeya Dam construction in the study area. Dam building has turned the forest region into a lake of more than 210 km^2 from 1975 to 1988. The bulk of affected forested areas contained spruce trees and oak-birch forests. The analysis also used Landsat indices to differentiate between forest and disturbance groups. Both indices have decreased dramatically since 2000 in most of the forest groups, based on study results. The areas of birch and larch forests and the vegetation recovery area were quickly decreased, resulting in a broad variation

of stableness for the outside of the Reserve. As the analysis measured the stableness, the report noticed the inside of the Reserve is the most stable for most of forest classes, which implies that the Reserve is very well shielded from disturbance and unexpected change. As a consequence, assessing the resilience of landscape transition through stableness from vegetation indices help to identify and target endangered areas for potential forest loss.

It has been vividly shown that the stableness of the forest inside and outside the Reserve could be measured on the basis of these advanced technology, which could aid in the decision-making phase involving surveillance, policy initiatives and numerous other planning aspects. The aid of short-term classification maps could be extremely captured by how the forest was modified after disturbance on a finer time scale, which could be extremely cost-effective if not required in labor-intensive field work. The technique may be used in other rural or remote areas. Such a method may be very useful in the primary sector for tracking natural resources such as tundra ecosystems, pine trees, spruce forests, birch and larch forests, grasslands, rivers and other water bodies, etc., and also for monitoring urbanization, logging, etc. Adverse disturbance impacts could be easily monitored by the stableness of the class from remote sensing data. Effective policy initiatives should be objectively designed for growing future activities such as mining, clearcutting, and road building.

References

A. I. Bedritsky, V. G. Blinov, & D. A. Gershinkova. (2008). ASSESSMENT REPORT ON CLIMATE CHANGE AND ITS CONSEQUENCES IN RUSSIAN FEDERATION. *FEDERAL SERVICE FOR HYDROMETEOROLOGY AND ENVIRONMENTAL MONITORING (ROSHYDROMET)*. https://pogoda.meteoinfo.ru/images/wmc/climate/obzhee_rezume_eng.pdf

Achard, F., Mollicone, D., Stibig, H.-J., Aksenov, D., Laestadius, L., Li, Z., Popatov, P., & Yaroshenko, A. (2006). Areas of rapid forest-cover change in boreal Eurasia. *Forest Ecology and Management*, *237*(1), 322–334. https://doi.org/10.1016/j.foreco.2006.09.080

Amici, V., Marcantonio, M., La Porta, N., & Rocchini, D. (2017). A multi-temporal approach in MaxEnt modelling: A new frontier for land use/land cover change detection. *Ecological Informatics*, *40*, 40–49. https://doi.org/10.1016/j.ecoinf.2017.04.005

Amiro, B. D., Orchansky, A. L., Barr, A. G., Blacks, T. A., Chambers, S. D., Chapin, F. S., Goulden, M. L., Litvak, M., Liu, H. P., McCaughey, J. H., McMillan, A., & Randerson, J. T. (2006a). The effect of post-fire stand age on the boreal forest energy balance. *Agricultural and Forest Meteorology*, *140*(1–4), 41–50. https://doi.org/10.1016/j.agrformet.2006.02.014

Anderson-Teixeira, K. J. (2018). Prioritizing biodiversity and carbon. *Nature Climate Change*, *8*(8), 667–668. https://doi.org/10.1038/s41558-018-0242-6

As-syakur, A. R., Adnyana, I. W. S., Arthana, I. W., & Nuarsa, I. W. (2012). Enhanced Built-Up and Bareness Index (EBBI) for Mapping Built-Up and Bare Land in an Urban Area. *Remote Sensing*, *4*(10), 2957–2970. https://doi.org/10.3390/rs4102957

Astrup, R., Bernier, P. Y., Genet, H., Lutz, D. A., & Bright, R. M. (2018). A sensible climate solution for the boreal forest. *Nature Climate Change*, *8*(1), 11–12. https://doi.org/10.1038/s41558-017-0043-3

Barber, C. P., Cochrane, M. A., Souza, C. M., & Laurance, W. F. (2014). Roads, deforestation, and the mitigating effect of protected areas in the Amazon. *Biological Conservation*, *177*, 203–209. https://doi.org/10.1016/j.biocon.2014.07.004

Bartalev, S. A., Loupian, E. A., Stytsenko, F. V., Panova, O. Y., & Efremov, V. Yu. (2014). Rapid mapping of forest burnt areas over Russia using Landsat data. *Current Problems in Remote Sensing of the Earth from Space*, *11*(1), 9–20. http://jr.rse.cosmos.ru/article.aspx?id=1260&lang=eng (In Russian)

Başay, L., & Ersan, R. (2015). COMPARISON OF PIXEL-BASED AND OBJECT-BASED CLASSIFICATION METHODS FOR SEPARATION OF CROP PATTERNS. *Earth Observation*, 6.

Beck, P. S. A., & Goetz, S. J. (2011). Satellite observations of high northern latitude vegetation productivity changes between 1982 and 2008: Ecological variability and regional differences. *Environmental Research Letters*, *6*(4), 045501. https://doi.org/10.1088/1748-9326/6/4/045501

Bergen, K. M., Loboda, T., Newell, J. P., Kharuk, V., Hitztaler, S., Sun, G., Johnson, T., Hoffman-Hall, A., Ouyang, W., Park, K., Fort, C., & Gargulinski, E. (2020). Long-term

trends in anthropogenic land use in Siberia and the Russian Far East: A case study synthesis from Landsat. *Environmental Research Letters*, *15*(10), 105007. https://doi.org/10.1088/1748-9326/ab98b7

Betts, R. A. (2000). Offset of the potential carbon sink from boreal forestation by decreases in surface albedo. *Nature*, *408*(6809), 187–190. https://doi.org/10.1038/35041545

Biswal, A., Jeyaram, A., Mukherjee, S., & Kumar, U. (2013). *Ecological significance of core, buffer and transition boundaries in biosphere reserve: A remote sensing study in Similipal, Odisha, India*. 12.

Blaschke, T. (2010). Object based image analysis for remote sensing. *ISPRS Journal of Photogrammetry and Remote Sensing*, *65*(1), 2–16. https://doi.org/10.1016/j.isprsjprs.2009.06.004

Bockel, L., Bernoux, M., Thapa, D., & Armstrong, A. (2014). *GHG and Natural Capital Impact of Russia Forest Fire Response Project*. 26.

Bonan, G. B., Pollard, D., & Thompson, S. L. (1992). Effects of boreal forest vegetation on global climate. *Nature*, *359*(6397), 716–718. https://doi.org/10.1038/359716a0

Bondur, V. G., Tsidilina, M. N., & Cherepanova, E. V. (2019a). Satellite Monitoring of Wildfire Impacts on the Conditions of Various Types of Vegetation Cover in the Federal Districts of the Russian Federation. *Izvestiya, Atmospheric and Oceanic Physics*, *55*(9), 1238–1253. https://doi.org/10.1134/S000143381909010X

Borisova, I. G., & Veklich, T. N. (2013, July 25). *Oak-black birch lespedetsy- forb forest*. https://mail.google.com/mail/u/1/#search/borisovagis%40mail.ru/FMfcgxmSdZHGlbLWHkcRcWjtnFvTHVCP?projector=1&messagePartId=0.1

Bowman, D. M. J. S., Moreira-Muñoz, A., Kolden, C. A., Chávez, R. O., Muñoz, A. A., Salinas, F., González-Reyes, Á., Rocco, R., de la Barrera, F., Williamson, G. J., Borchers, N., Cifuentes, L. A., Abatzoglou, J. T., & Johnston, F. H. (2019). Human–environmental drivers and impacts of the globally extreme 2017 Chilean fires. *Ambio*, *48*(4), 350–362. https://doi.org/10.1007/s13280-018-1084-1

Bragina, E. V., Radeloff, V. C., Baumann, M., Wendland, K., Kuemmerle, T., & Pidgeon, A. M. (2015a). Effectiveness of protected areas in the Western Caucasus before and after the transition to post-socialism. *Biological Conservation*, *184*, 456–464. https://doi.org/10.1016/j.biocon.2015.02.013

Bright, B. C., Hudak, A. T., Kennedy, R. E., Braaten, J. D., & Henareh Khalyani, A. (2019). Examining post-fire vegetation recovery with Landsat time series analysis in three western North American forest types. *Fire Ecology*, *15*(1), 8. https://doi.org/10.1186/s42408-018-0021-9

Chander, G., Markham, B. L., & Helder, D. L. (2009). Summary of current radiometric calibration coefficients for Landsat MSS, TM, ETM+, and EO-1 ALI sensors. *Remote Sensing of Environment*, *113*(5), 893–903. https://doi.org/10.1016/j.rse.2009.01.007

Chavez, P. (1996). *Image-Based Atmospheric Corrections—Revisited and Improved*. Undefined. /paper/Image-Based-Atmospheric-Corrections-Revisited-and-Chavez/45f12625ce130261c7d360d50e09c635355ca919

Chen, D., Loboda, T. V., Krylov, A., & Potapov, P. (2017a). Distribution of Estimated Stand Age Across Siberian Larch Forests, 1989-2012. *ORNL DAAC*. https://doi.org/10.3334/ORNLDAAC/1364

Chen, Dong, & Loboda, T. V. (2018). Surface forcing of non-stand-replacing fires in Siberian larch forests. *Environmental Research Letters*, *13*(4), 045008. https://doi.org/10.1088/1748-9326/aab443

Chen, Dong, Loboda, T. V., He, T., Zhang, Y., & Liang, S. (2018). Strong cooling induced by stand-replacing fires through albedo in Siberian larch forests. *Scientific Reports*, *8*(1), 4821. https://doi.org/10.1038/s41598-018-23253-1

Chistyakova, A. A., & Leonova, N. A. (2003). The State of Protected Forest Communities in the European Forest–Steppe Zone of Russia and Prospects for Their Reconstruction: A Case Study of Specially Protected Areas of Penza Oblast. *Russian Journal of Ecology*, *34*(5), 285–291. https://doi.org/10.1023/A:1025657822528

Chu, T., Guo, X., & Takeda, K. (2016). Remote sensing approach to detect post-fire vegetation regrowth in Siberian boreal larch forest. *Ecological Indicators*, *62*, 32–46. https://doi.org/10.1016/j.ecolind.2015.11.026

Chuvieco, E., Aguado, I., Jurdao, S., Pettinari, M. L., Yebra, M., Salas, J., Hantson, S., Riva, J. de la, Ibarra, P., Rodrigues, M., Echeverría, M., Azqueta, D., Román, M. V., Bastarrika, A., Martínez, S., Recondo, C., Zapico, E., & Martínez-Vega, F. J. (2014). Integrating geospatial information into fire risk assessment. *International Journal of Wildland Fire*, *23*(5), 606–619. https://doi.org/10.1071/WF12052

Cocke, A. E., Fulé, P. Z., & Crouse, J. E. (2005). Comparison of burn severity assessments using Differenced Normalized Burn Ratio and ground data. *International Journal of Wildland Fire*, *14*(2), 189–198. https://doi.org/10.1071/WF04010

Cohen, W. B., & Goward, S. N. (2004). Landsat's Role in Ecological Applications of Remote Sensing. *BioScience*, *54*(6), 535–545. https://doi.org/10.1641/0006-3568(2004)054[0535:LRIEAO]2.0.CO;2

Conard, S. G., & A. Ivanova, G. (1997). Wildfire in Russian Boreal Forests—Potential Impacts of Fire Regime Characteristics on Emissions and Global Carbon Balance Estimates. *Environmental Pollution*, *98*(3), 305–313. https://doi.org/10.1016/S0269-

Conard, S. G., Sukhinin, A. I., Stocks, B. J., Cahoon, D. R., Davidenko, E. P., & Ivanova, G. A. (2002). Determining Effects of Area Burned and Fire Severity on Carbon Cycling and Emissions in Siberia. *Climatic Change*, *55*(1), 197–211. https://doi.org/10.1023/A:1020207710195

Coppin, P., Jonckheere, I., Nackaerts, K., Muys, B., & Lambin, E. (2004). Review ArticleDigital change detection methods in ecosystem monitoring: A review. *International Journal of Remote Sensing*, *25*(9), 1565–1596. https://doi.org/10.1080/0143116031000101675

Damoah, R., Spichtinger, N., Forster, C., James, P., Mattis, I., Wandinger, U., Beirle, S., Wagner, T., & Stohl, A. (2004). Around the world in 17 days—Hemispheric-scale transport of forest fire smoke from Russia in May 2003. *Atmospheric Chemistry and Physics*, *4*(5), 1311–1321. https://doi.org/10.5194/acp-4-1311-2004

de Groot, W. J., Flannigan, M. D., & Cantin, A. S. (2013). Climate change impacts on future boreal fire regimes. *Forest Ecology and Management*, *294*, 35–44. https://doi.org/10.1016/j.foreco.2012.09.027

Degteva, S. V., Ponomarev, V. I., Eisenman, S. W., & Dushenkov, V. (2015). Striking the balance: Challenges and perspectives for the protected areas network in northeastern European Russia. *Ambio*, *44*(6), 473–490. https://doi.org/10.1007/s13280-015-0636-x

Drăguţ, L., Tiede, D., & Levick, S. R. (2010). ESP: A tool to estimate scale parameter for multiresolution image segmentation of remotely sensed data. *International Journal of Geographical Information Science*, *24*(6), 859–871. https://doi.org/10.1080/13658810903174803

Dubinin, M., Potapov, P., Lushchekina, A., & Radeloff, V. C. (2010). Reconstructing long time series of burned areas in arid grasslands of southern Russia by satellite remote sensing. *Remote Sensing of Environment*, *114*(8), 1638–1648. https://doi.org/10.1016/j.rse.2010.02.010

Dudov, S. V. (2018). Large-scale vegetation mapping of the Zeya State Nature Reserve. *География и природные ресурсы*, *4*. https://doi.org/10.21782/GiPR0206-1619-2018-4(66-75)

Elbakidze, M., Angelstam, P., Sobolev, N., Degerman, E., Andersson, K., Axelsson, R., Höjer, O., & Wennberg, S. (2013). Protected Area as an Indicator of Ecological Sustainability? A Century of Development in Europe's Boreal Forest. *AMBIO*, *42*(2), 201–214. https://doi.org/10.1007/s13280-012-0375-1

Escuin, S., Navarro, R., & Fernández, P. (2008). Fire severity assessment by using NBR (Normalized Burn Ratio) and NDVI (Normalized Difference Vegetation Index) derived from LANDSAT TM/ETM images. *International Journal of Remote Sensing*, *29*(4), 1053–1073. https://doi.org/10.1080/01431160701281072

Eskandari, S., Pourghasemi, H. R., & Tiefenbacher, J. P. (2020). Relations of land cover, topography, and climate to fire occurrence in natural regions of Iran: Applying new data mining techniques for modeling and mapping fire danger. *Forest Ecology and Management*, *473*, 118338. https://doi.org/10.1016/j.foreco.2020.118338

Federal State Statistic Service. (n.d.). *The Demographic Yearbook of Russia*. Retrieved November 26, 2020, from https://eng.gks.ru/Publications/document/13972

Fernández-Nogueira, D., & Corbelle-Rico, E. (2018). Land Use Changes in Iberian Peninsula 1990–2012. *Land*, *7*(3), 99. https://doi.org/10.3390/land7030099

Feurdean, A., Florescu, G., Tanţău, I., Vannière, B., Diaconu, A.-C., Pfeiffer, M., Warren, D., Hutchinson, S. M., Gorina, N., Gałka, M., & Kirpotin, S. (2020). Recent fire regime in the southern boreal forests of western Siberia is unprecedented in the last five millennia. *Quaternary Science Reviews*, *244*, 106495. https://doi.org/10.1016/j.quascirev.2020.106495

Fick, S. E., & Hijmans, R. J. (2017). WorldClim 2: New 1-km spatial resolution climate surfaces for global land areas. *International Journal of Climatology*, *37*(12), 4302–4315. https://doi.org/10.1002/joc.5086

Fiore, N. M., Goulden, M. L., Czimczik, C. I., Pedron, S. A., & Tayo, M. A. (2020). Do recent NDVI trends demonstrate boreal forest decline in Alaska? *Environmental Research Letters*, *15*(9), 095007. https://doi.org/10.1088/1748-9326/ab9c4c

Fiorino, T., & Ostergren, D. (2011). Institutional Instability and the Challenges of Protected Area Management in Russia. *Society & Natural Resources*, *25*(2), 191–202. https://doi.org/10.1080/08941920.2011.603142

Fisher, R. A. (1992). Statistical Methods for Research Workers. In S. Kotz & N. L. Johnson (Eds.), *Breakthroughs in Statistics: Methodology and Distribution* (pp. 66–70). Springer. https://doi.org/10.1007/978-1-4612-4380-9_6

Franco-Lopez, H., Ek, A. R., & Bauer, M. E. (2001). Estimation and mapping of forest stand density, volume, and cover type using the k-nearest neighbors method. *Remote Sensing of Environment*, *77*(3), 251–274. https://doi.org/10.1016/S0034-4257(01)00209-7

Freitas, S. R., Hawbaker, T. J., & Metzger, J. P. (2010). Effects of roads, topography, and land use on forest cover dynamics in the Brazilian Atlantic Forest. *Forest Ecology and Management*, *259*(3), 410–417. https://doi.org/10.1016/j.foreco.2009.10.036

Gao, B. (1996). NDWI—A normalized difference water index for remote sensing of vegetation liquid water from space. *Remote Sensing of Environment*, *58*(3), 257–266. https://doi.org/10.1016/S0034-4257(96)00067-3

García, M. J. L., & Caselles, V. (1991). Mapping burns and natural reforestation using thematic Mapper data. *Geocarto International*, *6*(1), 31–37. https://doi.org/10.1080/10106049109354290

Gaston, G. G. (1997). *Forest Ecosystem Modeling in the Russian Far East Using Vegetation and Land-Cover Regions Identified by Classification of GVI*. 8.

Giglio, L., Justice, C., Boschetti, L., & Roy, D. (2015). *MCD64A1 MODIS/Terra+Aqua Burned Area Monthly L3 Global 500m SIN Grid V006. NASA EOSDIS Land Processes DAAC.* https://doi.org/10.5067/MODIS/MCD64A1.006

Goetz, S. J., Mack, M. C., Gurney, K. R., Randerson, J. T., & Houghton, R. A. (2007). Ecosystem responses to recent climate change and fire disturbance at northern high

latitudes: Observations and model results contrasting northern Eurasia and North America. *Environmental Research Letters*, *2*(4), 045031. https://doi.org/10.1088/1748-9326/2/4/045031

Gong, P., Wang, J., Yu, L., Zhao, Y., Zhao, Y., Liang, L., Niu, Z., Huang, X., Fu, H., Liu, S., Li, C., Li, X., Fu, W., Liu, C., Xu, Y., Wang, X., Cheng, Q., Hu, L., Yao, W., … Chen, J. (2013). Finer resolution observation and monitoring of global land cover: First mapping results with Landsat TM and ETM+ data. *International Journal of Remote Sensing*, *34*(7), 2607–2654. https://doi.org/10.1080/01431161.2012.748992

Goodale, C. L., Apps, M. J., Birdsey, R. A., Field, C. B., Heath, L. S., Houghton, R. A., Jenkins, J. C., Kohlmaier, G. H., Kurz, W., Liu, S., Nabuurs, G.-J., Nilsson, S., & Shvidenko, A. Z. (2002). Forest Carbon Sinks in the Northern Hemisphere. *Ecological Applications*, *12*(3), 891–899. https://doi.org/10.1890/1051-0761(2002)012[0891:FCSITN]2.0.CO;2

Gromtsev, A., & Petrov, N. (2014). Natural and anthropogenic fire regimes in boreal landscapes of Northwest Russia. In D. X. Viegas, *Advances in forest fire research* (pp. 569–574). Imprensa da Universidade de Coimbra. https://doi.org/10.14195/978-989-26-0884-6_65

Hansen, M. C., Defries, R. S., Townshend, J. R. G., & Sohlberg, R. (2000). Global land cover classification at 1 km spatial resolution using a classification tree approach. *International Journal of Remote Sensing*, *21*(6–7), 1331–1364. https://doi.org/10.1080/014311600210209

Hansen, M. C., Potapov, P. V., Moore, R., Hancher, M., Turubanova, S. A., Tyukavina, A., Thau, D., Stehman, S. V., Goetz, S. J., Loveland, T. R., Kommareddy, A., Egorov, A.,

Chini, L., Justice, C. O., & Townshend, J. R. G. (2013). High-Resolution Global Maps of 21st-Century Forest Cover Change. *Science*, *342*(6160), 850–853. https://doi.org/10.1126/science.1244693

He, N., Fang, L., Li, S., Plaza, A., & Plaza, J. (2018). Remote Sensing Scene Classification Using Multilayer Stacked Covariance Pooling. *IEEE Transactions on Geoscience and Remote Sensing*, *56*(12), 6899–6910. https://doi.org/10.1109/TGRS.2018.2845668

Healey, S. P., Cohen, W. B., Zhiqiang, Y., & Krankina, O. N. (2005). Comparison of Tasseled Cap-based Landsat data structures for use in forest disturbance detection. *Remote Sensing of Environment*, *97*(3), 301–310. https://doi.org/10.1016/j.rse.2005.05.009

Hirata, Y. H., & Takahashi, T. T. (2010). Image segmentation and classification of Landsat Thematic Mapper data using a sampling approach for forest cover assessmentThis article is one of a selection of papers from Extending Forest Inventory and Monitoring over Space and Time. *Canadian Journal of Forest Research*. https://doi.org/10.1139/X10-130

Hitztaler, S. K., & Bergen, K. M. (2013). Mapping resource use over a Russian landscape: An integrated look at harvesting of a non-timber forest product in central Kamchatka. *Environmental Research Letters*, *8*(4), 045020. https://doi.org/10.1088/1748-9326/8/4/045020

Hu, M., & Xia, B. (2019). A significant increase in the normalized difference vegetation index during the rapid economic development in the Pearl River Delta of China. *Land Degradation & Development*, *30*(4), 359–370. https://doi.org/10.1002/ldr.3221

Jasinski, K., & Angelstam, P. (2002). Long-term differences in the dynamics within a natural forest landscape—Consequences for management. *Forest Ecology and Management*, *161*(1), 1–11. https://doi.org/10.1016/S0378-1127(01)00486-8

Jaynes, E. T. (1957). Information Theory and Statistical Mechanics. *Physical Review*, *106*(4), 620–630. https://doi.org/10.1103/PhysRev.106.620

Johnson, R. D., & Kasischke, E. S. (1998). Change vector analysis: A technique for the multispectral monitoring of land cover and condition. *International Journal of Remote Sensing*, *19*(3), 411–426. https://doi.org/10.1080/014311698216062

Ju, J., & Masek, J. G. (2016). The vegetation greenness trend in Canada and US Alaska from 1984–2012 Landsat data. *Remote Sensing of Environment*, *176*, 1–16. https://doi.org/10.1016/j.rse.2016.01.001

Justice, C. O., Vermote, E., Townshend, J. R. G., Defries, R., Roy, D. P., Hall, D. K., Salomonson, V. V., Privette, J. L., Riggs, G., Strahler, A., Lucht, W., Myneni, R. B., Knyazikhin, Y., Running, S. W., Nemani, R. R., Zhengming Wan, Huete, A. R., Leeuwen, W. van, Wolfe, R. E., … Barnsley, M. J. (1998). The Moderate Resolution Imaging Spectroradiometer (MODIS): Land remote sensing for global change research. *IEEE Transactions on Geoscience and Remote Sensing*, *36*(4), 1228–1249. https://doi.org/10.1109/36.701075

Kämpf, I., Mathar, W., Kuzmin, I., Hölzel, N., & Kiehl, K. (2016). Post-Soviet recovery of grassland vegetation on abandoned fields in the forest steppe zone of Western Siberia. *Biodiversity and Conservation*, *25*(12), 2563–2580. https://doi.org/10.1007/s10531-016-1078-x

Kareiva, P., Watts, S., McDonald, R., & Boucher, T. (2007). Domesticated Nature: Shaping Landscapes and Ecosystems for Human Welfare. *Science*, *316*(5833), 1866–1869. https://doi.org/10.1126/science.1140170

Kartika, T., Arifin, S., Sari, I. L., Tosiani, A., Firmansyah, R., Kustiyo, Carolita, I., Adi, K., Daryanto, A. F., & Said, Z. (2019). Analysis of Vegetation Indices Using Metric Landsat-8 Data to Identify Tree Cover Change in Riau Province. *IOP Conference Series: Earth and Environmental Science*, *280*(1), 012013. https://doi.org/10.1088/1755-1315/280/1/012013

Kasischke, E. S., & Stocks, B. J. (Eds.). (2000). *Fire, Climate Change, and Carbon Cycling in the Boreal Forest*. Springer-Verlag. https://doi.org/10.1007/978-0-387-21629-4

Kerr, J. T., & Ostrovsky, M. (2003). From space to species: Ecological applications for remote sensing. *Trends in Ecology & Evolution*, *18*(6), 299–305. https://doi.org/10.1016/S0169-5347(03)00071-5

Key, C. H., & Benson, N. C. (2006). Landscape Assessment (LA). *In: Lutes, Duncan C.; Keane, Robert E.; Caratti, John F.; Key, Carl H.; Benson, Nathan C.; Sutherland, Steve; Gangi, Larry J. 2006. FIREMON: Fire Effects Monitoring and Inventory System. Gen. Tech. Rep. RMRS-GTR-164-CD. Fort Collins, CO: U.S. Department of Agriculture, Forest Service, Rocky Mountain Research Station. p. LA-1-55*, *164*. https://www.fs.usda.gov/treesearch/pubs/24066

Kharuk, V. I., Ranson, K. J., & Dvinskaya, M. L. (2010). Wildfire Dynamics in Mid-Siberian Larch Dominated Forests. In H. Balzter (Ed.), *Environmental Change in Siberia: Earth Observation, Field Studies and Modelling* (pp. 83–100). Springer Netherlands. https://doi.org/10.1007/978-90-481-8641-9_6

Kharuk, V. I., Ranson, K. J., Oskorbin, P. A., Im, S. T., & Dvinskaya, M. L. (2013). Climate induced birch mortality in Trans-Baikal lake region, Siberia. *Forest Ecology and Management*, *289*, 385–392. https://doi.org/10.1016/j.foreco.2012.10.024

Kharuk, Viacheslav I., Dvinskaya, M. L., Petrov, I. A., Im, S. T., & Ranson, K. J. (2016). Larch forests of Middle Siberia: Long-term trends in fire return intervals. *Regional Environmental Change*, *16*(8), 2389–2397. https://doi.org/10.1007/s10113-016-0964-9

Kharuk, Viacheslav I., Ponomarev, E. I., Ivanova, G. A., Dvinskaya, M. L., Coogan, S. C. P., & Flannigan, M. D. (2021). Wildfires in the Siberian taiga. *Ambio*. https://doi.org/10.1007/s13280-020-01490-x

Kharuk, Viacheslav I., Ranson, K. J., Dvinskaya, M. L., & Im, S. T. (2011). Wildfires in northern Siberian larch dominated communities. *Environmental Research Letters*, *6*(4), 045208. https://doi.org/10.1088/1748-9326/6/4/045208

Kharuk, Vyacheslav I., Ranson, K. J., Im, S. T., & Vdovin, A. S. (2010). Spatial distribution and temporal dynamics of high-elevation forest stands in southern Siberia. *Global Ecology and Biogeography*, *19*(6), 822–830. https://doi.org/10.1111/j.1466-8238.2010.00555.x

Khatancharoen, C. (2017). *Evaluating Fire Disturbance and Forest Cover Changes using Remote Sensing in Zeya State Nature Reserve, Russia* [Master thesis]. The University of Tokyo.

Khatancharoen, C., Tsuyuki, S., Bryanin, S. V., Sugiura, K., Seino, T., Lisovsky, V. V., Borisova, I. G., et al. (2021). Long-Time Interval Satellite Image Analysis on Forest-

Cover Changes and Disturbances around Protected Area, Zeya State Nature Reserve, in the Russian Far East. *Remote Sensing*, 13(7), 1285. MDPI AG. Retrieved from http://dx.doi.org/10.3390/rs13071285

Kondrashov, L. G. (2004). Russian Far East forest disturbances and socio-economic problems of restoration. *Forest Ecology and Management*, *201*(1), 65–74. https://doi.org/10.1016/j.foreco.2004.06.012

Korovin, G. (1995). Problems of forest management in Russia. *Water, Air, and Soil Pollution*, *82*(1), 13–23. https://doi.org/10.1007/BF01182814

Kpienbaareh, D., Sun, X., Wang, J., Luginaah, I., Bezner Kerr, R., Lupafya, E., & Dakishoni, L. (2021). Crop Type and Land Cover Mapping in Northern Malawi Using the Integration of Sentinel-1, Sentinel-2, and PlanetScope Satellite Data. *Remote Sensing*, *13*(4), 700. https://doi.org/10.3390/rs13040700

Krankina, O., & Dixon, R. (1992). A HISTORICAL PERSPECTIVE OF FOREST MANAGEMENT IN THE USSR: CHALLENGES AND OPPORTUNITIES IN THE ERA OF PERESTROIKA. *Journal of Forestry*, *90*, 29–34.

Krylov, A., McCarty, J. L., Potapov, P., Loboda, T., Tyukavina, A., Turubanova, S., & Hansen, M. C. (2014). Remote sensing estimates of stand-replacement fires in Russia, 2002–2011. *Environmental Research Letters*, *9*(10), 105007. https://doi.org/10.1088/1748-9326/9/10/105007

Kukavskaya, E. A., Soja, A. J., Petkov, A. P., Ponomarev, E. I., Ivanova, G. A., & Conard, S. G. (2013). Fire emissions estimates in Siberia: Evaluation of uncertainties in area

burned, land cover, and fuel consumption. *Canadian Journal of Forest Research*, *43*(5), 493–506. https://doi.org/10.1139/cjfr-2012-0367

Lasslop, G., & Kloster, S. (2017). Human impact on wildfires varies between regions and with vegetation productivity. *Environmental Research Letters*, *12*(11), 115011. https://doi.org/10.1088/1748-9326/aa8c82

Li, W., & Guo, Q. (2010). A maximum entropy approach to one-class classification of remote sensing imagery. *International Journal of Remote Sensing*, *31*(8), 2227–2235. https://doi.org/10.1080/01431161003702245

Loboda, Tatiana V., & Chen, D. (2017). Spatial distribution of young forests and carbon fluxes within recent disturbances in Russia. *Global Change Biology*, *23*(1), 138–153. https://doi.org/10.1111/gcb.13349

Loboda, T.V., Zhang, Z., O'Neal, K. J., Sun, G., Csiszar, I. A., Shugart, H. H., & Sherman, N. J. (2012). Reconstructing disturbance history using satellite-based assessment of the distribution of land cover in the Russian Far East. *Remote Sensing of Environment*, *118*, 241–248. https://doi.org/10.1016/j.rse.2011.11.022

Loranty, M. M., Lieberman-Cribbin, W., Berner, L. T., Natali, S. M., Goetz, S. J., Alexander, H. D., & Kholodov, A. L. (2016). Spatial variation in vegetation productivity trends, fire disturbance, and soil carbon across arctic-boreal permafrost ecosystems. *Environmental Research Letters*, *11*(9), 095008. https://doi.org/10.1088/1748-9326/11/9/095008

Maclaurin, G. J., & Leyk, S. (2016). Extending the geographic extent of existing land cover data using active machine learning and covariate shift corrective sampling.

International Journal of Remote Sensing, *37*(21), 5213–5233. https://doi.org/10.1080/01431161.2016.1230285

Makoto, K., Bryanin, S. V., Lisovsky, V. V., Kushida, K., & Wada, N. (2016). Dwarf pine invasion in an alpine tundra of discontinuous permafrost area: Effects on fine root and soil carbon dynamics. *Trees*, *30*(2), 431–439. https://doi.org/10.1007/s00468-015-1192-5

Malila, W. A. (1980). *Change Vector Analysis: An Approach for Detecting Forest Changes with Landsat*. 12.

Marcot, B. G., Ganzei, S. S., Zhang, T., & Voronov, B. A. (1997). A sustainable plan for conserving forest biodiversity in far East Russia and northeast China. *The Forestry Chronicle*, *73*(5), 565–571. https://doi.org/10.5558/tfc73565-5

Marozas, V., Racinskas, J., & Bartkevicius, E. (2007). Dynamics of ground vegetation after surface fires in hemiboreal Pinus sylvestris forests. *Forest Ecology and Management*, *250*(1), 47–55. https://doi.org/10.1016/j.foreco.2007.03.008

Matsypura, D., Prokopyev, O. A., & Zahar, A. (2018). Wildfire fuel management: Network-based models and optimization of prescribed burning. *European Journal of Operational Research*, *264*(2), 774–796. https://doi.org/10.1016/j.ejor.2017.06.050

Melillo, J. M., McGuire, A. D., Kicklighter, D. W., Moore, B., Vorosmarty, C. J., & Schloss, A. L. (1993). Global climate change and terrestrial net primary production. *Nature*, *363*(6426), 234–240. https://doi.org/10.1038/363234a0

Miller, C., & Urban, D. L. (2011). Interactions between forest heterogeneity and surface fire regimes in the southern Sierra Nevada. *Canadian Journal of Forest Research*. https://doi.org/10.1139/x98-188

Miller, J. D., & Thode, A. E. (2007). Quantifying burn severity in a heterogeneous landscape with a relative version of the delta Normalized Burn Ratio (dNBR). *Remote Sensing of Environment*, *109*(1), 66–80. https://doi.org/10.1016/j.rse.2006.12.006

Ministry of Natural Resources of the Russian Federation. (last). (2011). *General information of Zeya State Nature Reserve.* http://www.zapoved.ru/catalog/36/

Mishina, N. V. (2015). Land-Use Dynamics in the Amur River Basin in the Twentieth Century: Main Tendencies, Driving Forces and Environmental Consequences. In S. Haruyama & T. Shiraiwa (Eds.), *Environmental Change and the Social Response in the Amur River Basin* (pp. 231–262). Springer Japan. https://doi.org/10.1007/978-4-431-55245-1_11

Morresi, D., Vitali, A., Urbinati, C., & Garbarino, M. (2019). Forest Spectral Recovery and Regeneration Dynamics in Stand-Replacing Wildfires of Central Apennines Derived from Landsat Time Series. *Remote Sensing*, *11*(3), 308. https://doi.org/10.3390/rs11030308

Naprasnikov, A. T., Bogojavlensky, B. A., & Bufal, V. V. (1983). *Hydroclimatic resources of the Amur Region* (I.F.Mavrina). Blagoveshchensk: Khabarovsk publishing house.

Newell, J. P., & Henry, L. A. (2016). The state of environmental protection in the Russian Federation: A review of the post-Soviet era. *Eurasian Geography and Economics*, *57*(6), 779–801. https://doi.org/10.1080/15387216.2017.1289851

Norton, T. W. (1996). Conservation of biological diversity in temperate and boreal forest ecosystems. *Forest Ecology and Management*, *85*(1), 1–7. https://doi.org/10.1016/S0378-1127(96)03745-0

ORNL DAAC. (2018). *MODIS and VIIRS Land Products Global Subsetting and Visualization Tool. ORNL DAAC, Oak Ridge, Tennessee, USA. Accessed December 02, 2020. Subset obtained for MCD64A1 product at Spatial Range: N=60.41N, S=59.73N, E=140.68W, W=141.71W, time period: 2000-01-02 to 2016-05-02, and subset size: 0.5 x 0.5 km.* https://doi.org/10.3334/ORNLDAAC/1379

Ostroukhov, A. V., Klimina, E. M., & Kuptsova, V. A. (2020). Landscape mapping of hard-to-reach areas. A case study for the Bolonsky State Nature Reserve (Russia). *Nature Conservation Research*, *5*(2), Article 2. https://doi.org/10.24189/ncr.2020.015

Peterson, L. K., Bergen, K. M., Brown, D. G., Vashchuk, L., & Blam, Y. (2009). Forested land-cover patterns and trends over changing forest management eras in the Siberian Baikal region. *Forest Ecology and Management*, *257*(3), 911–922. https://doi.org/10.1016/j.foreco.2008.10.037

Phan, T. N., & Kappas, M. (2018). Comparison of Random Forest, k-Nearest Neighbor, and Support Vector Machine Classifiers for Land Cover Classification Using Sentinel-2 Imagery. *Sensors*, *18*(1), 18. http://dx.doi.org/10.3390/s18010018

Phillips, S. J., Anderson, R. P., & Schapire, R. E. (2006). Maximum entropy modeling of species geographic distributions. *Ecological Modelling*, *190*(3), 231–259. https://doi.org/10.1016/j.ecolmodel.2005.03.026

Potapov, P., Hansen, M. C., Laestadius, L., Turubanova, S., Yaroshenko, A., Thies, C., Smith, W., Zhuravleva, I., Komarova, A., Minnemeyer, S., & Esipova, E. (2017). The last frontiers of wilderness: Tracking loss of intact forest landscapes from 2000 to 2013. *Science Advances*, *3*(1), e1600821. https://doi.org/10.1126/sciadv.1600821

Potapov, P., Turubanova, S., & Hansen, M. C. (2011). Regional-scale boreal forest cover and change mapping using Landsat data composites for European Russia. *Remote Sensing of Environment*, *115*(2), 548–561. https://doi.org/10.1016/j.rse.2010.10.001

Potapov, P., Hansen, M. C., Stehman, S. V., Loveland, T. R., & Pittman, K. (2008a). Combining MODIS and Landsat imagery to estimate and map boreal forest cover loss. *Remote Sensing of Environment*, *112*(9), 3708–3719. https://doi.org/10.1016/j.rse.2008.05.006

Potapov, P., Yaroshenko, A., Turubanova, S., Dubinin, M., Laestadius, L., Thies, C., Aksenov, D., Egorov, A., Yesipova, Y., Glushkov, I., Karpachevskiy, M., Kostikova, A., Manisha, A., Tsybikova, E., & Zhuravleva, I. (2008b). Mapping the World's Intact Forest Landscapes by Remote Sensing. *Ecology and Society*, *13*(2), Article 2. https://doi.org/10.5751/ES-02670-130251

R Core Team. (2017). *R: A Language and Environment for Statistical Computing*. R Foundation for Statistical Computing. https://www.R-project.org/

Randerson, J. T., Liu, H., Flanner, M. G., Chambers, S. D., Jin, Y., Hess, P. G., Pfister, G., Mack, M. C., Treseder, K. K., Welp, L. R., Chapin, F. S., Harden, J. W., Goulden, M. L., Lyons, E., Neff, J. C., Schuur, E. a. G., & Zender, C. S. (2006). The Impact of Boreal Forest Fire on Climate Warming. *Science*, *314*(5802), 1130–1132. https://doi.org/10.1126/science.1132075

Roy, D. P., Jin, Y., Lewis, P. E., & Justice, C. O. (2005). Prototyping a global algorithm for systematic fire-affected area mapping using MODIS time series data. *Remote Sensing of Environment*, *97*(2), 137–162. https://doi.org/10.1016/j.rse.2005.04.007

Ruiz-Ramos, J., Marino, A., Boardman, C., & Suarez, J. (2020). Continuous Forest Monitoring Using Cumulative Sums of Sentinel-1 Timeseries. *Remote Sensing*, *12*(18), 3061. https://doi.org/10.3390/rs12183061

Ryzhkova, N., Pinto, G., Kryshen', A., Bergeron, Y., Ols, C., & Drobyshev, I. (2020). Multi-century reconstruction suggests complex interactions of climate and human controls of forest fire activity in a Karelian boreal landscape, North-West Russia. *Forest Ecology and Management*, *459*, 117770. https://doi.org/10.1016/j.foreco.2019.117770

Schroeder, T. A., Wulder, M. A., Healey, S. P., & Moisen, G. G. (2011). Mapping wildfire and clearcut harvest disturbances in boreal forests with Landsat time series data. *Remote Sensing of Environment*, *115*(6), 1421–1433. https://doi.org/10.1016/j.rse.2011.01.022

Scullion, J. J., Vogt, K. A., Drahota, B., Winkler-Schor, S., & Lyons, M. (2019). Conserving the Last Great Forests: A Meta-Analysis Review of the Drivers of Intact Forest Loss and the Strategies and Policies to Save Them. *Frontiers in Forests and Global Change*, *2*. https://doi.org/10.3389/ffgc.2019.00062

Sellers, P., Hall, F., Margolis, H., Kelly, B., Baldocchi, D., den Hartog, G., Cihlar, J., Ryan, M. G., Goodison, B., Crill, P., Ranson, K. J., Lettenmaier, D., & Wickland, D. E. (1995). The Boreal Ecosystem–Atmosphere Study (BOREAS): An Overview and Early Results from the 1994 Field Year. *Bulletin of the American Meteorological Society*, *76*(9), 1549–1577. https://doi.org/10.1175/1520-0477(1995)076<1549:TBESAO>2.0.CO;2

Shishov, V. V., & Vaganov, E. A. (2010). Dendroclimatological Evidence of Climate Changes Across Siberia. In H. Balzter (Ed.), *Environmental Change in Siberia* (Vol. 40, pp. 101–114). Springer Netherlands. https://doi.org/10.1007/978-90-481-8641-9_7

Shuman, Jacquelyn K., Foster, A. C., Shugart, H. H., Hoffman-Hall, A., Krylov, A., Loboda, T., Ershov, D., & Sochilova, E. (2017). Fire disturbance and climate change: Implications for Russian forests. *Environmental Research Letters*, *12*(3), 035003. https://doi.org/10.1088/1748-9326/aa5eed

Shuman, Jacquelyn Kremper, Shugart, H. H., & O'halloran, T. L. (2011). Sensitivity of Siberian larch forests to climate change. *Global Change Biology*, *17*(7), 2370–2384. https://doi.org/10.1111/j.1365-2486.2011.02417.x

Shvetsov, E. G., Kukavskaya, E. A., Buryak, L. V., & Barrett, K. (2019). Assessment of post-fire vegetation recovery in Southern Siberia using remote sensing observations. *Environmental Research Letters*, *14*(5), 055001. https://doi.org/10.1088/1748-9326/ab083d

Sieber, A., Kuemmerle, T., Prishchepov, A. V., Wendland, K. J., Baumann, M., Radeloff, V. C., Baskin, L. M., & Hostert, P. (2013). Landsat-based mapping of post-Soviet land-use change to assess the effectiveness of the Oksky and Mordovsky protected areas in European Russia. *Remote Sensing of Environment*, *133*, 38–51. https://doi.org/10.1016/j.rse.2013.01.021

Smirnov, D. Y., Kabanets, A. G., Milakovsky, B. J., Lepeshkin, E. A., & Sychikov, D. V. (2013). *Illegal Logging in the Russian Far East: Global Demand and Taiga Destruction*. WWF Moscow. https://www.worldwildlife.org/publications/illegal-logging-in-the-russian-far-east-global-demand-and-taiga-destruction

Smith, A. M. S., Kolden, C. A., Paveglio, T. B., Cochrane, M. A., Bowman, D. M., Moritz, M. A., Kliskey, A. D., Alessa, L., Hudak, A. T., Hoffman, C. M., Lutz, J. A., Queen, L. P., Goetz, S. J., Higuera, P. E., Boschetti, L., Flannigan, M., Yedinak, K. M., Watts, A. C., Strand, E. K., … Abatzoglou, J. T. (2016). The Science of Firescapes: Achieving Fire-Resilient Communities. *BioScience*, *66*(2), 130–146. https://doi.org/10.1093/biosci/biv182

Sofronov, M. A., & Volokitina, A. V. (2010). Wildfire Ecology in Continuous Permafrost Zone. In A. Osawa, O. A. Zyryanova, Y. Matsuura, T. Kajimoto, & R. W. Wein (Eds.), *Permafrost Ecosystems: Siberian Larch Forests* (pp. 59–82). Springer Netherlands. https://doi.org/10.1007/978-1-4020-9693-8_4

Soja, A. J., Tchebakova, N. M., French, N. H. F., Flannigan, M. D., Shugart, H. H., Stocks, B. J., Sukhinin, A. I., Parfenova, E. I., Chapin, F. S., & Stackhouse, P. W. (2007). Climate-induced boreal forest change: Predictions versus current observations. *Global and Planetary Change*, *56*(3), 274–296. https://doi.org/10.1016/j.gloplacha.2006.07.028

Sommerfeld, A., Senf, C., Buma, B., D'Amato, A. W., Després, T., Díaz-Hormazábal, I., Fraver, S., Frelich, L. E., Gutiérrez, Á. G., Hart, S. J., Harvey, B. J., He, H. S., Hlásny, T., Holz, A., Kitzberger, T., Kulakowski, D., Lindenmayer, D., Mori, A. S., Müller, J., … Seidl, R. (2018). Patterns and drivers of recent disturbances across the temperate forest biome. *Nature Communications*, *9*. https://doi.org/10.1038/s41467-018-06788-9

Song, C., Woodcock, C. E., Seto, K. C., Lenney, M. P., & Macomber, S. A. (2001). Classification and Change Detection Using Landsat TM Data: When and How to Correct Atmospheric Effects? *Remote Sensing of Environment*, *75*(2), 230–244. https://doi.org/10.1016/S0034-4257(00)00169-3

Soverel, N. O., Perrakis, D. D. B., & Coops, N. C. (2010). Estimating burn severity from Landsat dNBR and RdNBR indices across western Canada. *Remote Sensing of Environment*, *114*(9), 1896–1909. https://doi.org/10.1016/j.rse.2010.03.013

Stocks, B. J., Fosberg, M. A., Lynham, T. J., Mearns, L., Wotton, B. M., Yang, Q., Jin, J.-Z., Lawrence, K., Hartley, G. R., Mason, J. A., & McKENNEY, D. W. (1998). Climate Change and Forest Fire Potential in Russian and Canadian Boreal Forests. *Climatic*

Suleymanova, G. F., Saratov State University, Boldyrev, V. A., Saratov State University, Savinov, V. A., & National park «Khvalynsky». (2019). Post-fire restoration of plant communities with Paeonia tenuifolia in the Khvalynsky National Park (Russia). *Nature Conservation Research*, *4*(Suppl.1), Article Suppl.1. https://doi.org/10.24189/ncr.2019.048

Suzuki, R., Kobayashi, H., Delbart, N., Asanuma, J., & Hiyama, T. (2011). NDVI responses to the forest canopy and floor from spring to summer observed by airborne spectrometer in eastern Siberia. *Remote Sensing of Environment*, *115*(12), 3615–3624. https://doi.org/10.1016/j.rse.2011.08.022

Sw, M., M, Y., Rs, C., & Cp, G. (2008). Comparison of Remote Sensing Image Processing Techniques to Identify Tornado Damage Areas from Landsat TM Data. *Sensors (Basel, Switzerland)*, *8*(2), 1128–1156. https://doi.org/10.3390/s8021128

Tei, S., Sugimoto, A., Kotani, A., Ohta, T., Morozumi, T., Saito, S., Hashiguchi, S., & Maximov, T. (2019). Strong and stable relationships between tree-ring parameters and forest-level carbon fluxes in a Siberian larch forest. *Polar Science*, *21*, 146–157. https://doi.org/10.1016/j.polar.2019.02.001

Tishkov, A. A., Belonovskaya, E. A., Zolotukhin, N. I., Titova, S. V., Tsarevskaya, N. G., & Chendev, Yu. G. (2020). Preserved Sections of Steppes as the Basis for the Future Ecological Framework of Belgorod Oblast. *Arid Ecosystems*, *10*(1), 36–43. https://doi.org/10.1134/S2079096120010114

Townsend Peterson, A., Papeş, M., & Eaton, M. (2007). Transferability and model evaluation in ecological niche modeling: A comparison of GARP and Maxent. *Ecography*, *30*(4), 550–560. https://doi.org/10.1111/j.0906-7590.2007.05102.x

Tucker, C. J. (1979). Red and photographic infrared linear combinations for monitoring vegetation. *Remote Sensing of Environment*, *8*(2), 127–150. https://doi.org/10.1016/0034-4257(79)90013-0

Tucker, C. J. (1980). Remote sensing of leaf water content in the near infrared. *Remote Sensing of Environment*, *10*(1), 23–32. https://doi.org/10.1016/0034-4257(80)90096-6

Tucker, C. J., Grant, D. M., & Dykstra, J. D. (2004). NASA's Global Orthorectified Landsat Data Set. *Photogrammetric Engineering & Remote Sensing*, *70*(3), 313–322. https://doi.org/10.14358/PERS.70.3.313

Turner, M. G. (2010). Disturbance and landscape dynamics in a changing world. *Ecology*, *91*(10), 2833–2849. https://doi.org/10.1890/10-0097.1

Turner, W., Spector, S., Gardiner, N., Fladeland, M., Sterling, E., & Steininger, M. (2003). Remote sensing for biodiversity science and conservation. *Trends in Ecology & Evolution*, *18*(6), 306–314. https://doi.org/10.1016/S0169-5347(03)00070-3

Uotila, A., Kouki, J., Kontkanen, H., & Pulkkinen, P. (2002). Assessing the naturalness of boreal forests in eastern Fennoscandia. *Forest Ecology and Management*, *161*(1), 257–277. https://doi.org/10.1016/S0378-1127(01)00496-0

USGS. (2017). *What are the band designations for the Landsat satellites?* [Government]. https://www.usgs.gov/faqs/what-are-band-designations-landsat-satellites?qt-news_science_products=3#qt-news_science_products

Uvsh, D., Gehlbach, S., Potapov, P. V., Munteanu, C., Bragina, E. V., & Radeloff, V. C. (2020). Correlates of forest-cover change in European Russia, 1989–2012. *Land Use Policy*, *96*, 104648. https://doi.org/10.1016/j.landusepol.2020.104648

Volokitina, A., Nazimova, D., Sofronova, T., & Korets, M. (2019). Improvement of fire danger rating and vegetation fire behaviour prediction on protected areas. *BIO Web of Conferences*, *16*, 00040. https://doi.org/10.1051/bioconf/20191600040

Wade, C. M., Austin, K. G., Cajka, J., Lapidus, D., Everett, K. H., Galperin, D., Maynard, R., & Sobel, A. (2020). What Is Threatening Forests in Protected Areas? A Global Assessment of Deforestation in Protected Areas, 2001–2018. *Forests*, *11*(5), 539. https://doi.org/10.3390/f11050539

Wear, D. N., & Bolstad, P. (1998). Land-Use Changes in Southern Appalachian Landscapes: Spatial Analysis and Forecast Evaluation. *Ecosystems*, *1*(6), 575–594. https://doi.org/10.1007/s100219900052

Wendland, K. J., Baumann, M., Lewis, D. J., Sieber, A., & Radeloff, V. C. (2015). Protected Area Effectiveness in European Russia: A Postmatching Panel Data Analysis. *Land Economics*, *91*(1), 149–168. https://doi.org/10.3368/le.91.1.149

Wickham, H. (2009). *ggplot2: Elegant Graphics for Data Analysis.* http://ggplot2.org

World Resources Institute. (2014). *Global Forest Watch*. www.globalforestwatch.org

Wu, C., Wang, M., Lu, C., Venevsky, S., Sorokina, V., Kulygin, V., & Berdnikov, S. (2018). Climate-induced fire regimes in the Russian biodiversity hotspots. *Global Ecology and Conservation*, *16*, e00495. https://doi.org/10.1016/j.gecco.2018.e00495

Wulder, M. A., & Coops, N. C. (2014). Satellites: Make Earth observations open access. *Nature News*, *513*(7516), 30. https://doi.org/10.1038/513030a

Zeya State Nature Reserve. (2020). *Biodiversity* [Government]. https://zeyzap.ru/sohranyaem/zejskij-zapovednik/bioraznoobrazie/

Zhao, F., Liu, Y., & Shu, L. (2020). Change in the fire season pattern from bimodal to unimodal under climate change: The case of Daxing'anling in Northeast China. *Agricultural and Forest Meteorology*, *291*, 108075. https://doi.org/10.1016/j.agrformet.2020.108075

Zyryanova, O. A., Abaimov, A. P., Bugaenko, T. N., & Bugaenko, N. N. (2010). Recovery of Forest Vegetation After Fire Disturbance. In A. Osawa, O. A. Zyryanova, Y. Matsuura, T. Kajimoto, & R. W. Wein (Eds.), *Permafrost Ecosystems: Siberian Larch Forests* (pp. 83–96). Springer Netherlands. https://doi.org/10.1007/978-1-4020-9693-8_5

Appendices

Appendix 1. Overview images of each class in the field.

BURN

CCTA

MD





GRASS





OBF

BLF

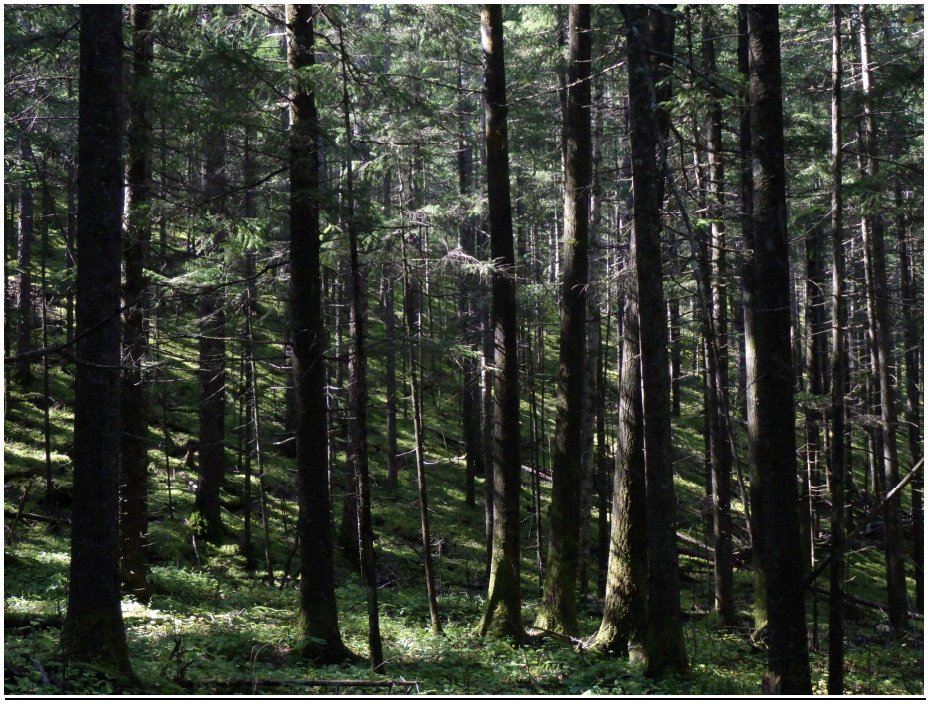

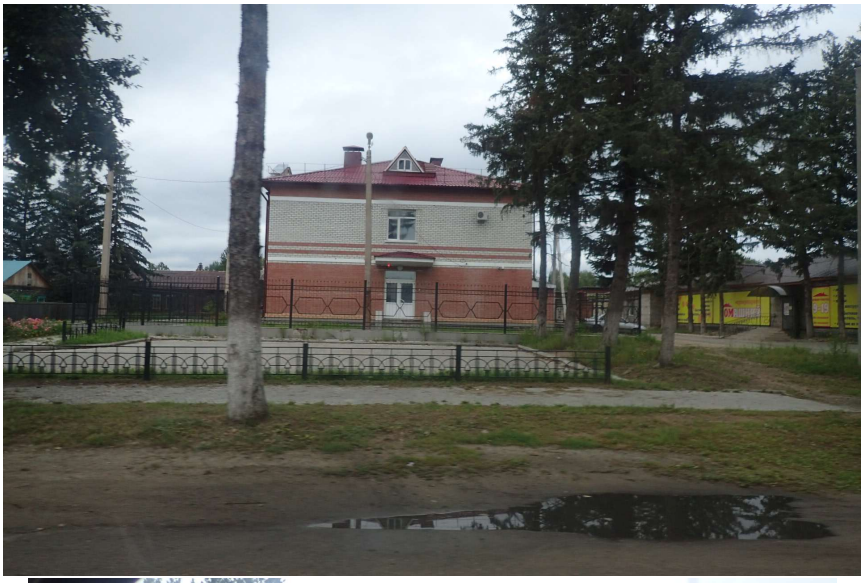

ROCK

Appendix 2. Post-classification algorithms for a) 1988–1999, b) 1999–2010, and c) 2010–2016 scripted in eCognition software by Culabush Khatancharoen (2020, unpublished)

a)

b)


multi-resolution: 10 [shape:0.1 compct.:0.5] creating 'Level1'
at Level1: Bog Muddy Floodplain (Grassland), Mixed Disturbance, Burn, Clearcut for Timber and Agrculture, Clearcut for Electricity, Dwarf Pine Woodland
unclassified with Mean NIR1999 < 80 or Mean NIR2010 < 80 at Level1: Water
Mt.Tundra Vegetation with Mean SRTM < 1100 at Level1: Bog Muddy Floodplain (Grassland)
Dwarf Pine Woodland with Mean SRTM < 1100 at Level1: Larch and Birch Forest
Mt.Spruce Forest with Mean SRTM < 700 at Level1: Spruce Forest in River Valley
Spruce Forest in River Valley with Mean SRTM >= 700 at Level1: Mt.Spruce Forest
Oak-Daurian Birch Forest with Mean SRTM > 800 at Level1: Larch and Birch Forest
Burn with dNBR1999-2010 < 150 at Level1: Larch and Birch Forest
Clearcut for Electricity with Border to Stream Bedrock > 0 Pxl at Level1: Stream Bedrock
Clearcut for Timber and Agrculture with Border to Stream Bedrock > 0 Pxl at Level1: Stream Bedrock
Clearcut for Timber and Agrculture with dNBR1999-2010 > 100 at Level1: Burn
Clearcut for Timber and Agrculture with Border to Burn > 5 Pxl at Level1: Burn
Clearcut for Timber and Agrculture with dNBR1999-2010 < -10 at Level1: unclassified
Stream Bedrock with Border to Clearcut for Electricity > 0 Pxl at Level1: Clearcut for Electricity
Stream Bedrock with NDWI1999 > 100 or NDWI2010 > 100 at Level1: Mixed Forest
Clearcut for Electricity with dNBR1999-2010 > 100 at Level1: Clearcut for Timber and Agrculture
Clearcut for Timber and Agrculture with dNBR1999-2010 < 100 at Level1: Mixed Forest
Vegetation recovery 1999-2010 with Border to Bog Muddy Floodplain (Grassland) > 10 Pxl at Level1: Bog Muddy Floodplain (Grassland)
Unpaved Road with Border to Bog Muddy Floodplain (Grassland) > 0 Pxl at Level1: Mixed Forest
Settlement with Border to Stream Bedrock > 1 Pxl at Level1: Stream Bedrock
Stream Bedrock with Border to Settlement > 5 Pxl at Level1: Settlement
Mixed Forest with dNBR1999-2010 > 100 at Level1: Burn
Burn with dNBR1999-2010 > 164.28 and dNBR1999-2010 < 164.3 at Level1: Clearcut for Timber and Agrculture
Burn, Mixed Forest with dNBR1999-2010 > 203.09 and dNBR1999-2010 < 203.11 at Level1: Clearcut for Timber and Agrculture
Burn with NDWI2010 < 90 or NDWI1999 < 90 at Level1: Stream Bedrock
Clearcut for Timber and Agrculture with dNBR1999-2010 > 137.9 and dNBR1999-2010 < 137.92 at Level1: Larch and Birch Forest
unclassified with dNBR1999-2010 > 191.9 and dNBR1999-2010 < 191.96 at Level1: Clearcut for Timber and Agrculture
Mixed Disturbance with dNBR1999-2010 > 184.55 and dNBR1999-2010 < 184.57 at Level1: Burn
Clearcut for Electricity with dNBR1999-2010 > 74.87 and dNBR1999-2010 < 74.89 at Level1: Larch and Birch Forest
Mixed Disturbance, Burn, Clearcut for Electricity with Rel. border to Water > 0.35 at Level1: Stream Bedrock
Burn with dNBR1999-2010 > 411.33 and dNBR1999-2010 < 411.35 at Level1: Stream Bedrock
Stream Bedrock with dNBR1999-2010 > 159.06 and dNBR1999-2010 < 159.08 at Level1: Burn
Unpaved Road with Border to Stream Bedrock > 10 Pxl at Level1: Stream Bedrock
unclassified at Level1: Larch and Birch Forest
Clearcut for Electricity, Clearcut for Timber and Agrculture, Mixed Disturbance, Settlement at Level1: Larch and Birch Forest
unclassified at Level1: Larch and Birch Forest

c)

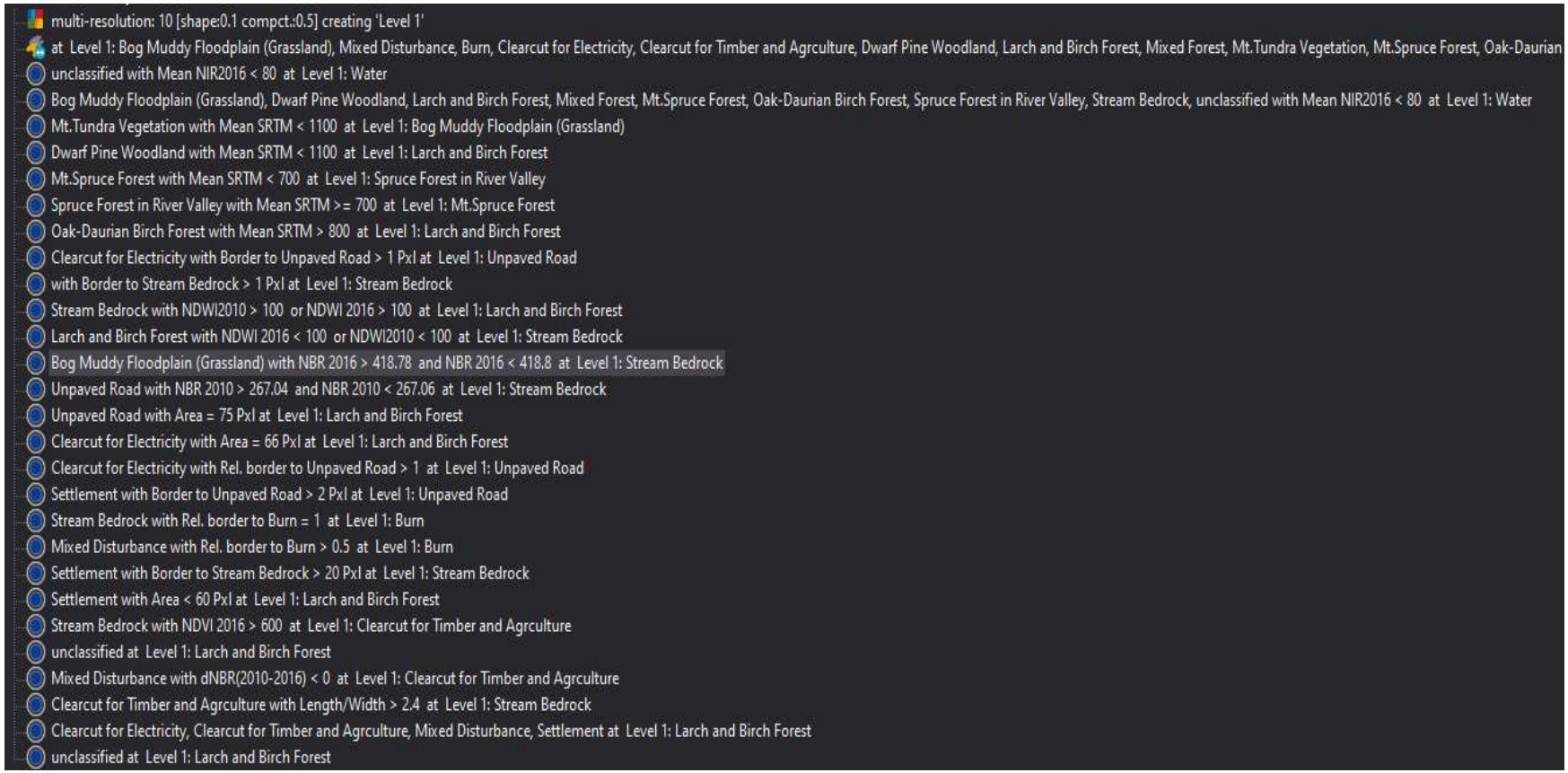
multi-resolution: 10 [shape:0.1 compct.:0.5] creating 'Level 1'
at Level 1: Bog Muddy Floodplain (Grassland), Mixed Disturbance, Burn, Clearcut for Electricity, Clearcut for Timber and Agrculture, Dwarf Pine Woodland, Larch and Birch Forest, Mixed Forest, Mt.Tundra Vegetation, Mt.Spruce Forest, Oak-Daurian
unclassified with Mean NIR2016 < 80 at Level 1: Water
Bog Muddy Floodplain (Grassland), Dwarf Pine Woodland, Larch and Birch Forest, Mixed Forest, Mt.Spruce Forest, Oak-Daurian Birch Forest, Spruce Forest in River Valley, Stream Bedrock, unclassified with Mean NIR2016 < 80 at Level 1: Water
Mt.Tundra Vegetation with Mean SRTM < 1100 at Level 1: Bog Muddy Floodplain (Grassland)
Dwarf Pine Woodland with Mean SRTM < 1100 at Level 1: Larch and Birch Forest
Mt.Spruce Forest with Mean SRTM < 700 at Level 1: Spruce Forest in River Valley
Spruce Forest in River Valley with Mean SRTM >= 700 at Level 1: Mt.Spruce Forest
Oak-Daurian Birch Forest with Mean SRTM > 800 at Level 1: Larch and Birch Forest
Clearcut for Electricity with Border to Unpaved Road > 1 PxI at Level 1: Unpaved Road
with Border to Stream Bedrock > 1 PxI at Level 1: Stream Bedrock
Stream Bedrock with NDWI2010 > 100 or NDWI 2016 > 100 at Level 1: Larch and Birch Forest
Larch and Birch Forest with NDWI 2016 < 100 or NDWI2010 < 100 at Level 1: Stream Bedrock
Bog Muddy Floodplain (Grassland) with NBR 2016 > 418.78 and NBR 2016 < 418.8 at Level 1: Stream Bedrock
Unpaved Road with NBR 2010 > 267.04 and NBR 2010 < 267.06 at Level 1: Stream Bedrock
Unpaved Road with Area = 75 PxI at Level 1: Larch and Birch Forest
Clearcut for Electricity with Area = 66 PxI at Level 1: Larch and Birch Forest
Clearcut for Electricity with Rel. border to Unpaved Road > 1 at Level 1: Unpaved Road
Settlement with Border to Unpaved Road > 2 PxI at Level 1: Unpaved Road
Stream Bedrock with Rel. border to Burn = 1 at Level 1: Burn
Mixed Disturbance with Rel. border to Burn > 0.5 at Level 1: Burn
Settlement with Border to Stream Bedrock > 20 PxI at Level 1: Stream Bedrock
Settlement with Area < 60 PxI at Level 1: Larch and Birch Forest
Stream Bedrock with NDVI 2016 > 600 at Level 1: Clearcut for Timber and Agrculture
unclassified at Level 1: Larch and Birch Forest
Mixed Disturbance with dNBR(2010-2016) < 0 at Level 1: Clearcut for Timber and Agrculture
Clearcut for Timber and Agrculture with Length/Width > 2.4 at Level 1: Stream Bedrock
Clearcut for Electricity, Clearcut for Timber and Agrculture, Mixed Disturbance, Settlement at Level 1: Larch and Birch Forest
unclassified at Level 1: Larch and Birch Forest